สารยับยั้งโคลีนเอสเทอเรสจากผลมะระขี้นก *Momordica charantia* L.

นางสาววิชุตา ควรหัตร์

วิทยานิพนธ์นี้เป็นส่วนหนึ่งของการศึกษาตามหลักสูตรปริญญาวิทยาศาสตรมหาบัณฑิต
สาขาวิชาเคมี ภาควิชาเคมี
คณะวิทยาศาสตร์ จุฬาลงกรณ์มหาวิทยาลัย
ปีการศึกษา 2555

CHOLINESTERASE INHIBITORS FROM FRUITS OF THAI BITTER GOURD *Momordica charantia* L.

Miss Wichuta Kuanhut

A Thesis Submitted in Partial Fulfillment of the Requirements
for the Degree of Master of Science Program in Chemistry
Department of Chemistry
Faculty of Science
Chulalongkorn University
Academic Year 2012

Thesis Title	CHOLINESTERASE INHIBITORS FROM FRUITS OF THAI BITTER GOURD *Momordica charantia* L.
By	Miss Wichuta Kuanhut
Field of Study	Chemistry
Thesis Advisor	Assistant Professor Pattara Sawasdee, Ph.D.

Accepted by the Faculty of Science, Chulalongkorn University in Partial Fulfillment of the Requirements for the Master's Degree

…… Dean of the Faculty of Science
(Professor Supot Hannongbua, Dr. rer. nat.)

THESIS COMMITTEE

…… Chairman
(Assistant Professor Warinthorn Chavasiri, Ph.D.)

…… Thesis Advisor
(Assistant Professor Pattara Sawasdee, Ph.D.)

…… Examiner
(Assistant Professor Preecha Phuwapraisirisan, Ph.D.)

…… External Examiner
(Assistant Professor Wimolpun Rungprom, Ph.D.)

วิชุตา ควรหัตร์ : สารยับยั้งโคลีนเอสเทอเรสจากผลมะระขี้นก *Momordica charantia* L. (CHOLINESTERASE INHIBITORS FROM FRUITS OF THAI BITTER GOURD *Momordica charantia* L.) อ.ที่ปรึกษาวิทยานิพนธ์หลัก : ผศ.ดร.พัฒฑราสวัสดี, 85 หน้า.

ได้แยกสิ่งสกัดไดคลอโรมีเทนของผลมะระขี้นก *Momordica charantia* L. เพื่อหาสารออกฤทธิ์ยับยั้งโคลีนเอสเทอเรส ได้สารบริสุทธิ์ 4 ชนิด กับสารผสม 3 ชนิด และพิสูจน์โครงสร้างของสารทั้งหมดจากสมบัติทางกายภาพ และวิธีทางสเปกโทรสโกปี รวมทั้งเปรียบเทียบกับข้อมูลที่มีการรายงานมาแล้ว สารที่แยกได้ คือ (19*R*,23*E*)-5β,19-epoxy-19-methoxycucurbita-6,23,25-trien-3β-ol (**1**), (23*E*)-5β,19-epoxycucurbita-6,23-diene-3β,25-diol (**2**), สารผสมระหว่าง 5β,19-epoxycucurbita-6,23(*E*),25(26)-triene-3β,19(*S*)-diol (**3a**) และ 5β,19-epoxycucurbita-6,23(*E*),25(26)-triene-3β,19(*R*)-diol (**3b**), สารผสมระหว่าง 5β,19-epoxy-25-methoxy-cucurbita-6,23-diene-3β,19(*S*)-diol (**4a**) และ 5β,19-epoxy-25-methoxy-cucurbita-6,23-diene-3β,19(*R*)-diol (**4b**), ligballinol (**5**), สารผสมระหว่าง 3β-O-D-glucopyranosyl-24ξ-ethyl-cholesta-5-ene-3β-ol (**6a**) และ3β-O-D-glucopyranosyl-24β-ethyl-cholesta-5,25-diene-3β-ol (**6b**) หรือ ชาแลนทิน, และ momordicoside K (**7**) จากสารที่แยกได้ทั้งหมดพบว่า 5β,19-epoxycucurbita-6,23(*E*),25(26)-triene-3β,19(*S*)-diol (**3a**) และ 5β,19-epoxy-25-methoxy-cucurbita-6,23-diene-3β,19(*S*)-diol (**4a**) เป็นสารที่มีการพบในธรรมชาติเป็นครั้งแรก นอกจากนี้ ยังเป็นการพบ ligballinol (**5**) เป็นครั้งแรกในมะระขี้นก ligballinol (**5**) แสดงฤทธิ์ยับยั้งเอนไซม์บิวทิริลโคลีนเอสเทอเรสได้ดีที่สุด ด้วยค่าความเข้มข้นที่สามารถยับยั้งฤทธิ์ของเอนไซม์ได้ร้อยละ 50 เท่ากับ 32.20 ไมโครโมลาร์ และเป็นการยับยั้งแบบแข่งขันจากการศึกษาทางจลนศาสตร์

ภาควิชา เคมี ลายมือชื่อนิสิต .....

สาขาวิชา เคมี ลายมือชื่อ อ.ที่ปรึกษาวิทยานิพนธ์หลัก .....

ปีการศึกษา 2555

5372411823 : MAJOR CHEMISTRY
KEYWORDS : *Momordica charantia* L. / CUCURBITACEAE / ANTI-CHOLINESTERASE

WICHUTA KUANHUT : CHOLINESTERASE INHIBITORS FROM FRUITS OF THAI BITTER GOURD *Momordica charantia* L. ADVISOR : ASST. PROF. PATTARA SAWASDEE, Ph.D., 85 pp.

Anti-acetylcholinesterase compounds were separated from the dichloromethane extract of *Momordica charantia* L. Four compounds and three inseparable mixtures were afforded and their chemical structures were elucidated on the basis of physical properties and spectroscopic analysis as well as comparing with the previous publication data. The isolated substances were (19*R*,23*E*)-5β,19-epoxy-19-methoxycucurbita-6,23,25-trien-3β-ol (**1**), (23*E*)-5β,19-epoxycucurbita-6,23-diene-3β,25-diol (**2**), a mixture of 5β,19-epoxycucurbita-6,23(*E*),25(26)-triene-3β,19(*S*)-diol (**3a**) and 5β,19-epoxycucurbita-6,23(*E*),25(26)-triene-3β,19(*R*)-diol (**3b**), a mixture of 5β,19-epoxy-25-methoxy-cucurbita-6,23-diene-3β,19(*S*)-diol (**4a**) and 5β,19-epoxy-25-methoxy-cucurbita-6,23-diene-3β,19(*R*)-diol (**4b**), ligballinol (**5**), a mixture of 3β-O-D-glucopyranosyl-24ξ-ethyl-cholesta-5-ene-3β-ol (**6a**) and 3β-O-D-glucopyranosyl-24β-ethyl-cholesta-5,25-diene-3β-ol (**6b**) or charantin and momordicoside K (**7**). Among them, 5β,19-epoxycucurbita-6,23(*E*),25(26)-triene-3β,19(*S*)-diol (**3a**) and 5β,19-epoxy-25-methoxy-cucurbita-6,23-diene-3β,19(*S*)-diol (**4a**) were first identified from nature. Moreover, ligballinol (**5**) was first isolated from this plant. Ligballinol (**5**) exhibited the most potent butyrylcholinesterase (BChE) inhibitory activity with the IC_{50} value of 32.20 μM with a competitive mode of inhibition in a kinetic study.

Department : Chemistry Student's Signature .....
Field of Study : Chemistry Advisor's Signature .....
Academic Year : 2012

ACKNOWLEDGEMENTS

I would like to convey my faithful gratitude to my advisor Assistant Professor Dr. Pattara Sawasdee, for her recommendation, assistance, encouragement and supporting during in the course of this research. I also gratefully thank to the committee of my thesis, Assistant Professor Dr. Warinthorn Chavasiri, Assistant Professor Dr. Preecha Phuwapraisirisan, Department of chemistry, Faculty of science, Chulalongkorn University and Assistant Professor Dr. Wimolpun Rungprom, Faculty of Science and Technology, Phra Nakorn Sri Ayutthaya Rajaphat University, for discussion, guidance and valuable commentary.

My appreciation is expressed to acknowledge Associate Professor Dr. Thammarat Aree, Materials Chemistry and Catalysis Research Unit (MATCAT), Department of Chemistry, Faculty of Science, Chulalongkorn University, who kindly performed X-ray Crystallographic analysis. I would like to thank Associate Professor Dr. Nijsiri Ruangrungsi, Department of Pharmacognosy and Pharmaceutical Botany, Faculty of Pharmaceutical Science, Chulalongkorn University, for the plant identification and making the voucher specimen of *Momordica charantia* L. in this research.

I would like to convey my appreciation to my family. Furthermore, my specially thank to Miss Wisuttaya Worawalai, Mr. Thiendanai Sermboonpaisarn and Mr. Setthakorn Niamthiang for their technical assistance. On the other hand, I would like to thank all of my friends in the laboratory for their friendships and help during the course of my graduate research.

I would like to express my gratitude to the Natural Products Research Unit, Department of Chemistry, Faculty of Science, Chulalongkorn University for providing the chemicals and facilities throughout the course of study. A deep affectionate gratitude is acknowledged to my family for their understanding, encouragement and support throughout the education course.

CONTENTS

Page

LIST OF TABLES

LIST OF FIGURES

Figure **Page**

Figure **Page**

LIST OF SCHEMES

LIST OF ABBREVIATIONS

br	=	broad (NMR)
br s	=	broad singlet (NMR)
BuOH	=	butanol
C	=	carbon
^{13}C-NMR	=	carbon-13 nuclear magnetic resonance
cm	=	centimeter (s)
$CHCl_3$	=	chloroform
COSY	=	correlation spectroscopy
J	=	coupling constant
acetone-d_6	=	deuterated acetone
chloroform-d_1	=	deuterated chlorofrom
CH_2Cl_2	=	dichloromethane
d	=	doublet (NMR)
dd	=	doublet of doublet (NMR)
ESI-MS	=	electrospray ionization mass spectroscopy
EtOAC	=	ethyl acetae
U	=	enzyme unit
g	=	gram (s)
Hz	=	hertz (NMR)
HMBC	=	heteronuclear multiple bond correlation
HSQC	=	heteronuclear single quantum coherence
HRESIMS	=	high resolution electrospray ionization mass spectrometry
H	=	hydrogen
OH	=	hydroxy group
kg	=	kilogram (s)
in vitro	=	literally in glass
MHz	=	megahertz (NMR)
Me	=	methyl

MeOH	=	methanol
OMe	=	methoxy group
µL	=	microliter (s)
µM	=	micromolar
mg	=	milligram (s)
mL	=	milliliter (s)
mM	=	millimolar
min	=	minute (s)
M	=	molarity
M. charantia	=	*Momordica charantia* L.
m	=	multiplet (NMR)
NOSEY	=	nuclear overhauser effect spectroscopy
$[\alpha]_D$	=	optical rotation
ppm	=	part per million
%	=	percentage
^{1}H-NMR	=	proton-1 nuclear magnetic resonance
pyridene-d_5	=	deuterated pyridene
q-TOF	=	quadrupole time-of-flight tandem
R_f	=	retarding factor in chromatography
n	=	sample size (statistic)
sat. BuOH	=	saturated butanol
s	=	singlet (NMR)
S.D.	=	standard deviation (statistic)
t	=	triplet (NMR)
δ	=	unit of chemical shift
δ_C	=	chemical shift of carbon
δ_H	=	chemical shift of proton
UV	=	ultraviolet
v	=	volume
in vivo	=	within a living organism
H_2O	=	water

CHAPTER I

INTRODUCTION

A nature is a rich source of biological and chemical diversity. Many drugs are derived from natural sources which are, for examples, plants, microorganisms and marine organisms. Due to the unusual and complex structures of natural products, they cannot be gain easily by chemical synthesis. Moreover, some synthetic drugs might have significant side effects in clinical use. Hence, exploring of novel biological activity compounds from natural resources is interested for scientists and researchers. Thailand is a tropical country which has abundant kinds of plants. They have been utilized as food and folk medicine treatment. Many studies have reported the investigation of active constituents from Thai herbs and their bioactivities such as neurodegenerative disorder, anti-oxidant, anti-diabetic, anti-inflammatory and anti-cancer activities. Thai traditional herbs related to a neurodegenerative disorder are known as "rejuvenating" and "neurotonic" agents. They have been believed in the prevention of forgetfulness and the improvement of memory in the elderly persons. Previous reports have shown that the extract of roots of *Stephania suberosa* Forman. and *Tabernaemontana divaricata* (L.) R. Br. Ex Roem. & Schult (Ingkaninan *et al*., 2003), the flower of *Quisqualis indica* L. (Wetwitayaklung *et al*., 2007) exhibited high acetylcholinesterase (AChE) inhibitory activity. In addition, the essential oils from the rhizomes of *Curcuma longa* L., *Alpinia galanga* (L.) Willd and *Boesenbergia pandurata* (Roxb.) Schltr. (Kitphati *et al*., 2012) were also found to inhibit this enzyme. Besides, gnetol, active compound from the vines of *Ficus foveolata* Wall., were found to exhibit a high inhibition towards butyrylcholinesterase (BChE) (Sermboonpaisarn and Sawasdee, 2012). Herein, more than ten extracts of Thai herbs were screened for the preliminary cholinesterase inhibitory activity by the TLC-autobiography assay. The results revealed that the extract from the fruits of *Momordica charantia* L. or Thai bitter gourd showed potential anti-butyrylcholinesterase activity. Interestingly, there are no publications reported the cholinesterase inhibitory activity of this plant. Therefore, the objectives of this

research were to investigate the constituents of *M. charantia* fruits and determine their anti-cholinesterase activity. This research will be demonstrated both phytochemical informations and benefits to the development of Thai medicine for the treatment and prevention of Alzheimer's disease and also other neurodegenerative disorders in a future.

1.1 Botanical Aspects and Distribution of *M. charantia*.

Momordica charantia L., belonging to the family of Cucurbitaceae, is commonly known as bitter gourd or bitter melon. Other names, for examples, are Balsamina (India), Karawila (Sri Lanka), fu kwa (Chinese), nigai uri (Japanese), Mara Khee Nok (Thailand). The classification of *M. charantia* has been categorized as wild and cultivated forms. Generally, there are two different varieties of *M. charantia* including the cultivated variety with large fruit (*M. charantia* var. *charantia*) and the wild variety with small fruit (var. *muricata*) as shown in Figure 1.1. The latter are mostly used in a medicinal folklore (Chakravarty, 1990; Bharathi *et al*., 2012). Later, Reyes and others (1994) reclassified the botanical varieties in India and South-East Asia based on fruit with diameter less (var. *minima* Williams & Ng) and larger (var. *maxima* Williams & Ng) than 5 centimeters.

(a) (b)

Figure 1.1 Fruits of *M. charantia* (a) var. *charantia* (b) var. *muricata*.

In Thailand, two types of *M. charantia* are found. One is the light green and larger fruit which is called Chinese bitter gourd. Another is smaller and has a dark green fruit which is known as Thai bitter gourd or Mara Khee Nok. However, both

types use the same scientific name. However, the variety has not yet been identified (Bunyamahotama, 2004). The botanical characteristics of Thai bitter gourd (Figure 1.2) can be described as follows:

Stem: Long up to 5 meters, slender-stemmed tendril climber, flattened and fluted old stem.

Flower: Monoecious, solitary, approximately 3 cm in diameter, yellow, female flowers solitary in the axils of the leaves, male flowers subtended by a conspicuous kidney or heart shape, peduncle is 0.5-3 cm (male) and 0.2-5 cm (female), an apical bract in diameter is 2 cm (male) and 1 cm (female), the pedicel long is 2-2.5 cm (male) and 1-10 cm (female), corolla about 2.5 cm across and 5 petals free.

Leaves: Broadly blade-leaves, cordate at base, palmately vein, petiole long up to 7 cm, palmately cut into 5-7 lobes, the longest central lobe, irregular and sinuate-toothed margins.

Fruit: Unripe fruit is green, mostly long about 8.4 cm, very variable in shape and size, rough longitudinal rows of clear wart. Ripe fruit is orange-yellow and then becoming softly fleshly and opening to reveal pendulous seeds.

Seeds: Drip-shape seeds are covered with red pulp, brown seeds, which have a ridged surface and a thick jagged margin.

(a) (b) (c)

Figure 1.2 The parts of Thai bitter gourd: (a) unripe fruit and seeds, b) ripe fruit and seeds and (c) stem, leaves and flower.

1.2 The Literature Reviews of *M. charantia*

M. charantia is commonly found in the several regions of Thailand, and is grown all over the tropics, including India, South-East Asia, India, South America, East Africa and the Caribbean (Pornsuriya, Pornsuriya and Numuen, 2011). The leaves and fruits of *M. charantia* are edible and traditionally used as medicine such as anti-diabetic, anti-tumor, antioxidant, antibacterial, anti-virus and anti-cancer studied on its pharmacological actions (Dhiman *et al*., 2012). The several classes of secondary metabolites have been investigated from this plant such as glycosides, triterpenes, proteins, phenolic compounds, alkaloids, fixed oils and steroids (Grover and Yadav, 2004). Many reports have been studied phytochemicals and theirs bioactivities of this plant. According to the scientific name of Chinese and Thai bitter gourd are the same. The literature reviews of present works are described only Thai variety known as Mara Khee Nok.

In the previous works, many parts of *M. charantia*, especially unripe fruit and leaf, were screened for their biological activities. The fruit extract showed anti-mutagenic and anti-carcinogenic in rats (Kusamran, Tepsuwan, and Kupradinu, 1998). The leaf extract possessed the modulation of the function of Pgp and the MDR phenotype in the multidrug-resistant human cervical carcinoma KB-V1 cells (Limtrakul, Khantamat, and Pintha, 2004). Moreover, both extracts displayed a potential anti-oxidant activity because they had the high content of total phenolics (Kubola and Siriamornpu, 2008). The phenolic compounds found in these extracts are, for examples, gallic acid, caffeic acid and catechin as displayed in Figure 1.3.

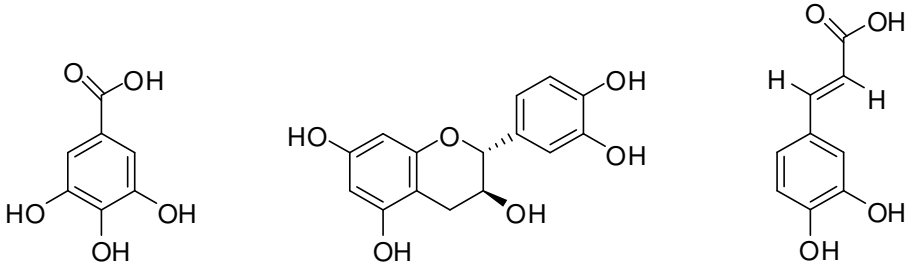

gallic acid (+)-catechin caffeic acid

Figure 1.3 Structures of phenolic compounds isolated from Thai bitter gourd.

Furthermore, charantin which is a mixture of sitosteryl glucoside and clerosteryl glucoside (Figure 1.4) was isolated from fruit and this mixture was a hypoglycemic agent (Raman and Lau, 1996). Generally, charantin was obtained by a silica gel column chromatography. However, it could be extracted by the high efficiency approach including soxhlet and pressurized liquid extraction (PLE) (Pitipanapong *et al*., 2007).

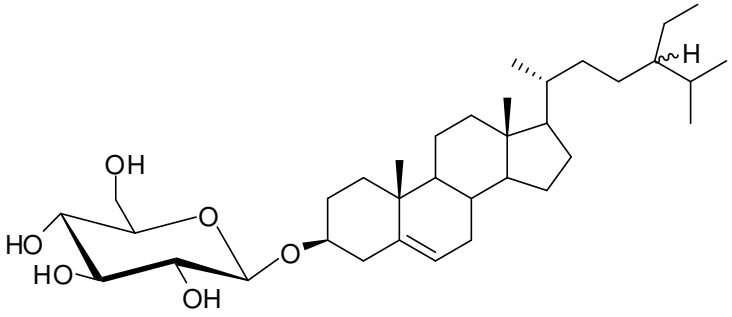

3β-O-D-glucopyranosyl-24ξ-ethyl-cholesta-5-ene-3β-ol (sitosteryl glucoside)

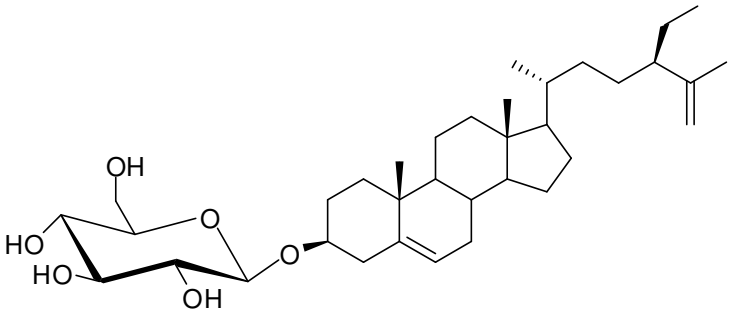

3β-O-D-glucopyranosyl-24β-ethyl-cholesta-5,25-diene-3β-ol (clerosteryl glucoside)

Figure 1.4 Chemical structures of charantin (a mixture of sitosteryl glucoside and clerosteryl glucoside).

Jiratchariyakul and colleagues (2001) investigated protein MRK29 which was isolated from ripe fruits and seeds of Thai bitter gourd. This protein possessed a human immunodeficiency virus (HIV) inhibitory activity. It inhibited the HIV-1 reverse transcriptase with 50% relative inhibitory ratio (IR) at 18 mg/mL and reduced 82% of viral core protein p24 expression in HIV-infected cells at 0.175 mg/mL.

Triterpene kuguacin J (Figure 1.5), isolated from the leaves of Thai bitter gourd, induced apoptosis on the several cancer cell lines. Pitchakarn *et al*. (2012a)

reported that kuguacin J could modulate the function of P-glycoprotein and the multidrug resistance (MDR) phenotype on a human cervical carcinoma cell line (KB-V1) *in vitro*. Thus, it was able to increase the sensitivity of KB-V1 cancer cell line to chemotherapeutic drugs. Moreover, Pitchakarn and colleagues (2010, 2011 and 2012b) indicated that kugucin J showed high anti-metastatic effect on a prostate cancer cell line such as PLS10, LNCaP and PC3 cancer cell lines. Nevertheless, it exhibited a low toxicity in a normal human prostate cell line.

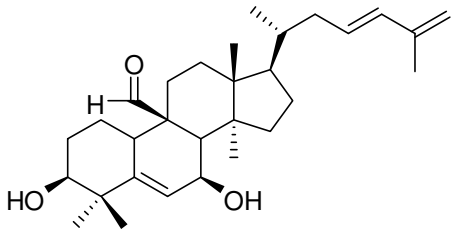

Figure 1.5 Chemical structure of kuguacin J.

In addition, several phytochemicals had been isolated from Chinese bitter gourds. The major class of constituents was triterpenoids. Terpenoids are a class of natural products which related to compounds formally derived from five carbon isoprene units. Of isolated triterpeniods, cucurbitacins (cucurbitane type-triterpenoid) were the major principles which were discovered in many parts of this plant (Haque, Alam, and Hossain, 2011). They were noted for their biological activities such as anti-cancer, anti-inflammatory, and anti-fertility activities (Chen *et al*., 2005). Cucurbitacins B and K were firstly obtained from the seeds of *M. charantia* (Guha and Sen, 1975). Other cucurbitane type-triterpenoids (Figure 1.6), for examples, were momordicines I, II and III (Yasuda *et al*., 1984), 5*β*,19-epoxycucurbita-6,23-diene-3*β*,19,25-triol (Mulholland *et al*., 1997), karavilagenins A-E (Nakamura *et al*., 2006; Matsuda *et al*., 2007) and kuguacins A-S (Chen *et al*., 2008, 2009).

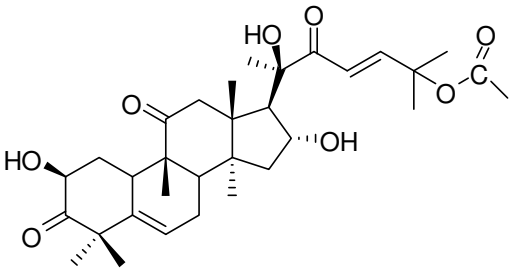

cucurbitacins B

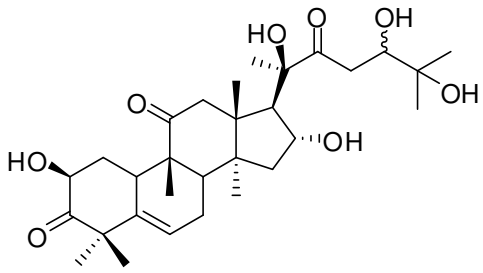

cucurbitacin K

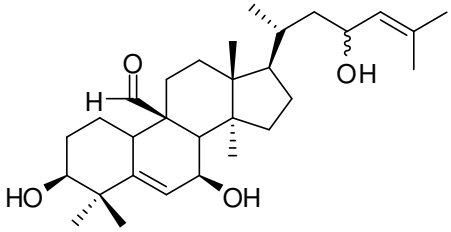

momordicine I

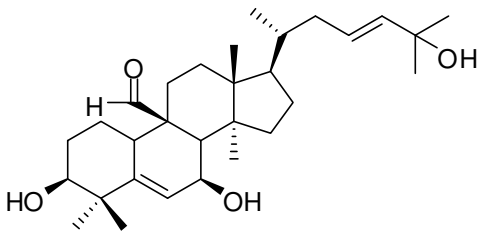

momordicine II

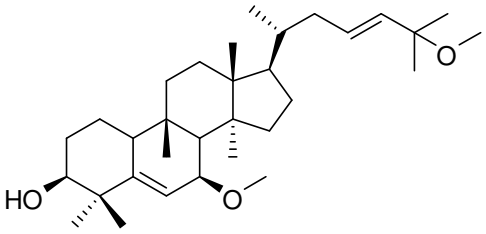

karavilagenin A

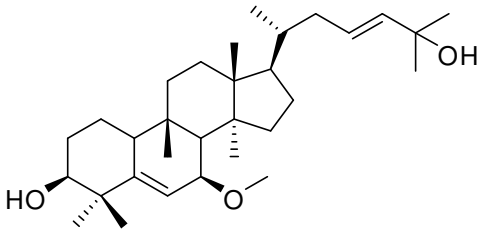

karavilagenin B

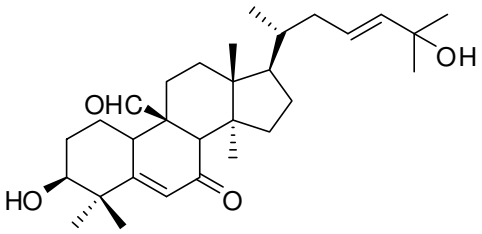

kuguacin A

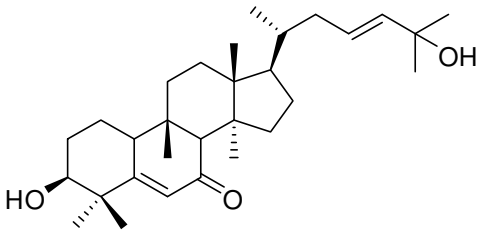

kuguacin B

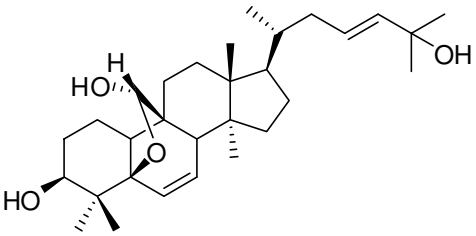

kuguacin R

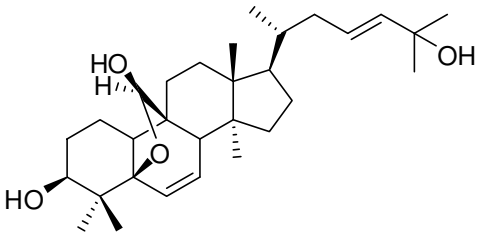

5β,19-epoxycucurbita-6,23-diene-3β,19,25-triol

Figure 1.6 Isolated cucurbitane type-triterpenoids from *M. charantia*.

Others chemical constituents including momordicosides A-E, F1, F2, G, I, K-O and Q-W (Okabe *et al*., 1980; Miyahara *et al*., 1981; Okabe *et al*., 1982a, 1982b; Li *et al*., 2007; Tan *et al*., 2008; Nhiem *et al*., 2010a), charantosides I-VIII (Akihisa *et al*., 2007) and charantosides A-C (Nhiem *et al*., 2010b) were curcurbitane type-triterpenoid glycosides which were isolated from the several parts of *M. chrantia*. Moreover, Liu *et al*. (2010) discovered a new multiflorane triterpenoid named 3*β*-hydroxymultiflora-8-en-17-oic acid in the stems of this plant. Recently, Panlilio and coworkers (2012) has been reported that charantal, a new lanostane type-triterpenoid, and 2,4-bis(2-phenylpropan-2-yl)phenol were isolated from the leaves of *M. charantia*. Recently, (4ξ)-*α*-terpineol 8-*O*-[*α*-larabinopyranosyl-(1→6)-*β*-D-glucopyranoside] and myrtenol 10-*O*-[*β*-D-apiofuranosyl-(1→6)-*β*-D-glucopyranoside] as novel compounds were also obtained from the leaves (Kikuchi *et al*., 2012). Examples of other chemical constituents isolated from *M. charantia* are presented in Figure 1.7.

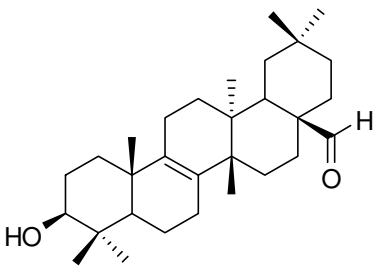

3β-hydroxymultiflora-8-en-17-oic acid

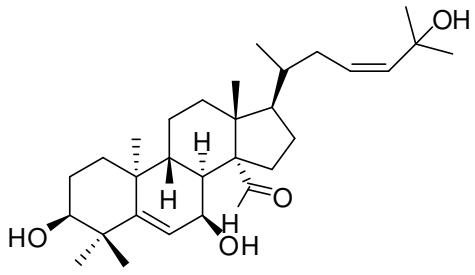

charantal

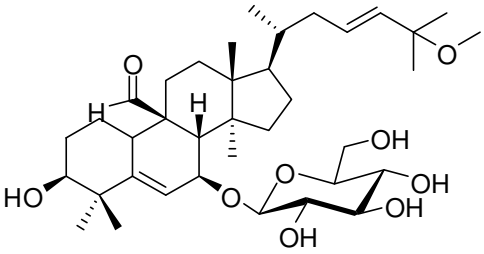

momordicosides K

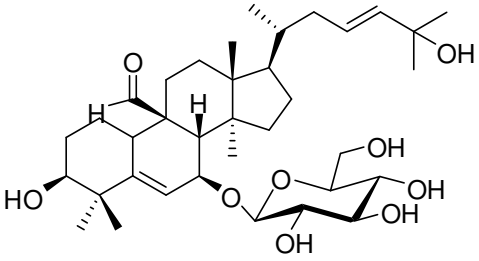

momordicosides L

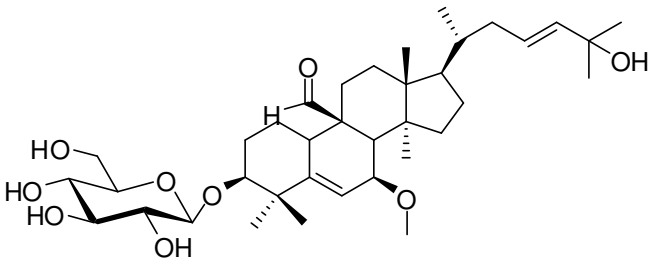

charantoside A

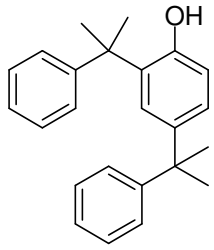

2,4-bis(2-phenylpropan-2-yl)phenol

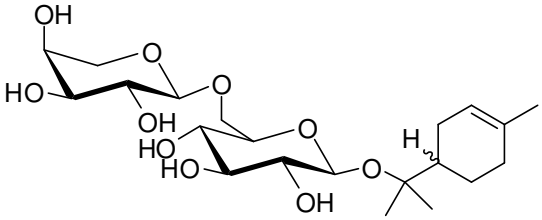

(4ξ)-α-terpineol 8-*O*-[α-larabinopyranosyl-(1→6)-β-D-glucopyranoside]

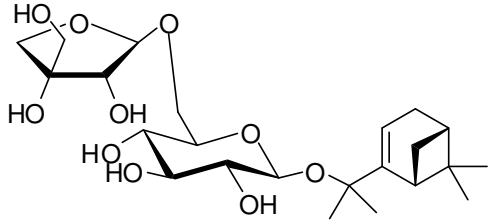

myrtenol 10-*O*-[β-D-apiofuranosyl-(1→6)-β-D-glucopyranoside]

Figure 1.7 Examples of other chemical constituents isolated from *M. charantia*.

1.3 Cholinesterase Inhibitory Activities

Alzheimer's disease (AD) has been the most regular type of dementia in the elderly persons, especially in Western part. Plassman *et al*. (2008) have reported that the most aged people of the United States with this disease are diagnosed at more or equal 70 years old. And women have risk to be Alzheimer's disease more than men. This disease has been determined for its causes, risk factors, symptoms and treatment only in the thirty years ago (Alzheimer's association, 2012). Alzheimer's disease involves with the death or malfunction of nerve cells and called neurons. It results in the progressively impaired cognitive function and behavior in the activities of daily living. The cognitive symptoms compose of memory loss, disorientation, confusion, thinking problem. Behavioral symptoms consist in agitation, anxiety, delusions, depression, hallucinations, insomnia and wandering. At last, they are fatal (Lahiri *et al*., 2002).

The conclusive causes of this disease are not yet known but many hypotheses have been proposed including cholinergic, amyloid and tau protein or tangle (Lahiri *et al*., 2002). However, cholinergic hypothesis is basically studied for the treatment of AD. It associates with the level of cholinergic neurotransmission in the brain.

In a cellular brain system, acetylcholine (ACh) is synthesized by the choline acetyltransferase (ChAT) in the pre-synaptic neuron and then release into the synaptic cleft (Figure 1.8). Binding of acetylcholine to the ACh receptor on the post-synaptic neuron begins a neurotransmission signal. Unbound acetylcholine is rapidly captured by acetylcholinesterase (AChE), following with a hydrolysis and a freeing choline. Choline returns to the pre-synaptic neuron for reuse. The acylated enzyme is hydrolysed to yield acetate (Scheme 1.1) and the restoration of AChE (Štěpánková and Komers, 2008).

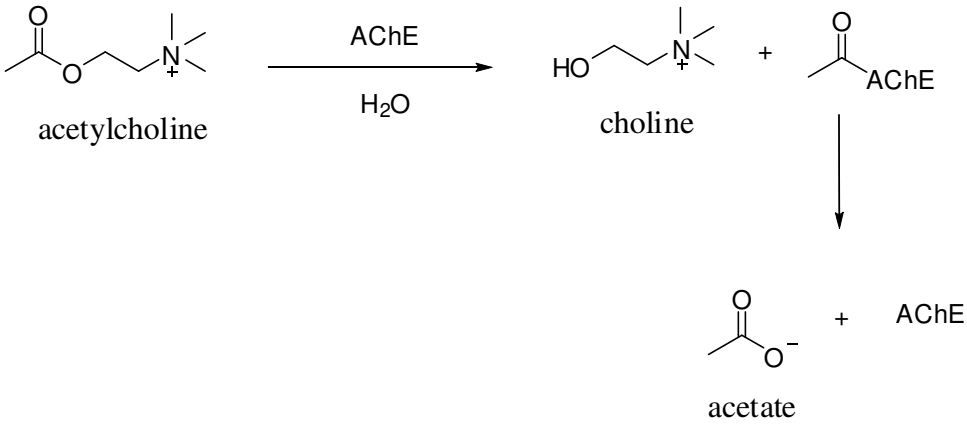

acetylcholine choline acetate

Scheme 1.1 The reaction during hydrolysis of acetylcholine.

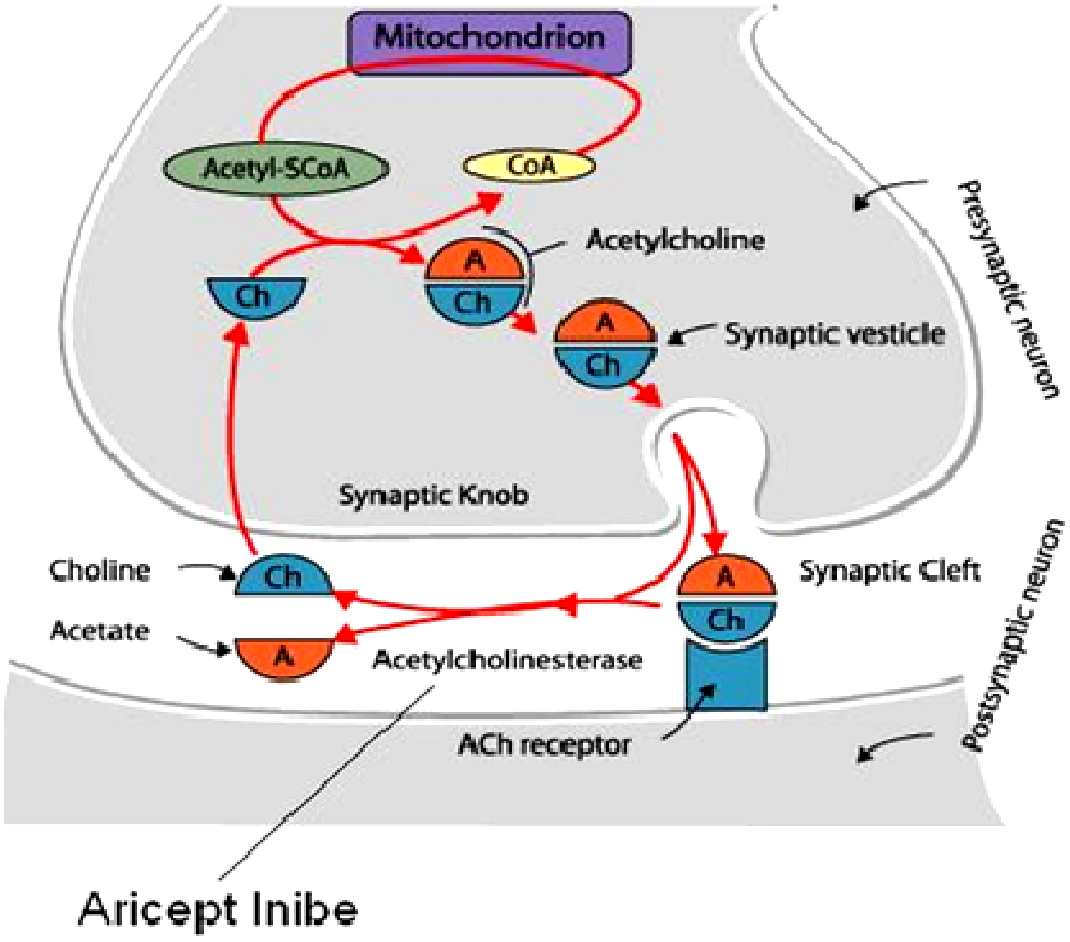

Figure 1.8 Synthesis and hydrolysis of acetylcholine (ACh) in neurons.

In Alzheimer's disease, the severe loss of cholinergic neurons in basal part of the brain results the 90% of reduction in the activity of enzyme, choline acetyltransferase (ChAT) (Sramek, Zarotsky, and Cutler, 2002). This is the rate-limiting synthesis of the neurotransmitter acetylcholine (ACh). The decreasing levels of ACh effects a decline of cholinergic neurotransmission process at brain synapses which is the causes of a cognitive and a memory. Moreover, there is also a matching reduction in the level of the enzyme, acetylcholinesterase, which is responsible for ending the physiological role of acetylcholine at cholinergic synapses (Atack *et al*.,

1986). Coincidental with these changes, a rise in the levels of the sister enzyme, butyrylcholinesterase, occurs predominantly in the brain. Its performance is likewise acetylcholinesterase to metabolize acetylcholine that also results a mismatching between acetylcholine release and its appropriate metabolism. So these results probably contribute to cholinergic dysfunction during AD progression (Greig, Lahiri, and Sambamurti, 2000). In addition, Darvesh and colleagues (1998) have demonstrated that some 10-15% of cholinergic neurons in the hippocampus and amygdala parts of healthy human brain have butyrylcholinesterase rather than acetylcholinesterase which maybe effects to therapeutics of AD.

All these discoveries, along with the known elements of the cholinergic system and cholinergic neurotransmission processing, lead to the development of the cholinergic hypothesis. The basic approach in the treatment of AD patient focuses on a rise of cholinergic or an expansion of acetylcholine's action in brain through the inhibition of enzymatic activities, acetylcholinesterase and butyrylcholinesterase. Cholinesterase (ChE) inhibitors work by binding to enzymes, so these are the preventing of acetylcholine from the hydrolysis of enzymes (Giacobini, 2000).

At present, cholinesterase inhibition is the most effective, widely researched and developed approach for the therapy of AD symptoms (Becker *et al*., 2001; Imbimbo, 2001). In this regard, the four administered drugs for Alzheimer's disease including tacrine, donepezil, rivastigmine and galantamine have been approved by the U.S. Food and Drug Administration (FDA) as shown in Figure 1.9. All drugs have been shown to improve moderately memory and cognition in some AD patients. However, their applications are limited due to side effects appear after several weeks of therapy. Generally, side effects have been occurred in AD patients if the dose of cholinesterase inhibitor is high enough. Their commonly side effects include nausea, vomiting, anorexia, diarrhoea, headache, bradycardia, muscle cramping or weakness (Grutzendler and Morris, 2001). Therefore, therapy inhibitors from a nature are a new alternative that is interesting and developing for the treatment and prevention of AD. Due to the scientists believe in the bioactive compounds from herbs less harmful than synthetic drugs.

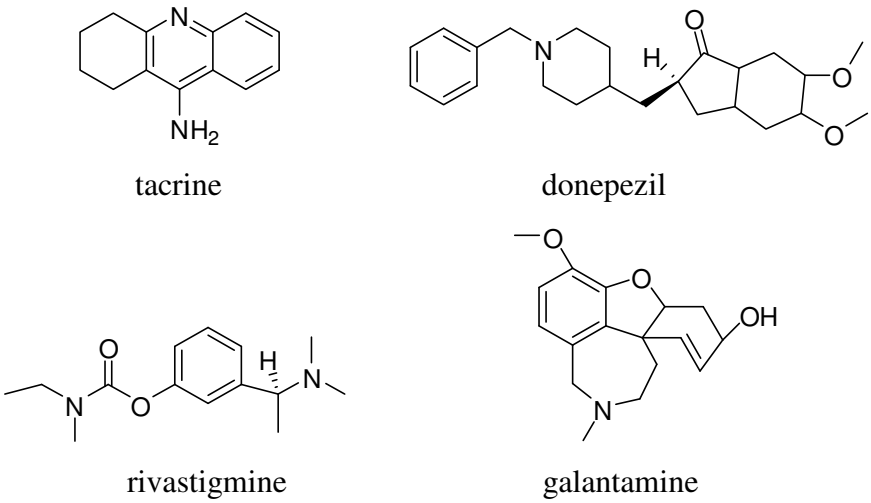

Figure 1.9 Chemical structures of AD drugs.

1.4 The Objectives of this Research

M. charantia extract showed high inhibition towards BChE and no reports have been investigated for anti-cholinesterase activity of this plant. Thus, the objectives of this study were

1.4.1 To extract and isolate the chemical constituents from the fruits of *M. charantia.*

1.4.2 To elucidate the chemical structures of isolated substances from the fruits of *M. charantia.*

1.4.3 To evaluate the acetylcholinesterase (AChE) and butyrylcholinesterase (BChE) inhibitory activities of isolated substances from the fruits of *M. charantia.*

CHAPTER II

EXPERIMENTAL

2.1 Plant Materials

The fruits of *M. charantia* collected from Phetchaburi Province of Thailand in January 2011 and indentified by Assoc. Prof. Nijsiri Ruangrungsi, Faculty of Pharmaceutical Sciences, Chulalongkorn University. A voucher of this plant material (No. NPRU 0003) has been deposited in the laboratory at Natural Products Research Unit, Department of Chemistry, Faculty of Science, Chulalongkorn University, Thailand.

2.2 Instruments and Equipments

The ^{1}H, ^{13}C, and 2D NMR spectra were recorded in chloroform-d_1 ($CDCl_3$), pyridene-d_5 (C_5D_5N) and acetone-d_6 (C_3D_6O) on a Varian model Mercury+ 400 and a Bruker Advance 400 NMR spectrometer (^{1}H 400 MHz; ^{13}C 100 MHz). The chemical shift (δ, ppm) was assigned with reference to the signal from the residual protons in deuterated solvent and using TMS as an internal standard in some cases. ESIMS and HRESIMS were recorded on a model VG TRIO 2000 MS and BrukermicrOTOF™-Q II mass spectrometer, respectively. Ultra Violet (UV) spectra were measured on a Shimadsu UV-160A photodiode array spectrophotometer. Optical rotations were carried out on a Jasco (P-1010) model polarimeter. Silica gel 60 (Merck), No. 7734 was used for open column chromatography and vacuum silica gel column chromatoghaphy (VCC). Silica gel 60 PF254 precoated on aluminium sheets (Merck Kieselgel) were used for thin layer chromatography (TLC). The spots on plate were detected under UV light at 254 nm and visualized by heating silica gel plates sprayed with anisaldehyde dipping reagent which were made with MeOH:anisaldehyde:conc.H_2SO_4 (95:3:3 (v/v) ratio). Column chromatography was carried out on Sephadex LH-20. A high performance liquid chromatography (HPLC) was performed by using ACE® 5 C18-AR column (150×4.6 mm). X-ray crystallographic analysis was performed on a Bruker APEX2 diffractometer by

Assoc. Prof. Thammarat Aree, Materials Chemistry and Catalysis Research Unit (MATCAT), Department of Chemistry, Faculty of Science, Chulalongkorn University. Crystal structures were solved by direct method SHELXS-97 and expanded using difference Fourier technique, refined by the program SHELXL-97.

2.3 Extraction Procedure of *M. charantia* Fruits

The air-dried fruits of *M. charantia* (2.5 kg) were extracted three times with MeOH and then it was concentrated *in vacuo* to give MeOH extract. This extract was further partitioned sequentially with *n*-hexane, dichloromethane (CH_2Cl_2) and saturated butanol (sat. BuOH), yielding *n*-hexane (18.8 g), CH_2Cl_2 (102.9 g) and BuOH (54.7 g) extracts. The extraction procedure is summarized as displayed in Scheme 2.1.

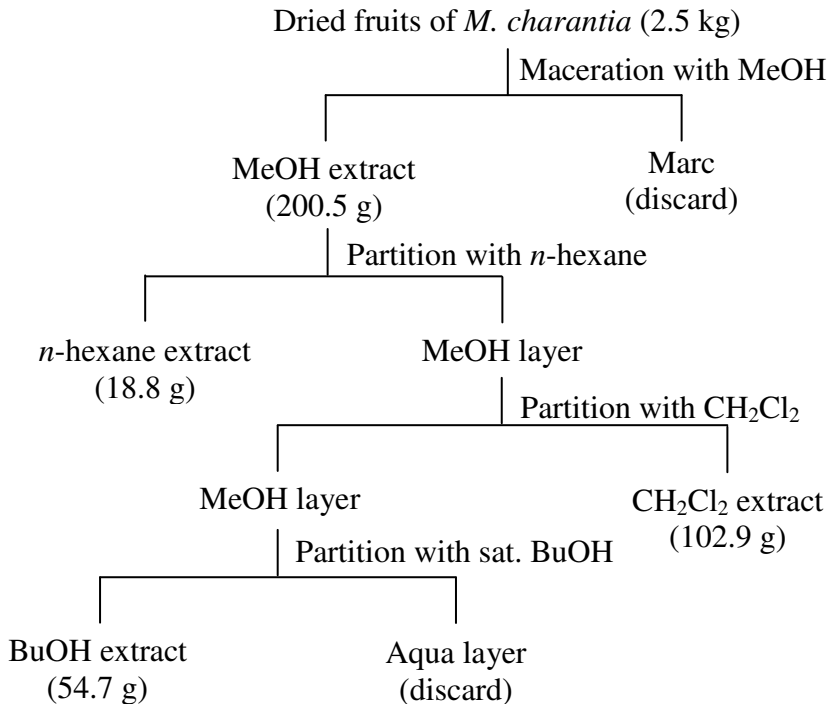

Scheme 2.1 Extraction procedure of *M. charantia* fruits.

Then, all four extracts were evaluated for preliminary anti-cholinesterase activities by microplate and TLC-autobiography assays.

2.4 Separation of Dichloromethane Extract from *M. charantia* Fruits

A portion of CH_2Cl_2 extract (83.9 g) was subjected to vacuum silica gel column chromatoghaphy (VCC) and eluted with a mixture of *n*-hexane:EtOAc and then EtOAc:MeOH by increasing polarity. Each fraction was combined monitoring by TLC analysis to give eight fractions (MD1 to MD8). Fraction MD2 was repeatedly separated on silica gel column, using a stepwise gradient of *n*-hexane-EtOAc and then EtOAc-MeOH to give six sub-fractions (MD2-1 to MD2-6). Recrystallization of fraction MD2-1 using the binary system of CH_2Cl_2 and MeOH gave compound **1** (45.5 mg). Fraction MD2-3 was purified by silica gel column chromatography and eluted with a mixture of *n*-hexane and acetone (9:1) to yield compound **2** (35.4 mg) and mixture **3** (21.7 mg). By the same way, compound **2** (60.8 mg) and mixture **4** (145.3 mg) were successively obtained from fraction MD2-4. The isolation diagram of fraction MD2 is presented in Scheme 2.2.

Fraction MD3 was fractionated on a silica gel column eluting with an increasingly polar mobile phase, in terms of *n*-hexane:EtOAc followed by EtOAc:MeOH to afford eight sub-fractions (MD3-1 to MD3-8). Afterwards, fraction MD3-1 was separated on a Sephadex LH-20 column using 50% of $CHCl_3$ in MeOH as eluent and then recrystallized using MeOH to furnish mixture **3** (10.0 mg). Fraction MD3-2 was purified on a Sephadex LH-20 column using $CHCl_3$:MeOH (1:1 (v/v) ratio) as eluent to furnish three fractions (MD3-2-1 to MD3-2-3). Fraction MD3-2-2 was then applied to a silica gel column eluting with a gradient system of CH_2Cl_2-acetone and recrytallization using MeOH to obtain mixture **4** (18.5 mg). Moreover, compound **5** (15.2 mg) was obtained from purification of MD3-3-3 on a Sephadex LH-20 column eluting with 50% of $CHCl_3$ in MeOH and recrytallization by MeOH. The separation diagram of fraction MD3 is described in Scheme 2.3.

Fraction MD4 was submitted to separate over a silica gel column and eluted with a stepwise system of *n*-hexane in EtOAc, EtOAc and MeOH in EtOAc, respectively, to afford eight sub-fractions (MD4-1 to MD4-8). The precipitated white solid from fraction MD4-5 was filtrated and purified by a silica gel column with a mixture of *n*-hexane:CH_2Cl_2 (3:3) and *n*-hexane:CH_2Cl_2:MeOH (3:6:1), respectively, as eluent to give mixture **6** (185.8 mg). Additionally, fraction MD4-7 was separated over a Sephadex LH-20 column using 50% of $CHCl_3$ in MeOH as eluent to provide

two fractions, MD4-7-1 and MD4-7-2. Fraction MD4-7-2 was further rechromatographed over silica gel eluting with a *n*-hexane-acetone gradient system and purified by recrystallization using MeOH to furnish compound **7** (42.7 mg). The separation procedure of fraction MD4 is exhibited in Scheme 2.4.

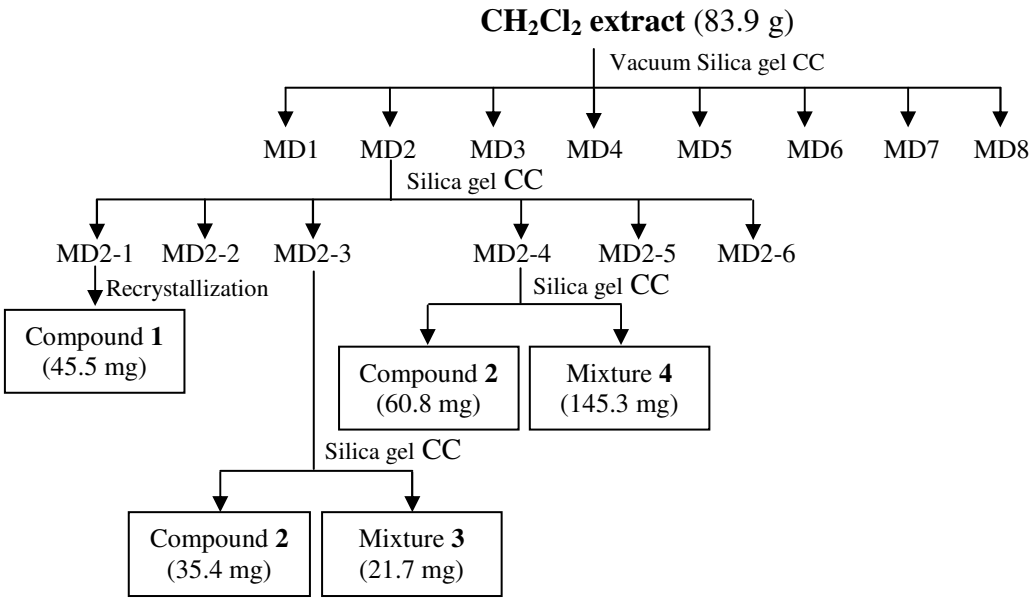

Scheme 2.2 Separation diagram of fraction MD2 from *M. charantia* fruits.

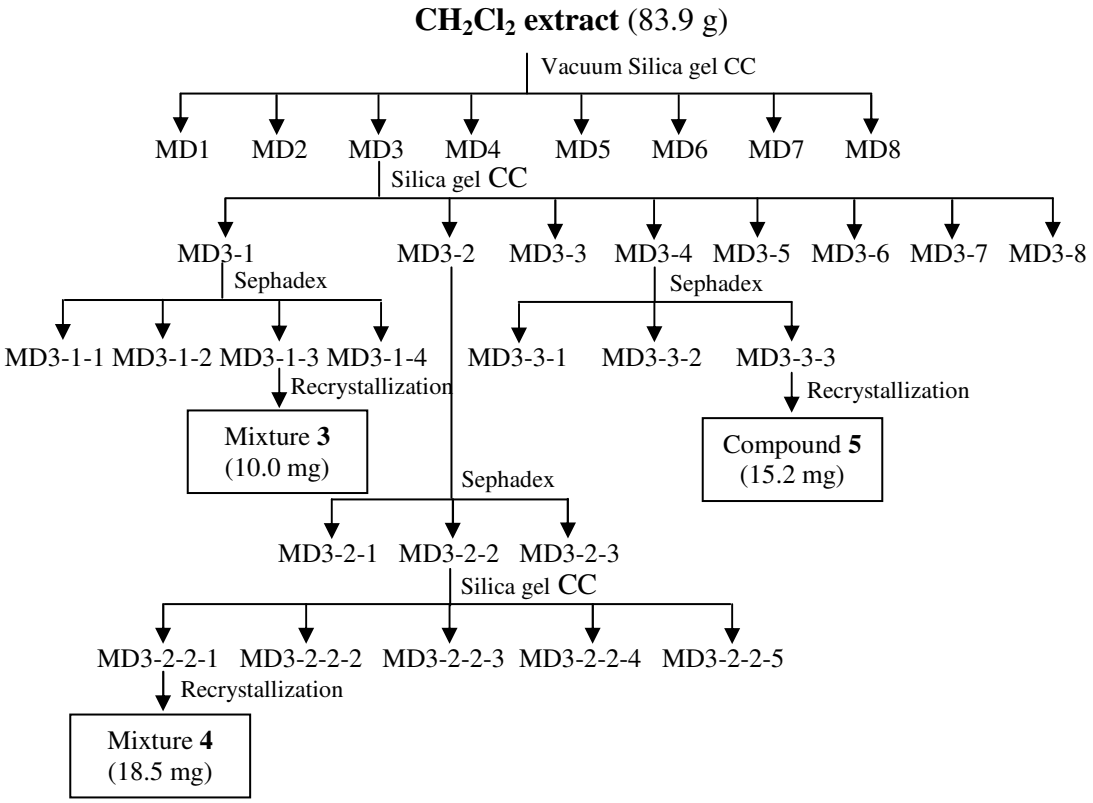

Scheme 2.3 Separation diagram of fraction MD3 from *M. charantia* fruits.

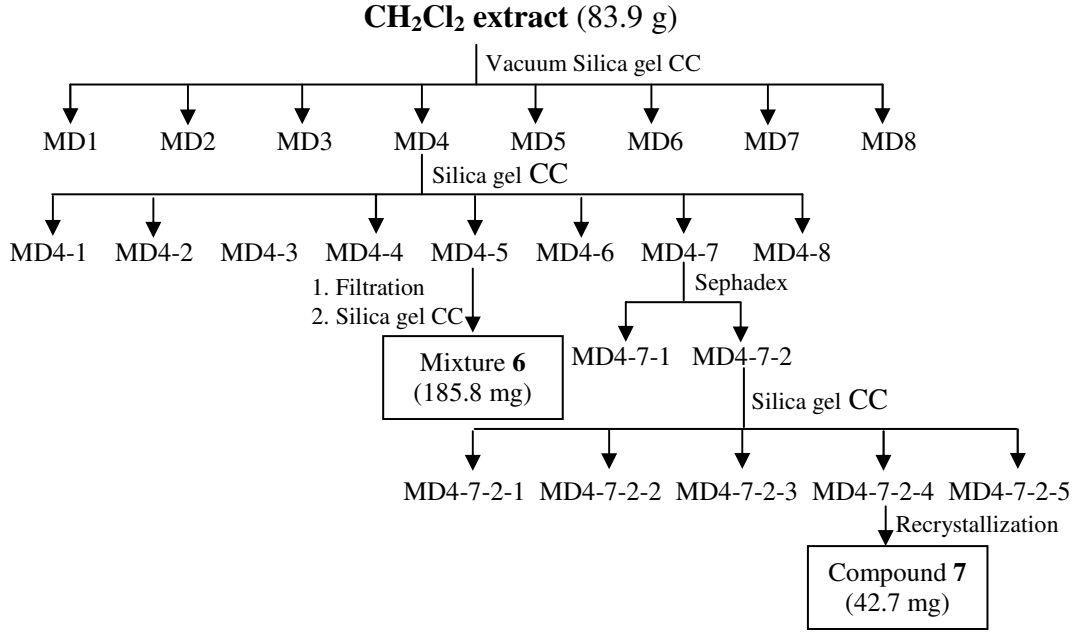

Scheme 2.4 Separation diagram of fraction MD4 from *M. charantia* fruits.

The structures of all isolated substances were established by spectroscopy techniques (^{1}H, ^{13}C NMR and MS spectroscopy) and compared the data with those from literature reviews. In addition, all isolated substances were evaluated their anti-cholinesterase activities.

2.5 Cholinesterase Inhibitory Assay

The cholinesterase inhibitions towards acetylcholinesterase (AChE) and butyrylcholinesterase (BChE) were evaluated by TLC bioautography and microplate methods (Ellman *et al*., 1961). The principle of assay was the hydrolysis of substrate acetylthiocholine (ATCI) by cholinesterase and give thiocholine and acetate as products. Then, thiocholine reacted with 5,5′-dithiobis(2-nitrobenzoic acid) (DTNB) to yield yellow product of 5-thio-2-nitrobenzoate. This reaction is shown in the Scheme 2.5. So if natural product compounds or synthetic molecules are able to decrease enzyme activity or preclude the reaction between substrate molecules and enzymes, the amount of yellow products are no happening.

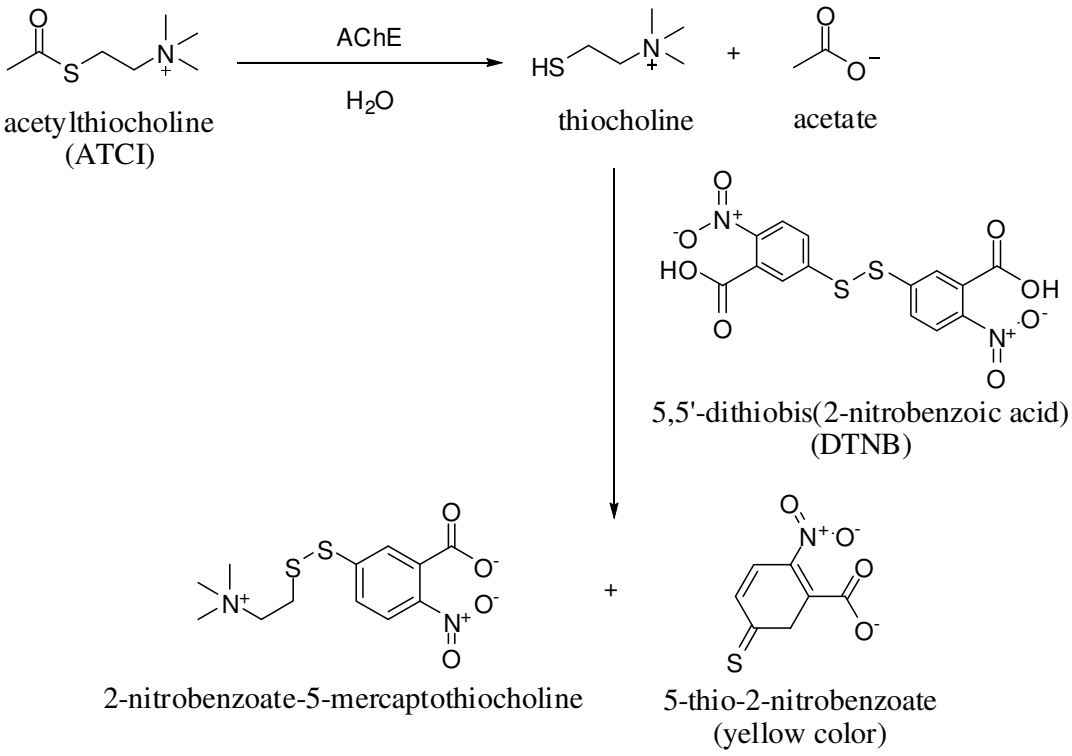

Scheme 2.5 Cholinesterase catalyzed hydrolysis of acetylthiocholine.

2.5.1 Chemical Reagents

Acetylthiocholine iodide (ATCI), butyrylthiocholine iodide (BTCI), DTNB, AChE from electric eels (Type-VI-S lypophilized powder, EC 3.1.1.7), BChE from horse serum (lypophilized powder, EC 3.1.1.8) and eserine (standard compound) were purchased from Sigma-Aldrich Co.Ltd. (St. Louis, MO, USA). Albumin from bovine serum (BSA) and *Tris*-(hydroxymethyl)-aminomethane (*Tris*-HCl) was purchased from Fluka chemical company and from Merck (Darmstadt, Germany), respectively.

2.5.2 Chemical Preparation (Rhee *et al*., 2001)

Buffers The following buffers were used;

Buffer A : 50 mM *Tris*–HCl, pH 8.

Buffer B : 50 mM *Tris*–HCl, pH 8 containing 0.1% bovine serum albumin (BSA).

Buffer C : 50 mM *Tris*–HCl, pH 8 containing 1 M sodium chloride (NaCl) and 0.2 mM magnesium chloride hexahydrate ($MgCl_2.6H_2O$).

Enzymes : cholinesterase enzymes (AChE and BChE) were dissolved in buffer A to prepare the 113 U/mL of stock solution for both the TLC-autobiography and microplate assays. These further diluted with buffer A and B to get 3 U/mL and 1 U/mL enzymes for the TLC-autobiography and microplate assays, respectively.

Substrates : Both ATCI and BTCI were dissolved in buffer A and Milli Q water to prepare 5 mM and 1.5 mM substrate for the TLC-autobiography and microplate assays, respectively.

Ellman reagent : 5 mM and 3 mM of DTNB in buffer A and C was used for the TLC-autobiography and microplate assays, respectively.

2.5.3 TLC-bioautographic Method

To assess the preliminary anti-cholinesterase activity of four extracts from *M. charantia* fruits, the TLC-autobiography assay was carried out. Each tested extract was dissolved in methanol to prepare a concentration of 10 mg/mL. Ten microliters of each tested extract were spotted on a silica gel TLC plate and the plate was further developed in *n*-hexane:EtOAc (1:1). After the TLC plate dried at room

temperature for 3 hours, was sprayed with a reagent of substrate (ATCI or BTCI) and DTNB mixture (1:1). It was permitted to dry for 5 min and then sprayed with an enzyme (AChE or BChE). After the incubated plate, white spots on a yellow background exhibited cholinesterase inhibition. These were observed and noted within 15 min (Salah and Jäger, 2005).

2.5.4 Microplate Method

All of extracts and isolated substances from *M. charantia* fruits were evaluated for their anti-cholinesterase effects by the modifying microplate assay (Ingkaninan *et al*., 2003). The concentrations of extracts for testing were 10 mg/mL, while three concentrations of each isolated substance and standard compound, eserine, were prepared as 5, 1 and 0.5 mg/mL. All samples were dissolved in MeOH. The activities of these samples were evaluated by using 96-wells plate. Briefly, 50 µL of buffer A, 25 µL of substrate (ATCI or BTCI), 25 µL of sample, 125 µL of DTNB, were added in the 96-well plates followed by 25 µL of enzyme (AChE or BChE). Then, the solutions were immediately measured at absorbance 415 nm every 5 s over 2 min period by Sunrise™ microplate reader (P-Intertrade Equipments, Australia). The resulting velocities were measured. Enzyme activity was determined from the percentage of velocities compared with blank without any inhibitor (25 µL of methanol instead of the sample). The percentage of enzyme inhibition was calculated according to the equation shown below.

$$\% \text{ inhibition} = \left(\frac{v_{blank} - v_{sample}}{v_{blank}} \right) \times 100$$

The v_{blank} is the velocity of reaction of blank without any inhibitors and v_{sample} is the velocity of reaction of sample.

If the activities of inhibitors showed higher than 50% cholinesterase inhibition at a concentration of 1 mg/mL, they were further determined for their IC_{50} values. The IC_{50} value was defined as the concentration of sample inhibited the 50% of the maximum observed enzymatic activity and graphically determined from a plot of percentage inhibition versus a log final concentration value using the Graph Pad Prism 5.01 software (Graph Pad Software Inc.) as displayed in Figure 2.1. In order to obtain the sigmoidal curve of enzyme inhibition, ten different concentrations of

inhibitors were measured. Eserine was used as positive control and this experiment was analyzed in duplicated.

Kinetic experiments were further performed using three inhibitor concentrations; 0, 30 and 60 μM. The activities of BChE were measured at six different substrate (BTCI) concentrations; 0.2, 0.5, 0.7, 1, 2, and 3 mM, in the absence (control) and presence of the inhibitor concentration. The Lineweaver–Burk graphs were plotted using the Graph-Pad Prism 5.01 software.

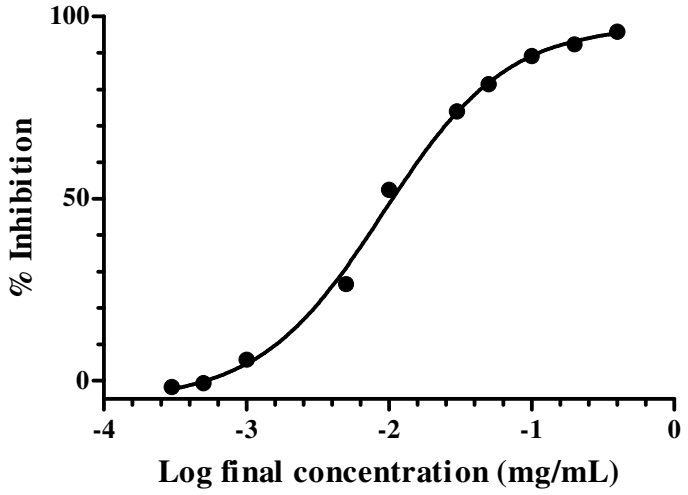

Figure 2.1 A plot of percentage inhibition of sample versus a log final concentration value.

CHEPTER III

RESULTS AND DISCUSSION

3.1 Preliminary Anti-cholinesterase Screening Test of *M. charantia* Extracts

The fruits of *M. charantia* were extracted with MeOH and then partitioned with *n*-hexane, CH_2Cl_2 and saturated BuOH, respectively, which represented in Scheme 2.1 of Chapter II. All extracts, MeOH, *n*-hexane, CH_2Cl_2 and BuOH extracts, were further examined for their cholinesterase inhibitory activities using both TLC-bioautographic and microplate methods. The results of microplate and TLC autobiography tests are presented in Table 3.1 and Figure 3.1, respectively.

Table 3.1 The anti-cholinesterase activities of extracts from *M. charantia* fruits by microplate assay.

Extract	% Inhibition*	
	AChE	BChE
MeOH	38.7	67.7
n-hexane	38.7	50.1
CH_2Cl_2	39.7	82.1
BuOH	6.8	59.1
eserine**	97.0	98.8

*At a final concentration of 1.0 mg/mL.

**Positive control.

a) AChE

b) BChE

1 : MeOH extract
2: BuOH extract
3: CH_2Cl_2 extract
4: *n*-hexane extract
Std: eserine

Figure 3.1 The anti-cholinesterase activities of extracts from *M. charantia* fruits by TLC-bioautographic assay (solvent system for TLC was *n*-hexane:EtOAc = 1:1).

According to Figure 3.1, MeOH extract showed many inhibition spots. However, this extract was then fractionated to obtain *n*-hexane, CH_2Cl_2 and BuOH extracts. Many inhibition spots were clearly found in *n*-hexane and CH_2Cl_2 extracts, and less in BuOH extract. In addition, the results of microplate assay (Table 3.1) indicated that CH_2Cl_2 extract exhibited the highest inhibition towards BChE. Therefore, the CH_2Cl_2 extract was further investigated to the active chemical constituents.

3.2 Elucidation Chemical Structure of Isolated Substances from *M. charantia* Fruits

According to the separation of CH_2Cl_2 extract of *M. charantia* fruits described in Scheme 2.2-2.4 of Chapter II, four compounds (**1**, **2**, **5** and **7**) and three inseparable mixtures (**3**, **4** and **6**) were obtained. Their chemical structures were identified based on spectroscopic data and compared with those of literature values. These isolated compounds could be divided into four main classes, based on NMR data, which were cucurbitane triterpenoids (**1**, **2**, **3** and **4**), lignan (**5**), steroid glycoside (**6**) and cucurbitane glycoside (**7**).

3.2.1 Structural Elucidation of Compounds 1-4

Triterpenoids are a class of natural compounds derived from six isoprene units to have a C30 skeleton. The triterpenes are subdivided into many groups, depending on their structures. The most predominant triterpenes in Cucurbitaceae family and also *M. charantia* are cucurbitane-type triterpenoids. This type is a highly oxygenated, tetracyclic triterpene as 19-(10→9*β*)-abeo-10*α*-lanostane (Figure 3.2) (Rahman, 2005).

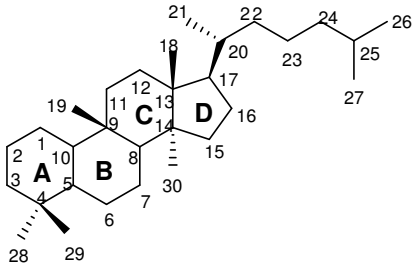

Figure 3.2 The cucurbitane-type triterpene skeleton.

3.2.1.1 Compound 1

Compound **1** (45.5 mg) was obtained as fine needles. It was determined to be $C_{31}H_{48}O_3$ by the positive ion at m/z 491.59 $[M+Na]^+$ in the ESI-MS technique (Figure A-3). Thus, the molecular weight of compound **1** was 468 g/mol. This compound had an optical rotation of $[\alpha]_D^{25}$ -154.8 (*c* 0.10 in acetone).

The ^{13}C NMR spectrum of **1** (Figure A-2) displayed the presence of 31 carbon signals of six methyls (δ_C 14.7, 18.7, 18.8, 19.8, 20.5, and 24.1), six olefinics (δ_C 114.1, 129.3, 131.0, 132.8, 134.2 and 142.2), two oxymethines (δ_C 76.2 and 112.1), one methoxyl (δ_C 58.2), seven methylenes (δ_C 17.4, 23.2, 27.2 28.1, 30.6, 33.5 and 39.8), four methines (δ_C 18.8, 40.5, 41.7 and 50.3) and five quaternary carbons (37.3, 45.1, 48.0, 48.3 and 86.8). The ^1H NMR spectrum (Figure A-1) revealed the typical signals for six tertiary methyls [δ_H 0.85 (Me×2), 0.87, 0.89, 1.22 and 1.83], one oxymethine proton (δ_H 3.41), one methoxyl proton (δ_H 3.44), one acetal group (δ_H 4.65) and five olefenic protons (δ_H 4.86, 5.99, 5.63, 5.64 and 6.12). The olefinic protons at δ_H 5.63 (*J* = 2.8, 9.2 Hz) and 5.63 (*J* = 2.8, 9.2 Hz) were

assigned as a *cis*-oriented double bond, whereas those of δ_H 5.64 (J = 15.2 Hz) and 6.12 (J = 15.6 Hz) were ascribed as a *trans*-oriented double bond. Further, comparison of ^{1}H and ^{13}C NMR data of compound **1** with those of cucurbitanes reported in the literature**,** compound **1** was identified as (19*R*,23*E*)-5*β*,19-epoxy-19-methoxycucurbita-6,23,25-trien-3*β*-ol (Figure 3.3) which was previously isolated from the fruit of Japanese bitter gourd (Kimura *et al*., 2005). The NMR data are shown in Table 3.2.

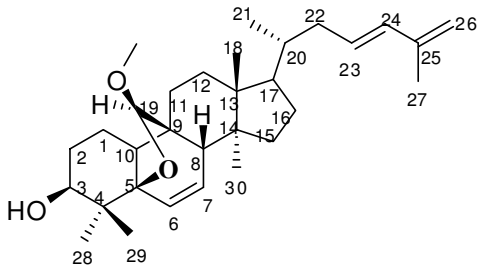

Figure 3.3 The chemical structure of compound **1**.

Table 3.2 The ^{1}H and ^{13}C NMR data of compound **1** compared with those of (19*R*,23*E*)-5*β*,19-epoxy-19-methoxycucurbita-6,23,25-trien-3*β*-ol (Kimura *et al*., 2005).

Position	**Compound 1** ($CDCl_3$)		**(19*R*,23*E*)-5*β*,19-epoxy-19-methoxycucurbita-6,23,25-trien-3*β*-ol** (Pyridine-d_5)	
	δ_C	δ_H (int., mult., *J* in Hz)	δ_C	δ_H (int., mult., *J* in Hz)
1	17.4	1.49 (1H, *m*), 1.54 (1H, *m*)	17.4	1.49 m (1H, *m*), 1.53 (1H, *m*)
2	27.2	1.76 (2H, *m*)	27.2	1.78 (2H, *m*)
3	76.2	3.41 (1H, *br s*)	76.2	3.41 (1H, *br d*, 6.9)
4	37.3		37.3	
5	86.8		86.8	
6	131.0	5.99 (1H, *dd*, 1.6, 9.6)	131.0	5.99 (1H, *dd*, 2.0, 9.8)
7	132.8	5.63 (1H, *dd*, 2.8, 9.2)	132.8	5.65 (1H, *dd*, 3.2, 9.8)
8	41.7	2.89 (1H, *br s*)	41.7	2.89 (1H, *dd*, 3.2, 3.2)
9	48.0		48.0	
10	40.5	2.40 (1H, *t,* 8.4)	40.5	2.41 (1H, *dd*, 7.6, 10.7)
11	23.2	1.75 (1H, *m*), 1.79 (1H, *m*)	23.2	1.60 (1H, *m*), 1.76 (1H, *m*)
12	30.6	1.63 (2H, *m*)	30.6	1.62 (2H, *m*)
13	45.1		45.1	
14	48.3		48.3	
15	33.5	1.33 (1H, *m*), 1.39 (1H, *m*)	33.5	1.34 (1H, *m*), 1.40 (1H, *m*)
16	28.1	1.42 (1H, *m*), 1.97 (1H, *m*)	28.1	1.39 (1H, *m*), 1.97 (1H, *m*)
17	50.3	1.47 (1H, *m*)	50.3	1.46 (1H, *m*)
18	14.7	0.87 (3H, *s*)	14.7	0.88 (3H, *s*)
19	112.1	4.65 (1H, *s*)	112.1	4.65 (1H, *s*)
20	36.6	1.57 (1H, *m*)	36.6	1.55 (1H, *m*)
21	18.8	0.89 (3H, *d*, 6.4)	18.8	0.91 (3H, *d*, 6.3)
22	39.8	1.83 (1H, *m*), 2.26 (1H, *m*)	39.8	1.81 (1H, *m*), 2.26 (1H, *m*)
23	129.3	5.64 (1H, *br d*, 15.2)	129.3	5.61 (1H, *br d*, 15.6)
24	134.2	6.12 (1H, *d*, 15.6)	134.2	6.12 (1H, *d*, 15.6)
25	142.2		142.2	
26	114.1	4.86 (2H, *s*)	114.1	4.86 (2H, *s*)
27	18.7	1.83 (3H, *s*)	18.7	1.84 (3H, *s*)
28	24.1	0.85 (3H, *s*)	24.1	0.85 (3H, *s*)
29	20.5	1.22 (3H, *s*)	20.5	1.22 (3H, *s*)
30	19.8	0.85 (3H, *s*)	19.8	0.86 (3H, *s*)
25-OMe	58.2	3.44 (3H, *s*)	58.2	3.44 (3H, *s*)

3.2.1.2 Compound 2

Compound **2** (96.2 mg) was isolated as colorless prism crystals with the molecular formula $C_{30}H_{48}O_3$. This compound had an optical rotation of $[\alpha]_D^{25}$ -97.5 (*c* 0.3 in $CHCl_3$).

Based on the ^1H, ^{13}C NMR and HSQC spectra of **2** (Figures A-4 to A-6), its signals was similar to those of compound **1** except for the absence of a terminal double bond and a methoxyl signals in compound **2**. Moreover, two methyl group signals at δ_H 1.31 (δ_C 30.0 and 29.9) of compound **2** showed a correlation to an oxygenated carbon at δ_C 70.7 in a HMBC spectrum (Figure A-7). These signals were assigned for C-26, C-27 and C-25, respectively. The downfield chemical shift of methine carbon (δ_C 112.1 and δ_H 4.65) of compound **1** was not found in compound **2** but a methylene signal at δ_C 79.9 (δ_H 3.51 and 3.66) appeared and showed a cross-peak with a quarternary carbon at δ_C 87.5 (C-5). Further comparison of ^1H and ^{13}C NMR data of compound **2** with those of cucurbitanes reported in the literature**,** compound **2** was identified as (23*E*)-5*β*,19-epoxycucurbita-6,23-diene-3*β*,25-diol (Figure 3.4) which was previously isolated from the stems of Chinese bitter gourd by Chang *et al*. (2006). The NMR data are shown in Table 3.3. The COSY correlations (Figure A-8) of olefinic protons (δ_H 5.63 and 6.03) with H-8 (δ_H 5.63) confirmed the presence of the double bond at C-6 and C-7 as shown in Figure 3.5.

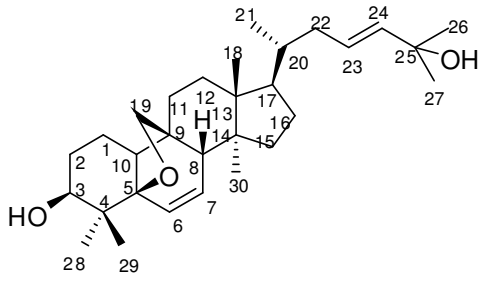

Figure 3.4 The chemical structure of compound **2**.

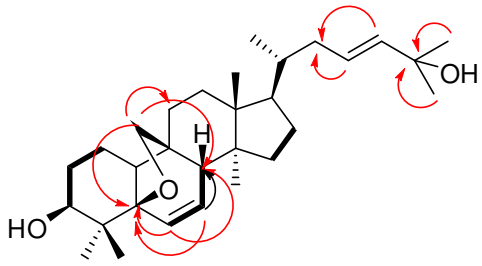

Figure 3.5 The selected HMBC (H→C) and COSY (bold lines) correlations of compound **2**.

Table 3.3 The ^{1}H and ^{13}C NMR data of compound **2** compared with those of (23*E*)-5*β*,19-epoxycucurbita-6,23-diene-3*β*,25-diol (Chang *et al*., 2006).

Position	**Compound 2** ($CDCl_3$)		**(23*E*)-5*β*,19-epoxycucurbita-6,23-diene-3*β*,25-diol** ($CDCl_3$)	
	δ_C	δ_H (int., mult., *J* in Hz)	δ_C	δ_H (int., mult., *J* in Hz)
1	17.6	1.46 (2H, *m*)	17.6	1.45 (2H, *m*)
2	27.4	1.77 (2H, *m*)	27.3	1.82 (2H, *m*)
3	76.2	3.40 (1H, *br s*)	76.1	3.36 (1H, *m*)
4	37.2		37.2	
5	87.5		87.5	
6	131.8	6.03 (1H, *dd*, 1.6, 9.6)	131.9	6.02 (1H, *dd*, 1.6, 9.6)
7	131.5	5.63 (1H, *dd*, 3.6, 9.6)	131.5	5.61 (1H, *dd*, 3.6, 9.6)
8	52.0	2.33 (1H, *br s*)	52.0	2.32 (1H, *br s*)
9	45.3		45.4	
10	38.9	2.27 (2H, *dd*, 6.8, 11.2)	38.8	2.24 (2H, *dd*, 6.8, 11.2)
11	23.6	1.48 (1H, *m*), 1.72 (1H, *m*)	23.5	1.46 (1H, *m*), 1.80 (1H, *m*)
12	30.8	1.63 (2H, *m*)	30.8	1.64 (2H, *m*)
13	45.5		45.4	
14	48.6		48.8	
15	33.2	1.36 (2H, *m*)	33.1	1.35 (2H, *m*)
16	28.0	1.43 (1H, *m*), 1.95 (1H, *m*)	28.0	1.42 (1H, *m*), 2.00 (1H, *m*)
17	50.0	1.49 (1H, *m*)	50.0	1.48 (1H, *m*)
18	14.9	0.86 (3H, *s*)	14.9	0.84 (3H, *s*)
19	79.9	3.51 (1H, *d*, 8.4), 3.66 (1H, *d*, 8.4)	79.8	3.50 (1H, *d*, 8.4), 3.65 (1H, *d*, 8.4)
20	36.2	1.41 (1H, *m*)	36.1	1.45 (1H, *m*)
21	18.6	0.88 (3H, *d*, 6.8)	18.6	0.87 (3H, *d*, 6.6)
22	39.1	1.79 (1H, *m*), 2.16 (1H, *m*)	39.1	1.80 (1H, *m*), 2.14 (1H, *m*)
23	125.2	5.59 (1H, *m*)	125.1	5.57 (1H, *m*)
24	139.6	5.59 (1H, *m*)	139.6	5.57 (1H, *m*)
25	70.7		71.0	
26	30.0	1.31 (3H, *s*)	29.9	1.29 (3H, *s*)
27	29.9	1.31 (3H, *s*)	29.8	1.29 (3H, *s*)
28	20.5	1.19 (3H, *s*)	20.5	1.18 (3H, *s*)
29	24.6	0.89 (3H, *s*)	24.5	0.87 (3H, *s*)
30	20.0	0.86 (3H, *s*)	20.0	0.84 (3H, *s*)
3-OH		4.01 (1H, *br s*)		3.98 (1H, *d*, 9.6)

3.2.1.3 Mixtures 3-4

Mixture **3** (31.7 mg), obtained as colorless prism crystals, had the molecular formula of $C_{30}H_{46}O_3$ based on positive ESI-Qq-TOFMS method (Figure A-15). Their HRESIMS spectra showed the $[M+Na]^+$ ion peak at m/z 477.3225 (calculated for $C_{30}H_{46}O_3Na$, 477.3447). Thus, the molecular weight of this mixture **3** was 454 g/mol. The UV spectrum presented an absorption maximum at 229 nm in MeOH.

Mixture **4** (163.8 mg) was isolated as white fine needles. Its empirical molecular formula of $C_{31}H_{50}O_4$ was determined to be $C_{31}H_{50}O_4$ establish by the HRESIMS at m/z 509.3421 $[M+Na]^+$ (calculated for $C_{31}H_{50}O_4Na$, 509.3709) (Figure A-23). Thus, its molecular weight was 486 g/mol. The UV absorptions at λ_{max} was 202 nm in MeOH.

Mixture **3** showed single spot on TLC analysis (a solvent system of *n*-hexane:acetone = 8:2). Mixture **3** was analyzed by ^1H and ^{13}C-NMR spectroscopic method as shown in Figures A-9 and A-10, respectively. Those spectra clearly showed a mixture of cucurbitanes. However, the HPLC analysis (Figure A-16) of this mixture showed two separated peaks with the peak areas of nearly 2:1 ratio (63%:37%). A major separated fraction was then analyzed by ^1H, ^{13}C NMR and HPLC methods. Interestingly, the analysis results revealed the same as before separation. However, mixture **3** could be re-crystallized and determined by X-ray crystallographic analysis. The ORTEP result (Figure 3.8) indicated that this mixture composed of two diastereomers with the occupancy of 64% and 36% for compound **3a** and compound **3b**, respectively. Both compounds differed only in the way that substituents oriented in space at C-19. The configuration of chiral C-19 of compound **3a** (δ_C 105.4) was *S*-epimer and that of compound **3b** (δ_C 107.5) was *R*-epimer. The isomer mixture of cucurbitanes like the mixture **3** was previously reported by Chen *et al*. (2009). They obtained the mixture of 5*β*,19-epoxycucurbita-6,23-diene-3*β*,19,25-triol and kuguacin R which were diastereomers at C-19 the same as the mixture **3** of this study. Thus, the mixture **3** was identified as the mixture of 5*β*,19-epoxycucurbita-6,23(*E*),25(26)-triene-3*β*,19(*S*)-diol (**3a**) and 5*β*,19-epoxycucurbita-6,23(*E*),25(26)-triene-3*β*,19(*R*)-diol or charantadiol A (**3b**). The latter was previously found by Zhang *et al*. in 2009 (could not access the spectroscopic data from that publication) while compound **3a**, a major component, was a new compound. In addition, the position

assignments of compounds **3a** and **3b** were confirmed by 2D NMR techniques (HSQC, HMBC, COSY and NOESY). Those spectra are shown in Figures A-11 to A-14 and conclusions are shown in Figure 3.7.

The same results were found in a mixture **4**. This mixture could not be purified by HPLC technique (Figure A-24). This mixture showed also two separated peaks with the peak areas of nearly 2:1 ratio (63%:37%). The 1D and 2D NMR spectra of the mixture **4** are shown in Figures A-17 to A-22. However, the NMR data of minor component ($\delta_{C\text{-}19}$ 107.5) in the mixture **4** were in agreement with those of 5*β*,19-epoxy-25-methoxy-cucurbita-6,23-diene-3*β*,19(*R*)-diol (**4b**) (Mulholland *et al*., 1997; Chang *et al*., 2011). Thus, another ($\delta_{C\text{-}19}$ 105.4) was 5*β*,19-epoxy-25-methoxy-cucurbita-6,23-diene-3*β*,19(*S*)-diol (**4a**) which was a new compound. The NMR data of each component in the mixtures **3** and **4** are shown in Tables 3.4 and 3.5, respectively.

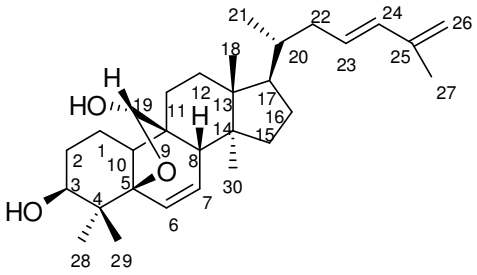

Compound **3a**

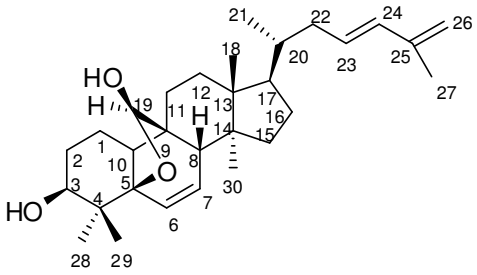

Compound **3b**

Figure 3.6 The chemical structure of mixture **3**.

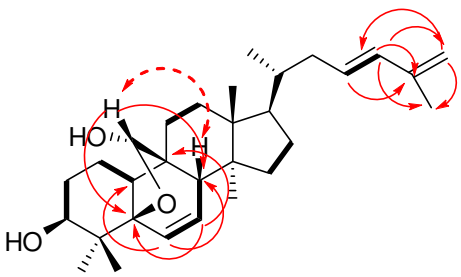

Compound **3a**

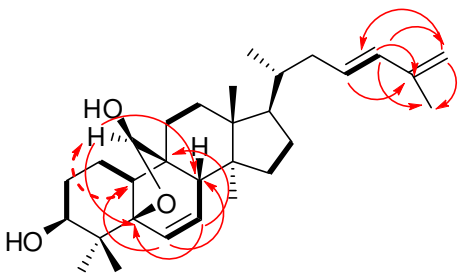

Compound **3b**

Figure 3.7 The selected HMBC (H→C), COSY (bold lines) and NOSEY (H↔H) correlations of mixture **3**.

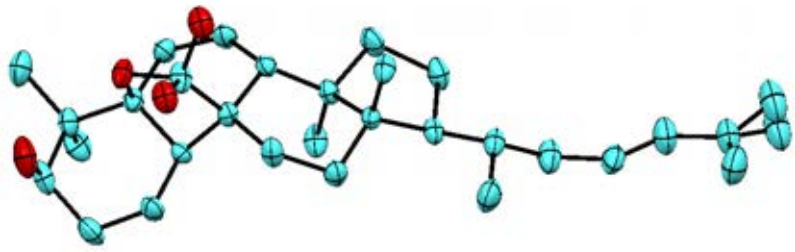

Figure 3.8 The ORTEP structure of mixture **3**.

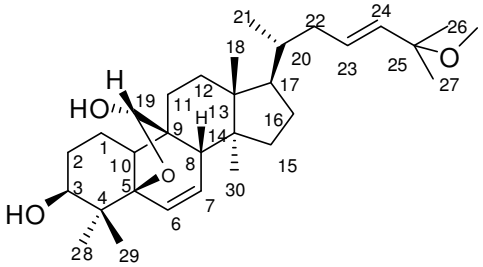

Compound **4a**

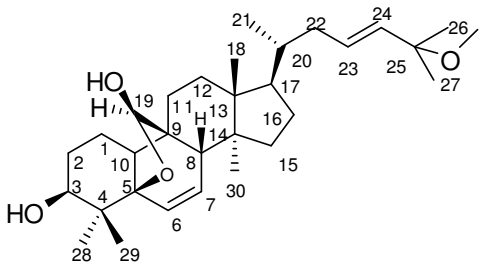

Compound **4b**

Figure 3.9 The chemical structure of mixture **4**.

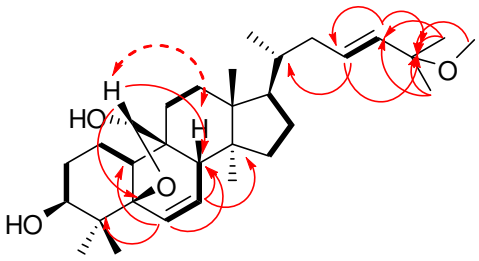

Compound **4a**

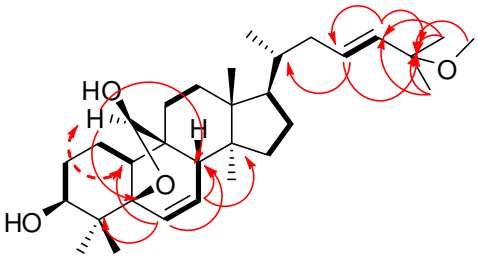

Compound **4b**

Figure 3.10 The selected HMBC (H→C), COSY (bold lines) and correlations and NOSEY (H↔H) of mixture **4**.

Table 3.4 The ^{1}H and ^{13}C NMR data of mixture **3**.

Position	**Mixture 3** ($CDCl_3$)		
	δ_C	**δ_H** (int., mult., *J* in Hz)	**HMBC**
1	17.3 [17.0]	1.50 (2H, *m*)	
2	23.1 [21.6]	1.69 (1H, *m*), 1.74 (1H, *m*)	
3	76.1 [76.3]	3.41 (1H, *br s*)	
4	37.2 [38.0]		
5	86.6		
6	132.7 [133.0]	6.09 (1H, *dd,* 2.0, 10.4)	C-8, C-10
7	132.4 [130.4]	5.67 (1H, *dd*, 3.6, 9.6) [5.52 (1H, *dd*, 3.6, 9.6)]	C-5, C-8, C-9
8	41.4	2.84 (1H, *br s*)	C-6, C-19
9	48.6 [49.7]		
10	40.6	2.47 (1H, *t*, 8.8) [2.32 (1H, *t*, 8.8)]	
11	30.5 [30.4]	1.63 (2H, *m*)	
12	39.8	1.80 (1H, *m*), 2.26 (1H, *m*)	
13	45.2		
14	48.1		
15	33.6 [33.5]	1.36 (2H, *m*)	
16	28.1 [27.9]	1.39 (1H, *m*), 1.98 (1H, *m*)	
17	50.3 [50.4]	1.46 (1H, *m*)	
18	14.7 [15.0]	0.89 (3H, *s*)	C-12, C-14
19	105.4 [107.5]	5.13 (1H, *s*) [4.88 (1H, *s*)]	C-5, C-8
20	36.6	1.54 (1H, *m*)	
21	18.8	0.90 (3H, *d*, 6.4)	
22	27.2	1.77 (2H, *m*)	
23	129.2	5.61 (1H, *dd*, 8.4, 15.6)	C-25
24	134.2	6.12 (1H, *d*, 16.4)	C-25, C-26, C-27
25	142.2		
26	114.1	4.86 (2H, *s*)	C-24, C-27
27	18.7	1.83 (3H, *s*)	C-24, C-25, C-26
28	24.0 [24.4]	0.85 (3H, *s*)	C-3, C-4, C-5, C-29
29	20.5 [20.6]	1.21 (3H, *s*)	C-3, C-4, C-5, C-28
30	19.7 [20.0]	0.88 (3H, *s*)	C-8, C-13

[...] = Values of minor component.

Table 3.5 The ^{1}H and ^{13}C NMR data of mixture **4**.

Position	**Mixture 4** ($CDCl_3$)		
	δ_C	δ_H (int., mult., *J* in Hz)	**HMBC**
1	17.3 [17.0]	1.50 (2H, *m*)	
2	23.1 [21.6]	1.63 (1H, *m*), 1.74 (1H, *m*),	
3	76.1 [76.3]	3.40 (1H, *br s*)	C-1, C-4, C-5
4	37.2		
5	86.6		
6	132.8 [133.0]	6.08 (1H, *d,* 10.0)	C-4, C-5, C-8, C-10
7	132.4 [130.4]	5.66 (1H, *dd*, 3.2, 9.6) [5.33 (1H, *dd*, 3.2, 8.4)]	C-8, C-14,
8	41.4 [	2.84 (1H, *br s*)	C-6, C-9
9	48.1 [48.6]		
10	40.6 [38.0]	2.46 (1H, *t*, 8.8) [2.30 (1H, *m*)]	C-1, C-8, C-9, C-19
11	30.5	1.61 (2H, *m*)	
12	39.4	1.82 (1H, *m*), 2.17 (1H, *m*)	
13	45.1		
14	48.6 [49.7]		
15	33.6 [33.5]	1.33 (2H, *m*)	
16	27.9 [27.8]	1.38 (1H, *m*), 1.96 (1H, *m*)	
17	50.0 [50.1]	1.48 (1H, *m*), 2.21 (1H, *m*)	C-14, C-21
18	14.7 [15.0]	0.88 (3H, *s*)	C-13, C-14
19	105.4 [107.5]	5.13 (1H, *s*) [4.87 (1H, *s*)]	C-5, C-8
20	36.1	1.54 (1H, *m*)	
21	18.7	0.90 (3H, *d*, 8.0)	C-17, C-20
22	27.2	1.77 (2H, *m*)	C-20, C-21, C-23, C-24
23	128.3	5.50 (1H, *m*)	C-20, C-24, C-25
24	136.9	5.40 (1H, *d*, 15.6)	C-23, C-25, C-26, C-27
25	74.9		
26	25.8	1.25 (3H, *s*)	C-24, C-25, C-27
27	26.1	1.25 (3H, *s*)	C-24, C-25, C-26
28	20.4 [20.6]	1.21 (3H, *s*)	C-3, C-4, C-5, C-29
29	24.0 [24.4]	0.85 (3H, *s*)	C-3, C-4, C-5, C-28
30	19.7 [19.6]	0.86 (3H, *s*)	C-8, C-15
25-OMe	50.2	3.15 (3H, *s*)	C-25
3-OH		3.79 (1H, *s*)	C-3, C-4

[...] = Values of minor component.

3.2.2 Structural Elucidation of Compound 5

Compound **5** (15.2 mg) was obtained as colorless plates. Its molecular formula, $C_{18}H_{18}O_4$, was established by the $[M+Na]^+$ ion peak at m/z 321.0967 and the $[M-H]^-$ ion peak at m/z 297.1165 in the HRESIMS (Figure A-30 and A-31). Thus, the molecular weight of this compound was 298 g/mol. It had an optical rotation of $[\alpha]_D^{28}$ +5.2 (*c* 0.06 in MeOH). The UV of maximum absorption exhibited at 227 nm in MeOH.

The ^{13}C NMR and HSQC spectra (Figure A-26 and A-27) of compound **5** revealed the characteristic signals of aromatic (δ_C 116.0, 128.3, 133.6 and 157.7), an oxymethine (δ_C 86.5), an oxymetheylene (δ_C 72.1) and a methine (δ_C 55.2) carbons. The ^1H NMR data (Figure A-25) showed the resonances of di-substituted aromatic (δ_H 6.68 *(d, J* = 8.4 Hz) and 7.10 (*d*, *J* = 8.4 Hz), an oxymethine (δ_H 4.53), an oxymetheylene (δ_H 3.41), a methine (δ_H 2.93) protons. In the HMBC spectrum (Figure A-28), the highly deshielded protons at δ_H 8.20 correlated to carbon signals at δ_C 116.0 and 157.7 and di-subsubstituted aromatic protons at δ_H 6.68 and 7.10 correlated to carbon signal at δ_C 86.5. Moreover, HMBC correlations observed between δ_H 4.53 and δ_C 55.2 as well as between δ_H 2.93 and δ_C 72.1. This compound was re-crytallized and also determined their structure by X-ray crystallographic analysis. The ORTEP figure (Figure 3.13) indicated that this compound composed of two *para*-substituted benzene rings which joined by two oxolane rings with an 8-8' linkage. This structure was a lignan named ligballinol (Figure 3.11) which was previously isolated from *Vigna angularis* bean (Kobayashi and Ohta, 1983) and *Gynostemma pentaphyllum* roots (Wang *et al*., 2009). However, there was no report in isolation of this compound from *M. charantia*. Comparison of ^1H and ^{13}C NMR data of compound **5** are displayed in Table 3.6.

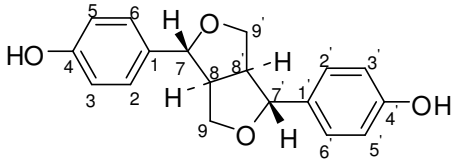

Figure 3.11 The chemical structure of compound **5**.

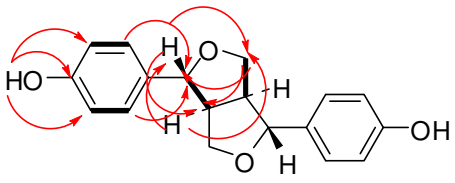

Figure 3.12 The selected HMBC (H→C) and COSY (bold lines) correlations of compound **5**.

Figure 3.13 The ORTEP diagram of compound **5**.

Table 3.6 The ^{1}H and ^{13}C NMR data of compound **5** compared with those of ligballinol (Wang *et al*., 2009).

Position	**Compound 5** (acetone-d_6)		**Ligballinol** (CD_3OD)	
	δ_C	δ_H (int., mult., *J* in Hz)	δ_C	δ_H (int., mult., *J* in Hz)
1	133.6		133.3	
2	128.3	7.10 (1H, *d*, 8.4)	129.0	7.07 (1H, *d*, 8.5)
3	116.0	6.68 (1H, *d*, 8.4)	116.5	6.63 (1H, *dd*, 2.0, 8.5)
4	157.7		158.5	
5	116.0	6.68 (1H, *d*, 8.4))	116.5	6.63 (1H, *dd*, 2.0, 8.5)
6	128.3	7.10 (1H, *d*, 8.4)	129.0	7.07 (1H, *d*, 8.5)
7	86.5	4.53 (1H, *d*, 4.0)	87.7	4.57 (1H, *d*, 4.4)
8	55.2	2.93 (1H, *m*)	55.6	3.01 (*m*, 1H)
9	72.1	3.65 (1H, *dd*, 3.6, 9.2), 4.05 (1H, *dd*, 7.2, 9.2)	72.8	3.70 (1H, *dd*, 4.0, 8.4), 4.07 (1H, *dd*, 7.0, 8.0)
4-OH		8.20 (1H, *br s*)		
1′	133.6		133.3	
2′	128.3	7.10 (1H, *d*, 8.4)	129.0	7.07 (1H, *d*, 8.5)
3′	116.0	6.68 (1H, *d*, 8.4)	116.5	6.63 (1H, *dd*, 8.5, 2.0)
4′	157.7		158.5	
5′	116.0	6.68 (1H, *d*, 8.4)	116.5	6.63 (1H, *dd*, 8.5, 2.0)
6′	128.3	7.10 (1H, *d*, 8.4)	129.0	7.07 (1H, *d*, 8.5)
7′	86.5	4.53 (1H, *d*, 4.0)	87.7	4.57 (1H, *d*, 4.4)
8′	55.2	2.93 (1H, *m*)	55.6	3.01 (1H, *m*)
9′	72.1	3.65 (1H, *dd*, 3.6, 9.2), 4.05 (1H, *dd*, 7.2, 9.2)	72.8	3.70 (1H, *dd*, 4.0, 8.4), 4.07 (1H, *dd*, 7.0, 8.0)
4′-OH		8.20 (1H, *br s*)		

3.2.3 Structural Elucidation of Mixture 6

Mixture **6** (185.8 mg) was obtained as white powder. The ^{1}H and ^{13}C NMR spectra of mixture **6** (Figure A-33 and A-34) presented more than one compound. Mixture **6** was suspected to be glycosides due to the signals of an anomeric proton at δ_H 5.10 and other sugar moiety at δ_H 4.02-4.60 together with carbon signals at δ_C 63.4-79.1. This sugar was assigned to be D-glucose because the *J*-coupling value of an anomeric proton was 7.6 Hz. Moreover, the signals of olefinic protons at δ_H 4.83, 4.90 and 5.37 and olefinic carbons at δ_C 112.4, 122.4, 140.1, 141.4 and 148.2 were found in its NMR spectra. The NMR data of mixture **6** were in agreement with those of charantin (Tables 3.7 and 3.8). Charantin was a sterol glucoside mixture which was a major component previously isolated from Thai bitter gourd (Suwannaroj, 1997). Thus, mixture **6** was identified as charantin, a mixture of 3*β*-O-D-glucopyranosyl-24ξ-ethyl-cholesta-5-ene-3*β*-ol (**6a**) and 3*β*-O-D-glucopyranosyl-24*β*-ethyl-cholesta-5,25-diene-3*β*-ol (**6b**). The structure of this mixture was additionally confirmed by the HMBC correlations (Figure A-35) as shown in Figure 3.15.

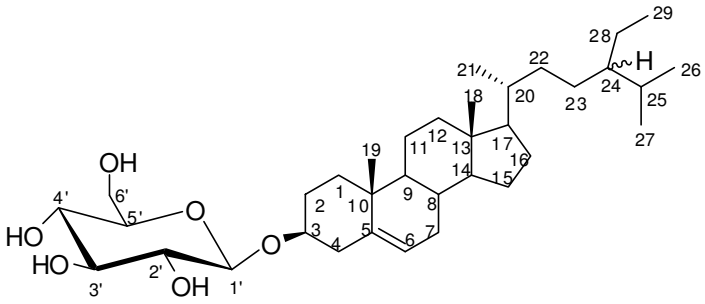

Compound **6a**

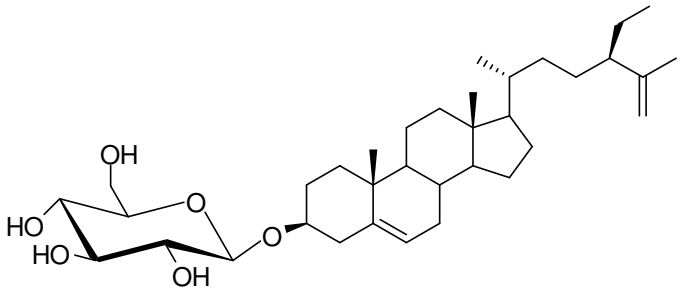

Compound **6b**

Figure 3.14 The chemical structure of mixture **6**.

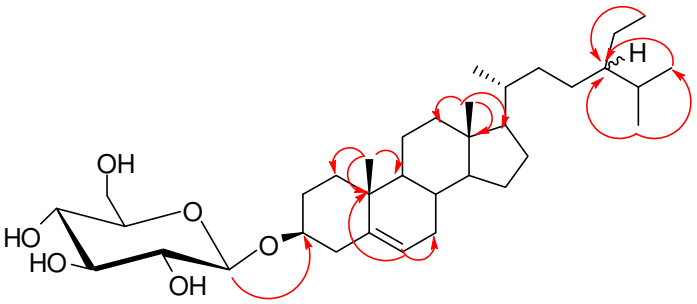

Compound **6a**

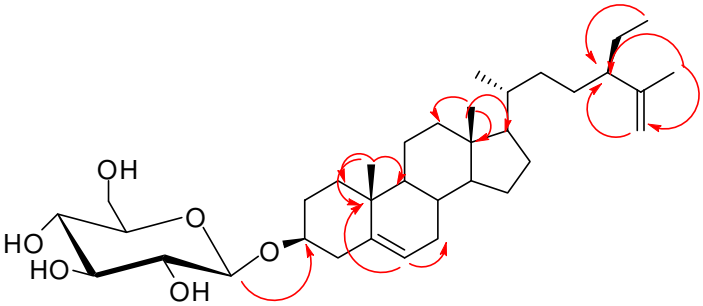

Compound **6b**

Figure 3.15 The selected HMBC (H→C) correlations of mixture **6**.

Table 3.7 The ^{1}H and ^{13}C NMR data of compound **6a** compared with those of 3β-O-D-glucopyranosyl-24ξ-ethyl-cholesta-5-ene-3β-ol (Suwannaroj, 1997).

Position	**Compound 6a** (pyridine-d_5)		**3β-O-D-glucopyranosyl-24β-ethyl-cholesta-5-ene-3β-ol** (pyridine-d_5)	
	δ_C	δ_H (int., mult., *J* in Hz)	δ_C	δ_H (int., mult., *J* in Hz)
1	38.0	1.00 (1H, *m*), 1.75 (1H, *m*)	37.5	0.90-1.02 (1H, *m*), 1.69 (1H, *m*)
2	30.8	1.72 (1H, *m*), 2.16 (1H, *m*)	30.2	1.69 (1H, *m*), 2.12 (1H, *m*)
3	78.6	3.98 (1H, *m*)	78.1	3.94 (1H, *m*)
4	39.8	2.50 (1H, *m*), 2.76 (1H, *dd*, 2.4, 13.2)	39.3	2.47 (1H, *m*), 2.71 (1H, *dd*, 2.7, 13.4)
5	140.1		139.6	
6	122.4	5.37 (1H, *m*)	121.9	5.35 (1H, *m*)
7	32.7	1.56 (1H, *m*), 1.90 (1H, *m*)	32.2	1.58 (1H, *m*), 1.84 (1H, *m*)
8	32.6	1.44 (1H, *m*)	32.0	1.40 (1H, *m*)
9	50.9	0.92 (1H, *m*)	50.3	0.90-0.094 (1H, *m*)
10	37.4		36.9	
11	21.8	1.47 (2H, *m*)	21.3	1.41 (2H, *m*)
12	40.5	1.13 (1H, *m*), 1.97 (1H, *m*)	40.0	1.10 (1H, *m*), 1.94 (1H, *m*)
13	43.0		42.5	
14	57.3	0.93 (1H, *m*)	56.8	0.90-0.94 (1H, *m*)
15	25.0	1.01 (1H, *m*), 1.52 (1H, *m*)	24.5	1.02 (1H, *m*), 1.56 (1H, *m*)
16	30.0	1.26 (1H, *m*)	28.5	1.22 (1H, *m*)
17	56.8	1.05 (1H, *m*)	56.3	0.92-1.12 (1H, *m*)
18	12.5	0.87 (3H, *s*)	11.9	0.65 (3H, *s*)
19	19.5	0.99 (3H, *s*)	19.0	0.95 (3H, *s*)
20	36.9	1.41 (1H, *m*)	36.4	1.38 (1H, *m*)
21	20.5	0.97 (3H, *s*)	19.9	0.90 (3H , *s*)
22	23.9	1.32 (1H, *m*)	23.4	1.28 (2H, *m*)
23	35.2	1.10 (1H, *m*), 1.41(1H, *m*)	34.2	1.07 (1H, *m*), 1.37 (1H, *m*)
24	46.6	1.04 (1H, *m*)	46.0	0.92-1.06 (1H, *m*)
25	30.2	1.69 (1H, *m*)	29.5	1.68 (1H, *m*)
26	19.7	0.90 (3H, *m*)	19.2	0.90 (3H, *m*)
27	19.9	0.89 (3H, *s*)	19.4	0.88 (3H, *m*)
28	28.6	1.28 (2H, *s*)	26.4	1.28 (2H, *m*)
29	12.6	0.91 (3H, *m*)	12.1	0.92 (3H, *m*)
1′	103.1	5.10 (1H, *d*, 7.6)	102.5	5.02 (1H, *d*, 7.8)
2′	75.8	4.09 (1H, *m*)	75.3	4.02 (1H, *m*)
3′	79.1	4.35 (1H *m*)	78.6	4.26 (1H, *m*)
4′	72.3	4.33 (1H, *m*)	71.7	4.24 (1H, *m*)
5′	79.0	4.02 (1H, *m*)	78.4	3.94 (1H, *m*)
6′	63.4	4.45 (1H, *dd*, 5.2, 12.0), 4.60 (1H, *dd*, 2.0, 11.6)	62.8	4.38 (1H, *dd*, 5.1, 11.6) 4.55 (1H, *dd*, 2.7, 11.7)

Table 3.8 The ^{1}H and ^{13}C NMR data of compound **6b** compared with those of 3β-O-D-glucopyranosyl-24β-ethyl-cholesta-5,25-diene-3β-ol (Suwannaroj, 1997).

Position	**Compound 6b** (pyridine-d_5)		**3β-O-D-glucopyranosyl-24β-ethyl-cholesta-5,25-diene-3β-ol** (pyridine-d_5)	
	δ_C	**δ_H** (int., mult., *J* in Hz)	**δ_C**	**δ_H** (int., mult., *J* in Hz)
1	38.0	1.00 (1H, *m*), 1.75 (1H, *m*)	37.5	0.90-1.02 (1H, *m*), 1.69 (1H, *m*)
2	30.8	1.72 (1H, *m*), 2.16 (1H, *m*)	30.2	1.69 (1H, *m*), 2.12 (1H, *m*)
3	78.6	3.98 (1H, *m*)	78.1	3.94 (1H, *m*)
4	39.8	2.50 (1H, *m*), 2.76 (1H, *dd*, 2.4, 13.2)	39.3	2.47 (1H, *m*), 2.71 (1H, *dd*, 2.7, 13.4)
5	141.4		140.9	
6	122.4	5.37 (1H, *m*)	121.9	5.35 (1H, *m*)
7	32.7	1.56 (1H, *m*), 1.90 (1H, *m*)	32.2	1.58 (1H, *m*), 1.84 (1H, *m*)
8	32.6	1.44 (1H, *m*)	32.0	1.40 (1H, *m*)
9	50.9	0.92 (1H, *m*)	50.3	0.90-0.094 (1H, *m*)
10	37.4		36.9	
11	21.8	1.47 (2H, *m*)	21.3	1.41 (2H, *m*)
12	40.5	1.15 (1H, *m*), 2.00 (1H, *m*)	40.0	1.14 (1H, *m*), 1.98 (1H, *m*)
13	43.0		42.5	
14	57.3	0.93 (1H, *m*)	56.8	0.90-0.94 (1H, *m*)
15	25.0	1.00 (1H, *m*), 1.52 (1H, *m*)	24.5	1.00 (1H, *m*), 1.56 (1H, *m*)
16	30.0	1.26 (1H, *m*), 1.82 (1H, *m*)	28.5	1.22 (1H, *m)*, 1.80 (1H, *m*)
17	56.8	1.05 (1H, *m*)	56.3	0.92-1.12 (1H, *m*)
18	12.5	0.68 (3H, *s*)	11.9	0.65 (3H, *s*)
19	19.9	0.95 (3H, *s*)	19.4	0.94 (3H, *s*)
20	36.2	1.44 (1H, *m*)	35.7	1.40 (1H, *m*)
21	19.4	0.89 (3H, *s*)	18.9	0.87 (3H , *s*)
22	34.5	1.07 (1H, *m*), 1.40 (1H, *m*)	34.0	1.05 (1H, *m*), 1.35 (1H, *m*)
23	30.5	1.79 (1H, *m*), 2.07 (1H, *m*)	29.7	1.71 (1H, *m*), 2.08 (1H, *m*)
24	50.2	1.94 (1H, *m*)	49.7	1.90 (1H, *m*)
25	148.2		147.7	
26	18.4	1.63 (3H, *s*)	17.9	1.62 (3H, *s*)
27	112.4	4.83 (1H, *m*), 4.90 (1H, *m*)	111.9	4.80 (1H, *m*), 4.87 (1H, *m*)
28	28.9	1.37 (2H, *m*)	26.7	1.34 (2H, *m*)
29	12.8	0.87 (3H, *s*)	12.2	0.86 (3H, *s*)
1′	103.1	5.10 (1H, *d*, 7.6)	102.5	5.02 (1H, *d*, 7.8)
2′	75.8	4.09 (1H, *m*)	75.3	4.02 (1H, *m*)
3′	79.1	4.35 (1H *m*)	78.6	4.26 (1H, *m*)
4′	72.3	4.33 (1H, *m*)	71.7	4.24 (1H, *m*)
5′	79.0	4.02 (1H, *m*)	78.4	3.94 (1H, *m*)
6′	63.4	4.45 (1H, *dd*, 5.2, 12.0), 4.60 (1H, *dd*, 2, 11.6)	62.8	4.38 (1H, *dd*, 5.1, 11.6) 4.55 (1H, *dd*, 2.7, 11.7)

3.2.4 Structural Elucidation of Compound 7

Compound **7** (42.7 mg) was obtained as colorless needles with $[\alpha]_D^{20}$ +68.7 (*c* 0.1 in $CHCl_3$:MeOH (1:1)). The molecular formula of compound **7** was determined to be $C_{30}H_{60}O_9$ on the basis of its ESI-MS at m/z 671.64 $[M+Na]^+$ (Figure A-42). Thus, the molecular weight of compound **7** was 648 g/mol.

The ^1H and ^{13}C NMR spectra (Figures A-37 and A-38) of compound **7** displayed signals of an anomeric (δ_H 4.17 (*d*, *J* = 7.6 Hz); δ_C 101.7) and sugar protons (δ_H 3.15-3.76; δ_C 61.8-76.3). Other signals suggested that it was a cucurbitane skeleton. The NMR data were similar to those of compound **4a**, except for the absence of hemi-acetal signal of C-19 in compound **7**. The signals at δ_C 210.1 and δ_H 9.74 of compound **7** indicated the presence of an aldehyde group. The correlations between this aldehyde proton (δ_H 9.74) and δ_C 22.4 (C-11) in HMBC experiment (Figure A-40) assured the assigment of the aldehyde group at C-9. In addition, the HMBC cross-peak from anomeric proton at δ_H 4.17 to C-7 at δ_C 73.4 confirmed the linkage of sugar moiety. The HMBC correlations of compound **7** were shown in Figure 3.17.

The ^1H and ^{13}C NMR data of compound **7** were found to be in agreement with those of momordicoside K (Okabe *et al.,* 1982b) as shown in Table 3.9. Thus, compound **7** was identified as momordicoside K.

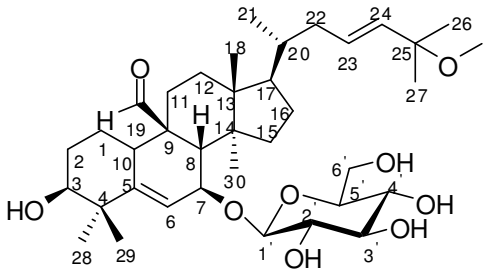

Figure 3.16 The chemical structure of compound **7**.

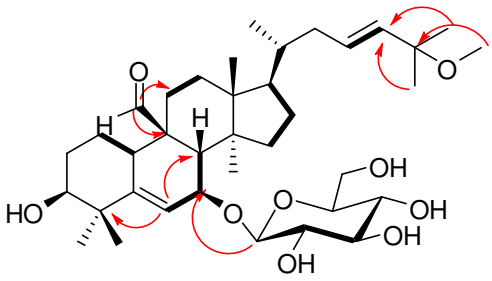

Figure 3.17 The selected HMBC (H→C) and COSY (bold lines) correlations of compound **7**.

Table 3.9 The ^{1}H and ^{13}C NMR data of compound **7** compared with those of momordicoside K (Okabe *et al.,* 1982b).

Position	**Compound 7** ($CDCl_3$)		**Momordicoside K** (pyridine-d_5)	
	δ_C	δ_H (int., mult., *J* in Hz)	δ_C	δ_H (int., mult., *J* in Hz)
1	21.0	1.53 (1H, *m*), 1.43 (1H, *m*)		
2	28.9	1.58 (2H, *m*)		
3	75.9	3.50 (1H, *br s*)	74.7	3.79 (1H, *br s*)
4	41.6			
5	146.9		147.1	
6	122.5	5.86 (1H, *d*, 5.2)	121.9	6.17 (1H, *br d*, 6.0)
7	73.4	3.92 (1H, *d*, 5.2)	71.5	
8	46.4	1.99 (1H, *s*)	50.6	2.39 (1H, *br s*)
9	50.0		47.9	
10	35.8	2.44 (1H, *m*)		
11	22.4	2.26 (2H, *m*)		
12	28.5	1.69 (1H, *m*), 1.85 (1H, *m*)		
13	45.6		41.8	
14	47.3		45.6	
15	34.8	1.23 (2H, *m*)		
16	27.4	1.29 (1H, *m*) ,1.82 (1H, *m*)		
17	49.4	1.40 (1H, *m*)		
18	14.9	0.84 (3H, *s*)	15.1	0.87 (3H, *s*)
19	210.1	9.74 (1H, *s*)	207.0	10.43 (1H, *s*)
20	36.1	1.47 (1H, *m*)		
21	18.8	0.84 (3H, *s*)	19.0	1.12 (3H, *s*)
22	39.4	2.12 (1H, *m*), 1.71 (1H, *m*)		
23	128.6	5.43 (1H, *m*)	128.0	5.57 (1H, *m*)
24	136.8	5.31 (1H, *d*, 15.6)	137.3	5.57 (1H, *m*)
25	75.2		74.7	
26	26.1	1.18 (3H, *s*)	26.5	1.31 (3H, *s*)
27	25.8	1.18 (3H, *s*)	26.1	1.31 (3H, *s*)
28	27.1	0.98 (3H, *s*)	27.4	0.95 (3H, *s*)
29	25.3	1.18 (3H, *s*)	26.2	1.42 (3H, *s*)
30	18.2	0.68 (3H, *s*)	18.2	0.78 (3H, *s*)
25-OMe	50.3	3.07 (3H, *s*)	50.0	3.21 (3H, *s*)
1′	101.7	4.17 (1H, *d*, 7.6)	106.8	4.58 (1H, *d*, 8.0)
2′	73.4	3.15 (1H, *d*, 8.0)	75.4	
3′	75.9	3.18 (1H, *d*, 9.2)	78.5	
4′	69.8	3.41 (1H, *dd*, 9.2, 8.8)	71.5	
5′	76.3	3.34 (1H, *dd*, 9.2, 8.8)	78.3	
6′	61.8	3.76 (2H, *m*)	62.7	

3.3 Cholinesterase Inhibitory Activities of Isolated Substances from *M. charantia* Fruits.

The separation of *M. charantia* fruits resulted in isolation of four compounds (**1**, **2**, **5** and **7**) and three inseparable mixtures (**3**, **4** and **6**). All substances were further evaluated for their anti-cholinesterase by colorimetric method. This experiment used eserine, a clinical drug, as a standard.

The AChE and BChE inhibition percentages of all substances, at the final concentrations of 0.5, 0.1 and 0.05 mg/mL, are expressed in Tables 3.10 and 3.11, respectively. The comparative activities of those substances are shown in Figures 3.18 and 3.19. All tested substances showed dose-dependent manners. However, they showed relatively low activities (< 50% inhibitory percentage), except for compound **5** towards BChE, compared with those of eserine. Compound **7** exhibited the highest inhibition towards AChE because the presence of an aldehyde group and a glycoside moiety on ring B seem to be increase inhibitory effect comparing with the absence of them in other isolated cucurbitanes, while compound **5** showed the highest inhibition and selectively towards BChE. According to less solubility of tested substances under assay condition, only compound **5** was further investigated for the IC_{50} value towards BChE. The dose response curves of compound **5** and eserine towards BChE are shown in Figure 3.20. By the Prism software calculation, the IC_{50} value of this compound was 32.20 μM which was 16-folds higher than that of eserine, 2.06 μM. However, the IC_{50} of compound **5** towards BChE was close to that of galanthamine. Galanthamine is a commercial AD drug which is isolated from natural plant. The IC_{50} of this compound towards BChE was 26.30 μM while that of eserine (or phytostigmine) was 10.20 μM in the previous report (Sermboonpaisarn and Sawasdee, 2012). In addition, this study is the first report of the BChE inhibitory effect of lignan. Thus, this result suggested that compound **5** or ligballinol could be a candidate in the improvement and development to be an effective drug for the treatment of AD and also other neurodegenerative disorders.

Table 3.10 AChE inhibitory activity of all isolated substances from the fruits of *M. charantia* at final concentrations 0.05, 0.1 and 0.5 mg/mL.

Substance	Structure	% AChE Inhibition[a] at the final concentration of (mg/mL)		
		0.05	**0.1**	**0.5**
1	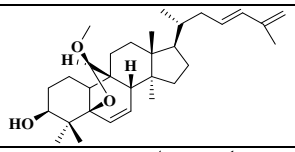	4.50	7.21	10.15
2	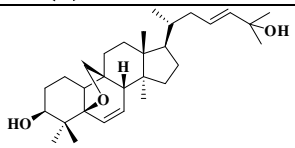	3.04	4.36	6.18
3	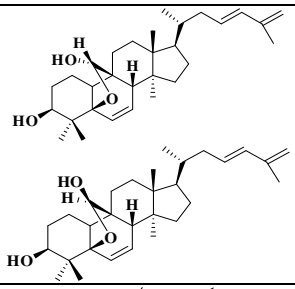	2.95	4.62	6.56
4	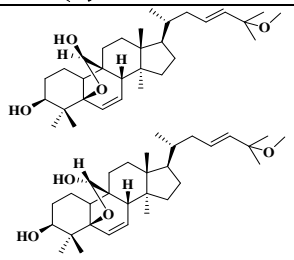	6.13	7.96	13.10
5	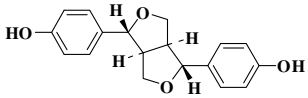	1.98	3.62	5.72
6	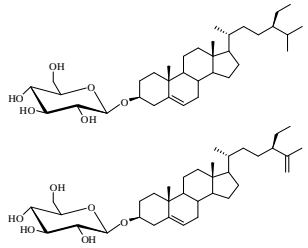	3.66	4.49	8.88
7	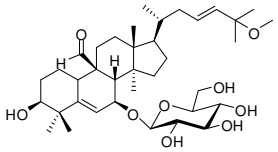	14.73	44.87	49.97
Eserine[b]	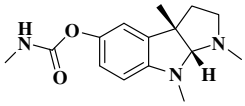	99.39	99.68	99.81

[a] *Results are expressed as means (n =2).*
[b] *Positive control.*

Table 3.11 BChE inhibitory activity of all isolated substances from the fruits of *M. charantia* at final concentrations 0.05, 0.1 and 0.5 mg/mL.

Substance	Structure	% BChE Inhibition[a] at the final concentration of (mg/mL)		
		0.05	**0.1**	**0.5**
1	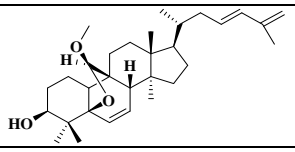	8.38	9.91	14.83
2	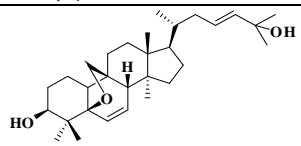	22.91	26.0	32.50
3	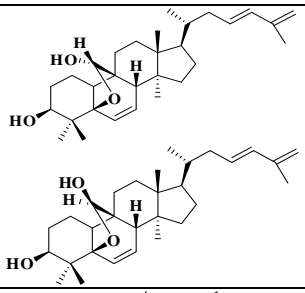	10.96	13.59	16.70
4	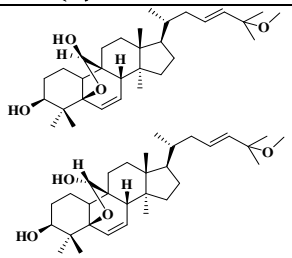	17.21	21.29	29.66
5	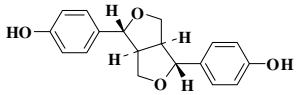	79.29	84.96	96.38
6	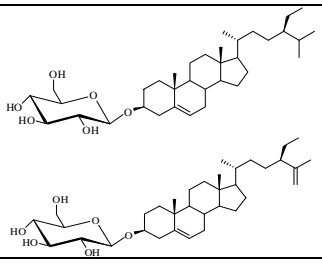	10.10	12.97	20.43
7	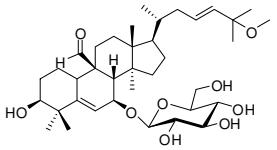	14.61	18.97	27.58
Eserine[b]	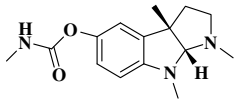	99.39	99.58	99.62

[a] *Results are expressed as means (n =2).*
[b] *Positive control.s*

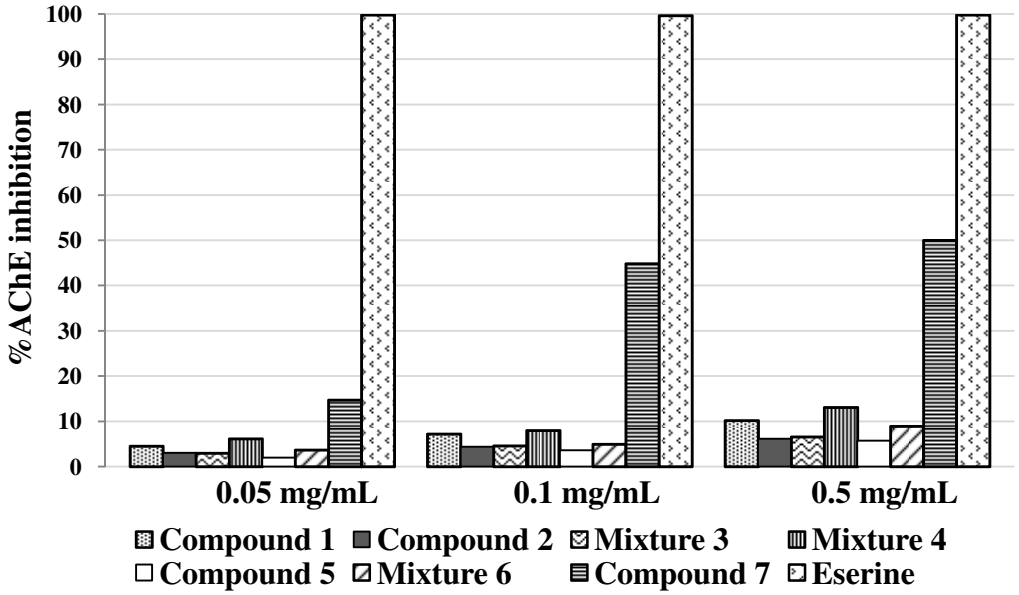

Figure 3.18 The AChE inhibitory activity of substances **1-7** from the fruits of *M. charantia* at final concentration 0.05, 0.1 and 0.5 mg/mL. Data are expressed as means (n=2).

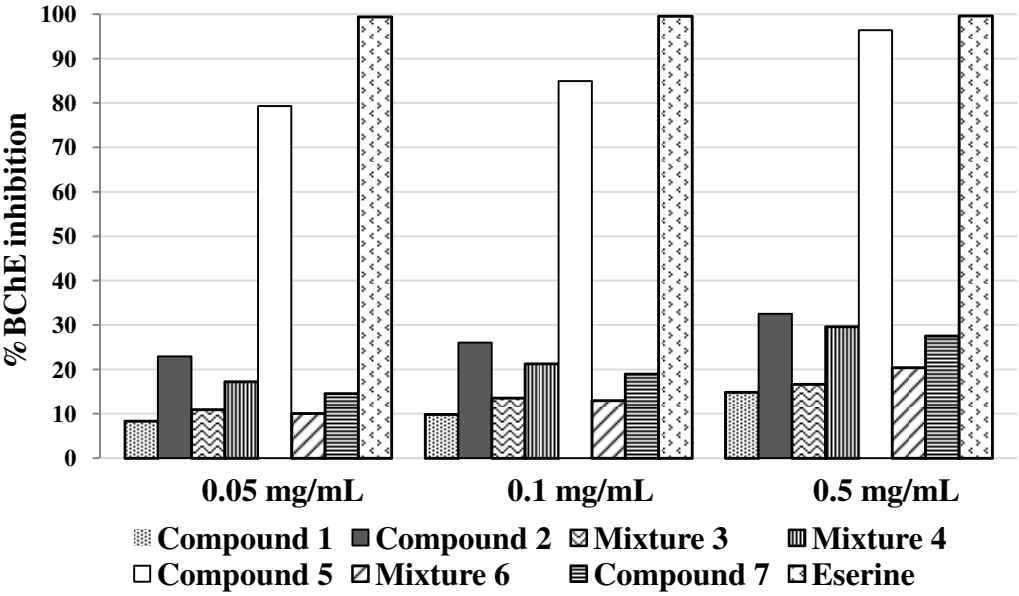

Table 3.19 The BChE inhibitory activity of substances **1-7** from the fruits of *M. charantia* at final concentration 0.05, 0.1 and 0.5 mg/mL. Data are expressed as means (n=2).

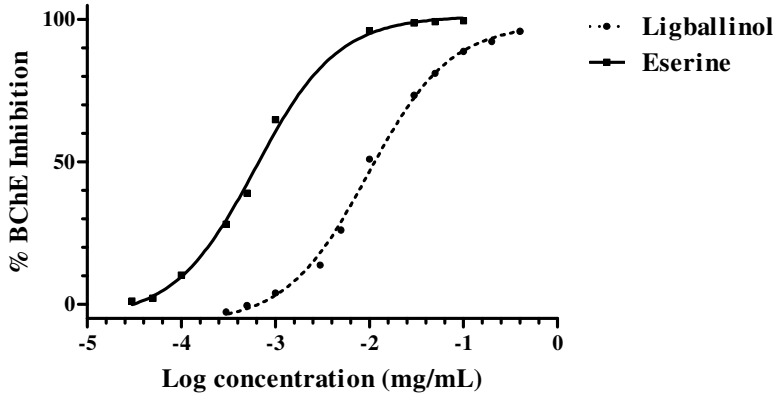

Figure 3.20 Dose response curves of ligballinol (**5**) and eserine (the standard inhibitor) against butyrylcholinesterase. Data are expressed as means (n =2).

To determine the mode of BChE inhibition of ligballinol (**5**), this compound was further examined for its kinetic studies. The Lineweaver–Burk plots of compound **5** (Figure 3.21) revealed the different K_m values (the negative reciprocal of the X-intercept) and the unchanged ν_{max} values (the reciprocal of the Y-intercept). These kinetic results indicated a competitive inhibition by binding to the catalytic site of free BChE. To gain comprehension into binding affinity of inhibitor to free enzyme, dissociation constant, K_i, were further determined.

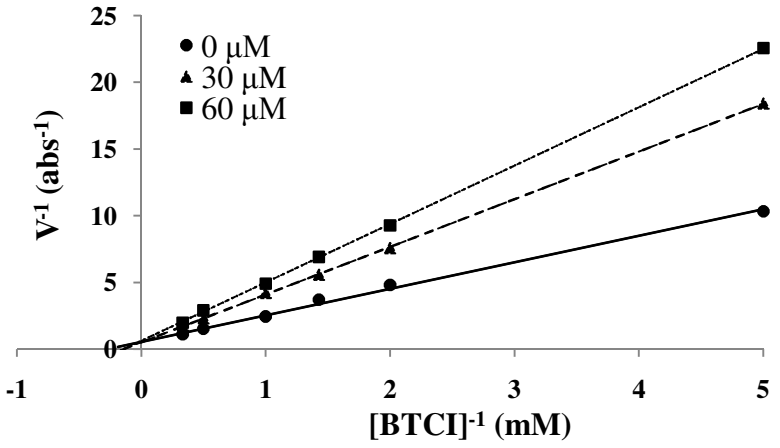

Figure 3.21 Lineweaver–Burk plots resulting of ligballinol (**5**) from the substrate velocity curves of BChE inhibitory activity.

For a calculation of K_i value, slopes from the Lineweaver-Burk plots (see Figure 3.21) were plotted versus concentrations of ligballinol (**5**) which afforded the secondary plot as shown in Figure 3.22. The derived equation for a calculation of K_i is

$$\text{slope} = \frac{K_m}{v_{max} \times K_i}$$

Where K_m or substrate constant is dissociation constant for the enzyme-substrate complex (ES) and v_{max} is the limiting velocity. Both values were calculated from a primary Lineweaver-Burk plot (see Figure 3.21) for the absence of inhibitor concentration using the following expression.

Which is;

$$v_{max} = \frac{1}{\text{C}} \text{ where; C = Y-intercept}$$

$$K_m = \text{slope} \times v_{max}$$

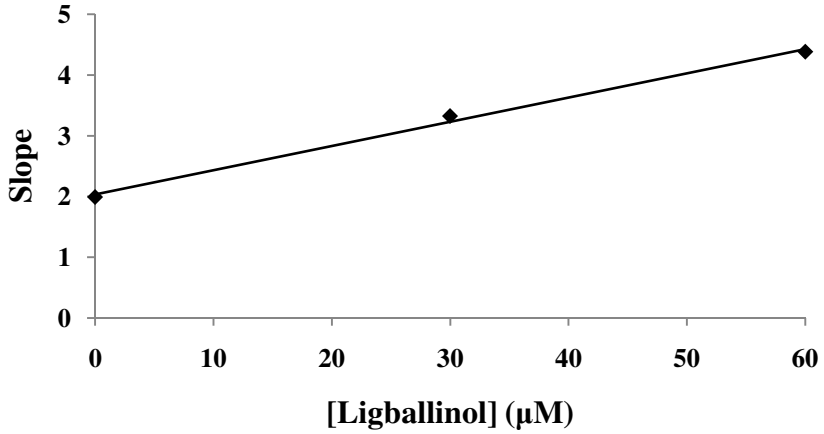

Figure 3.22 The secondary plot of slopes from the Lineweaver-Burk plots versus concentrations of ligballinol (**5**).

As shown above, the secondary plot indicated the binding of ligballinol (**5**) to free enzyme, BChE, (enzyme-inhibitor complex; EI complex) with K_i value of 49.86 µM in a competitive inhibition towards BChE.

CHEPTER IV

CONCLUSION

In this research, the fruits of *M. charantia* were investigated the chemical constituents and determined for their anti-cholinesterase activity. Four compounds and three inseparable mixtures were obtained from the dichloromethane extract and their chemical structures were elucidated on the basis of spectroscopic evidences and compared with the literature data. These isolated substances were (19*R*,23*E*)-5*β*,19-epoxy-19-methoxycucurbita-6,23,25-trien-3*β*-ol (**1**), (23*E*)-5*β*,19-epoxycucurbita-6,23-diene-3*β*,25-diol (**2**), a mixture of 5*β*,19-epoxycucurbita-6,23(*E*),25(26)-triene-3*β*,19(*S*)-diol (**3a**) and 5*β*,19-epoxycucurbita-6,23(*E*),25(26)-triene-3*β*,19(*R*)-diol or charantadiol A (**3b**), a mixture of 5*β*,19-epoxy-25-methoxy-cucurbita-6,23-diene-3*β*,19(*S*)-diol (**4a**) and 5*β*,19-epoxy-25-methoxy-cucurbita-6,23-diene-3*β*,19(*R*)-diol (**4b**), ligballinol (**5**), charantin (a mixture of 3*β*-O-D-glucopyranosyl-24*ξ*-ethyl-cholesta-5-ene-3*β*-ol (**6a**) and 3*β*-O-D-glucopyranosyl-24*β*-ethyl-cholesta-5,25-diene-3*β*-ol (**6b**)) and momordicoside K (**7**). All chemical structures of isolated substances are shown in Table 4.1.

Moreover, all substances were evaluated for their cholinesterase activities against acetylcholinesterase (AChE) and butyrylcholinesterase (BChE). Compound **5** or ligballinol exhibited the most potent butyrylcholinesterase inhibitory activities, with the IC_{50} value of 32.20 μM and a competitive inhibition mode. On the other hand, other compounds could be considered as low activity (% inhibition < 50% at a final concentration of 0.1 mg/mL). This study is the first report of anti-cholinesterase activity of chemical constituents from *M. charantia* and a lignan skeleton. This researching outcome suggested that *M. charantia* and ligballinol might be a new choice for the treatment and prevention of AD and also other neurodegenerative disorders.

Table 4.1 Isolated substances (**1-7**) from *M. charantia* fruits.

Substance	**Weight** (mg)	**% Yield**[*] (×10-2)
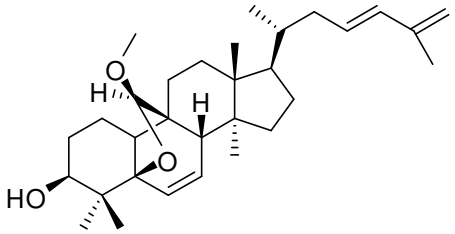 (19*R*,23*E*)-5*β*,19-epoxy-19-methoxycucurbita-6,23,25-trien-3*β*-ol (**1**)	45.5	5.4
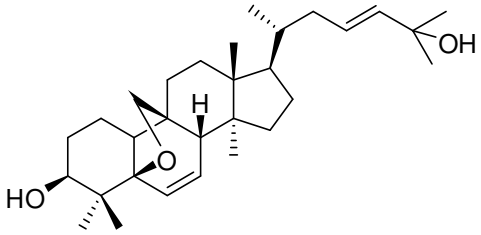 (23*E*)-5*β*,19-epoxycucurbita-6,23-diene-3*β*,25-diol (**2**)	96.2	11.5
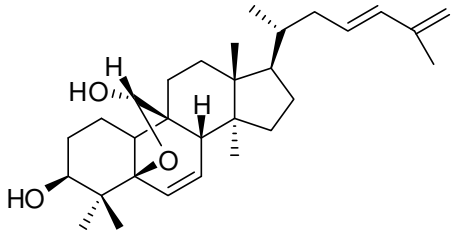 5*β*,19-epoxycucurbita-6,23(*E*),25(26)-triene-3*β*,19(*S*)-diol (**3a**) 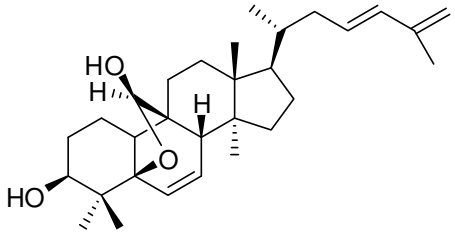 5*β*,19-epoxycucurbita-6,23(*E*),25(26)-triene-3*β*,19(*R*)-diol or charantadiol A (**3b**)	31.7	3.8
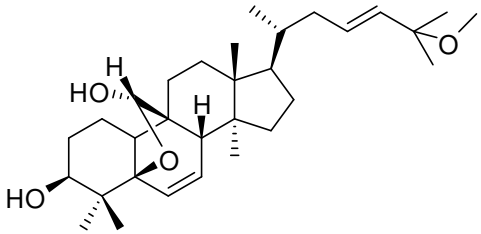 5*β*,19-epoxy-25-methoxy-cucurbita-6,23-diene-3*β*,19(*S*)-diol (**4a**) 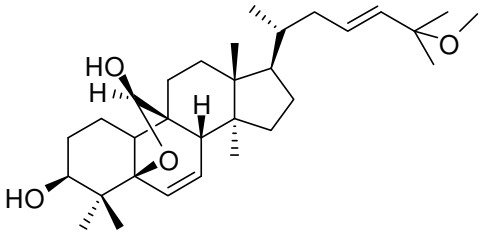 5*β*,19-epoxy-25-methoxy-cucurbita-6,23-diene-3*β*,19(*R*)-diol (**4b**)	163.8	19.5

Table 4.1 Isolated substances (**1-7**) from *M. charantia* fruits (continued).

Substance	**Weight** (mg)	**% Yield**[*] ($\times 10^{-2}$)
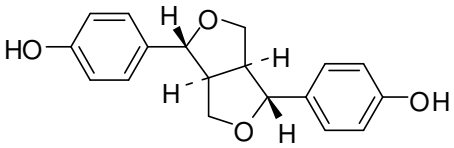 Ligballinol (**5**)	15.2	1.8
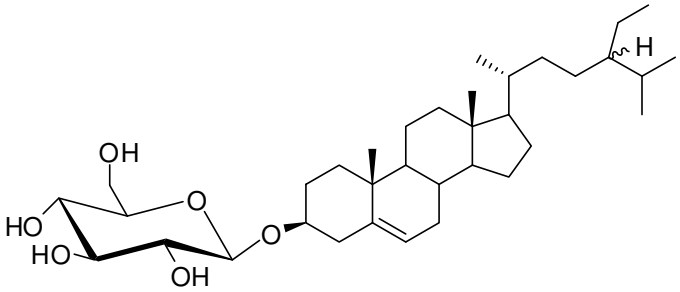 3β-O-D-glucopyranosyl-24ξ-ethyl-cholesta-5-ene-3β-ol (**6a**) 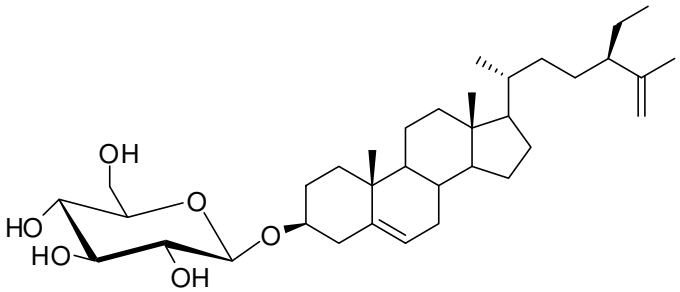 3β-O-D-glucopyranosyl-24β-ethyl-cholesta-5,25-diene-3β-ol (**6b**)	185.8	22.2
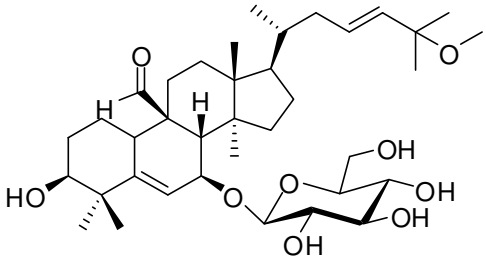 Momordicoside K (**7**)	42.7	5.1

**The percentage of yield substances was calculated based on the dichloromethane extract.*

REFERENCES

Alzheimer's association. Alzheimer's association report 2012: Alzheimer's disease facts and figures. Alzheimer's & Dementia 8 (2012): 131-168.

Atack, J.R., Perry, E.K., Bonham, J.R., Candy, J.M. and Perry, R.H. Molecular forms of acetylcholinesterase and butyrylcholinesterase in the aged human central nervous system. Journal of Neurochemistry 47 (1986): 263-277.

Becker, R.E., Moriearty, P., Unni, L. and Vicari, S. Cholinesterase inhibitors as therapy in Alzheimer's disease: Benefit to risk considerations in clinical application. In R. Becker, and E. Giacobini (eds.), Alzheimer's disease: From molecular biology to therapy, pp. 257-266. Boston: Brikhäuser, 1997.

Bharathi, L.K., Munshi, A.D., Behera1, T.K., Vinod, John, K.J., Das, A.B., Bhat, K.V., and Sidhu, A.S. Production and preliminary characterization of inter-specific hybrids derived from *Momordica* species. Current Science 103 (2012): 178-186.

Bunyamahotama, S. Acute hypoglycemic effects of *Momordica charantia* freezed dried powder in impair glucose tolerance cases (IGT). Master's thesis, Department of Clinical Pharmacy, Graduate School, Silpakorn University, 2004.

Ellman, G.L., Courtney, K.D., Andres, V., and Featherstone, R.M. A new and rapid colorimetric determination of acetylcholinesterase activity. Biochemical Pharmacology 7 (1961): 88-95.

Chakravarty, H.L. Cucurbits of India and their role in the development of vegetable crop. In D.M. Bates, R.W. Robinson, and C. Jeffrey (eds.), Biology and utilization of cucurbitaceae, pp. 325-334. New York: Cornell University Press, 1990.

Chang, C.I., Chen, C.R., Liao, Y.W., Cheng, H.L., Chen, Y.C., and Chou, C.H. Cucurbitane-type triterpenoids from *Momordica charantia*. Journal of Natural Products 69 (2006): 1168-1171.

Chang, C.I., Tseng, H.I., Liao, Y.W., Yen, C.H., Chen, T.M., Lin, C.C., and Cheng, H.L. *In vivo* and *in vitro* studies to identify the hypoglycaemic constituents of *Momordica charantia* wild variant WB24. Food Chemistry 125 (2011): 521-528.

Chen, J.C., Chiu, M.H., Nie, R.L, Cordell, G.A., and Qiu, S.X. Cucurbitacins and cucurbitane glycosides: Structures and biological activities. Natural Product Reports 22 (2005): 386-399.

Chen, J.C., Liu, H.Q., Lu, L., Qiu, M.H., Zheng, Y.T., Yang, L.M., Zhang, X.M., Zhou, L., and Li, Z.R. Kuguacins F-S, cucurbitane triterpenoids from *Momordica charantia*. Phytochemistry 70 (2009): 133-140.

Chen, J.C., Tian, R., Qiu, M., Lu, L., Zheng, Y., and Zhang, Z. Trinorcucurbitane and cucurbitane triterpenoids from the roots of *Momordica charantia*. Phytochemistry 69 (2008): 1043-1048.

Darvesh, S., Grantham, D.L. and Hopkins, D.A. Distribution of butyrylcholinesterase in human amygdala and hippocampal formation. Journal of Comparative Neurology 393 (1998): 374-390.

Dhiman, K., Sharma, D.K., Gill, N.S., and Goyal, A. A review on the medicinally important plants of the family Cucurbitaceae. Asian Journal of Clinical Nutrition 4 (2012): 16-26.

Dinan, L., Harmatha, J., and Lafont, R. Chromatographic procedures for the isolation of plant steroids. Journal of Chromatography A 935 (2001): 105-123.

Giacobini E. Cholinesterase inhibitors from the Calabar bean to Alzheimer therapy. In E. Giacobini (ed.), Cholinesterases and cholinesterase inhibitors, pp. 181-226. London: Martin Dunitz, 2000.

Greig, N.H., Lahiri, D.K. and Sambamurti, K. Butyrylcholinesterase: An important new target in Alzheimer's disease therapy. International Psychogeriatrics (2000)

Grover, J.K., and Yadav, S.P. Pharmacological actions and potential uses of *Momordica charantia*: A review. Journal of Ethnopharmacology 93 (2004): 123-132.

Grutzendler, J., and Morris, J.C. Cholinesterase inhibitors for Alzheimer's disease. Drugs 61 (2001): 41-52.

Guha. J., and Sen, S.P. The cucurbitacins-a review. Plant Biochemistry Journal 2 (1975): 12-28.

Haque, M.E., Alam, M.B., and Hossain, M.S. The efficacy of cucurbitane type triterpenoids, glycosides and phenolic compounds isolated from *Momordica charantia*: A review. International Journal of Pharmaceutical Sciences and Research 2 (2011): 1135-1146.

Imbimbo, B.P. Pharmacodynamic-tolerability relationships of cholinesterase inhibitors for Alzheimer's disease. CNS Drugs 15 (2001): 375-390.

Ingkaninan, K., Temkitthawon, P., Chuenchom, K., and Thongnoi, T.Y. Screening for acetylcholinesterase inhibitory activity in plants used in Thai traditional rejuvenating and neurotonic remedies. Journal of Ethnopharmacology 89 (2003): 261-264.

Jiratchariyakul, W., Wiwat, C., Vongsakul, M., Somanabandhu, A., Leelamanint, W., Fujii, I., Suwannaroj, N., and Ebizuka, Y. HIV inhibitor form Thai bitter gourd. Planta Medica 67 (2001): 350-353

Kikuchia, T., Zhanga, J., Huanga, Y., Watanabea, K., Ishiia, K., Yamamotoa, A., Fukatsua, M., Tanakab, R., and Akihisa, T. Glycosidic inhibitors of melanogenesis from leaves of *Momordica charantia*. Chemistry & Biodiversity 9 (2012):1221-1230.

Kimura, Y., Akihisa, T., Yuasa, N., Ukiya, M., Suzuki, T., Toriyama, M., Motohashi, S., and Tokuda, H. Cucurbitane-type triterpenoids from the fruit of *Momordica charantia*. Journal of Natural Products 68 (2005): 807-809.

Kitphati, W., Wattanakamolkul, K., Lomarat, P., Phanthong, P., Anantachoke, N., Nukoolkarn, V., Thirapanmethee, K., and Bunyapraphatsara, N. Anticholinesterase of essential oils and their constituents from Thai medicinal plants on purified and cellular enzymes. Journal of the American Academy of Spine Physicians 1 (2012): 58-67.

Kobayashi, M., and Ohta, Y. Induction of stress metabolite formation in suspension cultures of *Vigna angularis*. Phytochemistry 22 (1983): 1257-1261.

Kubola, J., and Siriamornpun, S. Phenolic contents and antioxidant activities of bitter gourd (*Momordica charantia* L.) leaf, stem and fruit fraction extracts *in vitro*. Food Chemistry 110 (2008): 881-890.

Kusamran, W.R., Tepsuwan, A., and Kupradinun, P. Antimutagenic and anticarcinogenic potentials of some Thai vegetables. Mutation Research 402 (1998): 247-258.

Lahiri, D.K., Farlow, M.R., Greig, N.H., and Sambamurti, K. Current drug targets for alzheimer's disease treatment. Drug Development Research 56 (2002): 267-281.

Li, Q.Y., Chen, H.B., Liu, Z.M., Wang, B., and Zhao, Y.Y. Cucurbitane triterpenoids from *Momordica charantia*. Magnetic Resonance Chemistry 45 (2007): 451-456.

Limtrakul, P., Khantamat, O., and Pintha, K. Inhibition of P-glycoprotein activity and reversal of cancer multidrug resistance by *Momordica charantia* extract. Cancer Chemother Pharmacol 54 (2004): 525-530.

Liu, C.H., Yen, M.H., Tsang, S.F, Gan, K.H., Hsu, H.Y., and Lin, C.N. Antioxidant triterpenoids from the stems of *Momordica charantia*. Food Chemistry 118 (2010): 751-756.

Matsuda, H., Nakamura, S., Murakami, T., and Yoshikawa, M. Structures of new cucurbitane-type triterpenes and glycosides, karavilagenins D and E and karavilosides VI, VII, VIII, IX, X and XI, from the fruit of *Momordica charantia*. Heterocycles 71 (2007): 331-341.

Miyahara, Y., Okabe, H., and Yamauchi, T. Studies on the constituents of *Momordica charantia* L.: II. Isolation and characterization of minor seed glycosides, momordicosides C, D and E. Chemical and Pharmaceutical Bulletin 29 (1981): 1561-1566.

Mulholland, D.A., Sewram, V., Osborne, R., Pegel, K.H., and Connolly, J.D. Cucurbitane triterpenoids from the leaves of *Momordica foetida*. Phytochemistry 45 (1997): 391-395.

Nakamura, S., Murakami, T., Nakamura, J., Kobayashi, H., Matsuda, H., and Yoshikawa, M. Structures of new cucurbitane-type triterpenes and glycosides, karavilagenins and karavilosides, from the dried fruit of *Momordica charantia* L. in Sri Lanka. Chemical and Pharmaceutical Bulletin 54 (2006): 1545-1550.

Nhiem, N.X., Kiem, P.V., Minh, C.V., Ban, N.K., Cuong, N.X., Ha, L.M., Tai, B.H., Quang, T.H., Tunga, N.H., and Kim, Y.H. Cucurbitane-type triterpene glycosides from the fruits of *Momordica charantia.* Magnetic Resonance in Chemistry 48 (2010a): 392-396.

Nhiem, N.X., Kiem, P.V., Minh, C.V., Ban, N.K., Cuong, N.X., Tung, N.H., Ha, L.M., HA, D.T., Tai, B.H., Quang, T.H., Ngoc, T.M., Kwon, Y.I., Jang, H.D., and Kim, Y.H. α-Glucosidase inhibition properties of cucurbitane-type triterpene glycosides from the fruits of *Momordica charantia.* Chemical and Pharmaceutical Bulletin 58 (2010b): 720-724.

Okabe, H., Miyahara, Y., and Yamaushi, T. Studies on the constituents of *Momordica charantia* L.: III. Characterization of the new cucurbitacin glycosides of the immature fruits: Structures of the bitter glycosides, momordicosides G, F1, F2, and I. Chemical and Pharmaceutical Bulletin 30 (1982a): 3977-3986.

Okabe, H., Miyahara, Y., and Yamaushi, T. Studies on the constituents of *Momordica charantia* L.: IV. Characterization of the new cucurbitacin glycosides of the immature fruits: Structures of the bitter glycosides, momordicosides K and L. Chemical and Pharmaceutical Bulletin 30 (1982b): 4334-4340.

Okabe, H., Miyahara, Y., Yamauchi, T., Miyahara, K., and Kawasaki, T. Studies on the constituents of *Momordica charantia* L.: I. Isolation and characterization of momordicosides A and B, glycosides of a pentahydroxy-cucurbitane triterpene. Chemical and Pharmaceutical Bulletin 28 (1980): 2753-2762.

Rahman, A.U., ed. Bioactive natural products (part L). 32 vols. 1st ed. The Netherlands: Amsterdam, 2005.

Panlilio, B.G., Macabeo, A.P.G., Knorn, M, Kohls, P., Richomme, P., Kouam, S.F., Gehle, D., Krohn, K., Franzblau, S.G., Zhang, Q., and Aguinaldo, M.A.M. A lanostane aldehyde from *Momordica charantia*. Phytochemistry Letters 5 (2012): 682-684.

Pitchakarn, P., Ohnumab, S., Pinthaa, K., Pompimonc, W., Ambudkar, S.V., and Limtrakul, P. Kuguacin J isolated from *Momordica charantia* leaves inhibits P-glycoprotein (ABCB1)-mediated multidrug resistance. Journal of Nutritional Biochemistry 23 (2012a): 76-84.

Pitchakarn, P., Ogawa, K., Suzuki, S., Takahashi, S., Asamoto, M., Chewonarin, T., Limtrakul, P., and Shirai, T. *Momordica charantia* leaf extract suppresses rat prostate cancer progression *in vitro* and *in vivo*. Cancer Science 101 (2010): 2234-2240.

Pitchakarn, P., Suzuki, S.,Ogawa, K., Pompimon, W., Takahashi, S., Asamoto, M., Limtrakul, P., and Shirai, T. Induction of G1 arrest and apoptosis in androgen-dependent human prostate cancer by kuguacin J, a triterpenoid from *Momordica charantia* leaf. Cancer Letters 306 (2011): 142-150.

Pitchakarn, P., Suzuki, S., Ogawa, K., Pompimon, W., Takahashi, S., Asamoto, M., Limtrakul, P., and Shirai, T. Kuguacin J, a triterpeniod from *Momordica charantia* leaf, modulates the progression of androgen-independent human prostate cancer cell line, PC3. Food and Chemical Toxicology 50 (2012b): 840-847.

Pitipanapong, J., Chitprasert, S., Goto, M., Jiratchariyakul, W., Sasaki, M., and Shotipruk, A. New approach for extraction of charantin from *Momordica charantia* with pressurized liquid extraction. Separation and Purification Technology 52 (2007): 416-422.

Plassman, B.L., Langa, K.M., Fisher, G.G., Heeringa, S.G., Weir, D.R., Ofstedal, M.B., Burke, J.R., Hurd, M.D., Potter, G.G., Rodgers, W.L., Steffens, D.C., Mcardle, J.J., Willis, R.J., and Wallace, R.B. Prevalence of cognitive impairment without dementia in the United States. Annals of Internal Medicine 148 (2008): 427-434.

Pornsuriya, P., Pornsuriya, P., and Numuen, C. Phenotypic diversity and classification of Thai bitter melon (*Momordica charantia* L.) landraces from three provinces in central region of Thailand. Journal of Agricultural Technology 7 (2011): 849-856.

Raman, A., and Lau, C. Anti-diabetic properties and phytochemistry of *Momordica charantia* L. (Cucurbitaceae). Phytomedicine 2 (1996): 349-362.

Rhee, I.K., Meent, M.V., Ingkaninan, K., and Verpoorte, R. Screening for acetylcholinesterase inhibitors from Amaryllidaceae using silica gel thin-layer chromatography in combination with bioactivity staining. Journal of Chromatography 915 (2001): 217-223.

Reyes, M.E.C., Gildemacher, B.H., and Jansen, G.J. *Momordica charantia* L. In J.S. Siemonsma, and K. Piluek, Plant resources of south-east Asia: Vegetables, pp. 206-210. The Netherlands: Pudoc Scientific, 1994.

Salah, S.M., and Jäger, A.K. Screening of traditionally used lebanese herbs for neurological activities. Journal of Ethnopharmacology 97 (2005): 145-149.

Sermboonpaisarn, T., and Sawasdee, P. Potent and selective butyrylcholinesterase inhibitors from *Ficus foveolata*. Fitoterapia 83 (2012): 780-784.

Sramek, J.J., Zarotsky, V., and Cutler, N.R. Review of drug development and therapeutic role cholinesterase inhibitors in alzheimer's disease. Drug Development Research 56 (2002): 347-353.

Štěpánková, S., and Komers, K. Cholinesterases and cholinesterase inhibitors. Current Enzyme Inhibition 4 (2008): 160-171.

Suwanmaroj, N. Chemical investigation of *Momordica charantia* L. fruits. Master's thesis, Department of Pharmacy, Graduate School, Mihidol University, 1997.

Tan, M.J., Ye, J.M., Turner, N., Hohnen, B.C, Ke, C.Q., Tang, C.P., Chen, T., Weiss, H.C., Gesing, E.R., Rowland, A., James, D.E., and Ye, Y. Antidiabetic activities of triterpenoids isolated from bitter melon associated with activation of the AMPK pathway. Chemistry and Biology 15 (2008): 263-273.

Wang, X.W., Zhang, H.P., Chen, F., Wang, X., and Wen, W.Y. A new lignan from *Gynostemma pentaphyllum*. Chinese Chemical Letters 20 (2009): 589-591.

Wetwitayaklung, P., Limmatvapirat, C., Phaechamud, T., and Keokitichai, S. Kinetics of acetylcholinesterase inhibition of *Quisqualis indica* Linn. flower extract. Silpakorn University Science and Technology Journal 1 (2007): 20-28.

Yasuda, M., Iwamoto, M., Okabe, H., and Yamauchi, T. Structures of momordicines I, II and III, the bitter principles in the leaves and vines of *Momordica charantia* L. Chemical and Pharmaceutical Bulletin 32 (1984): 2044-2047.

Zhang, Y., Cui, J.M., Piao, H.R., and Zhao, Y.Q. Novel compounds in *Momordica charantia.* Chinese Traditional and Herbal Drugs 40 (2009): 509-512.

APPENDIX

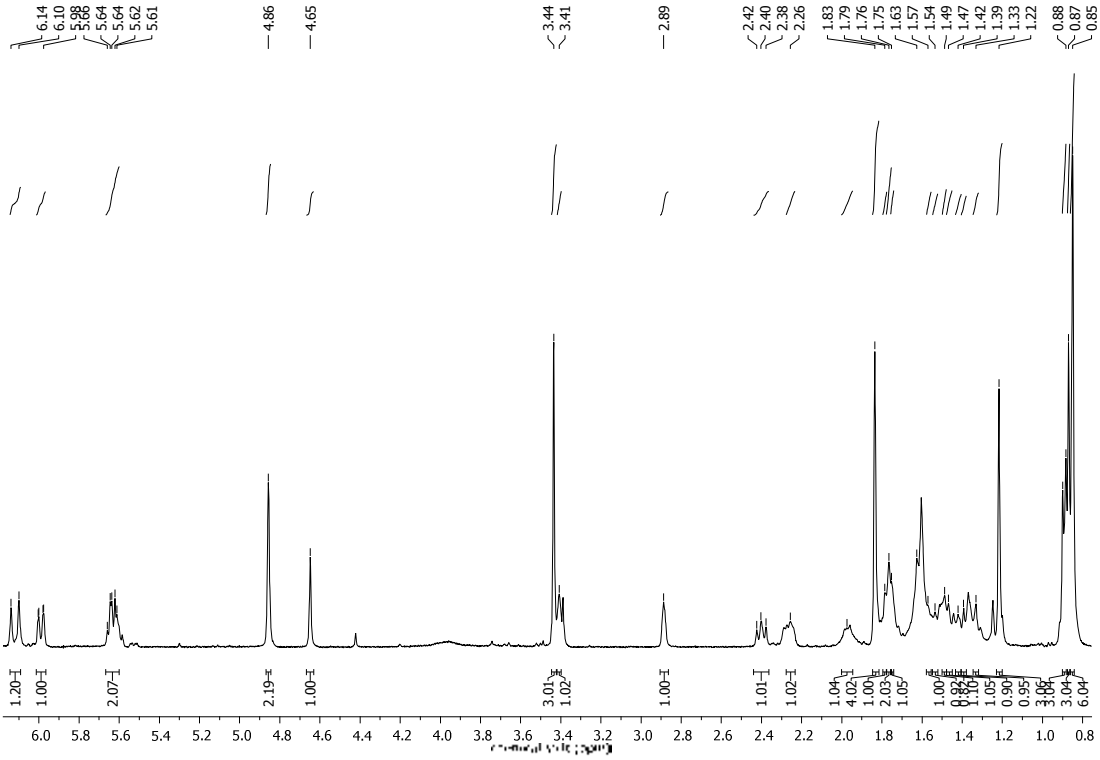

Figure A-1 The ^{1}H-NMR spectrum ($CDCl_3$) of compound **1**.

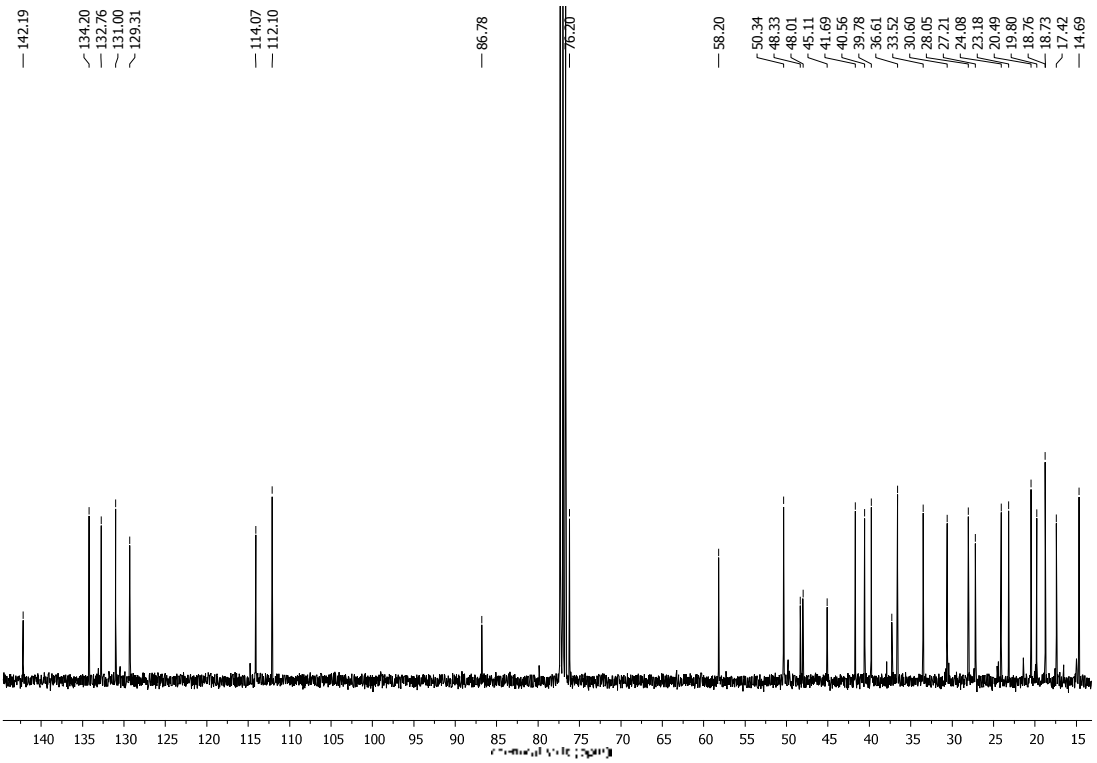

Figure A-2 The ^{13}C-NMR spectrum ($CDCl_3$) of compound **1**.

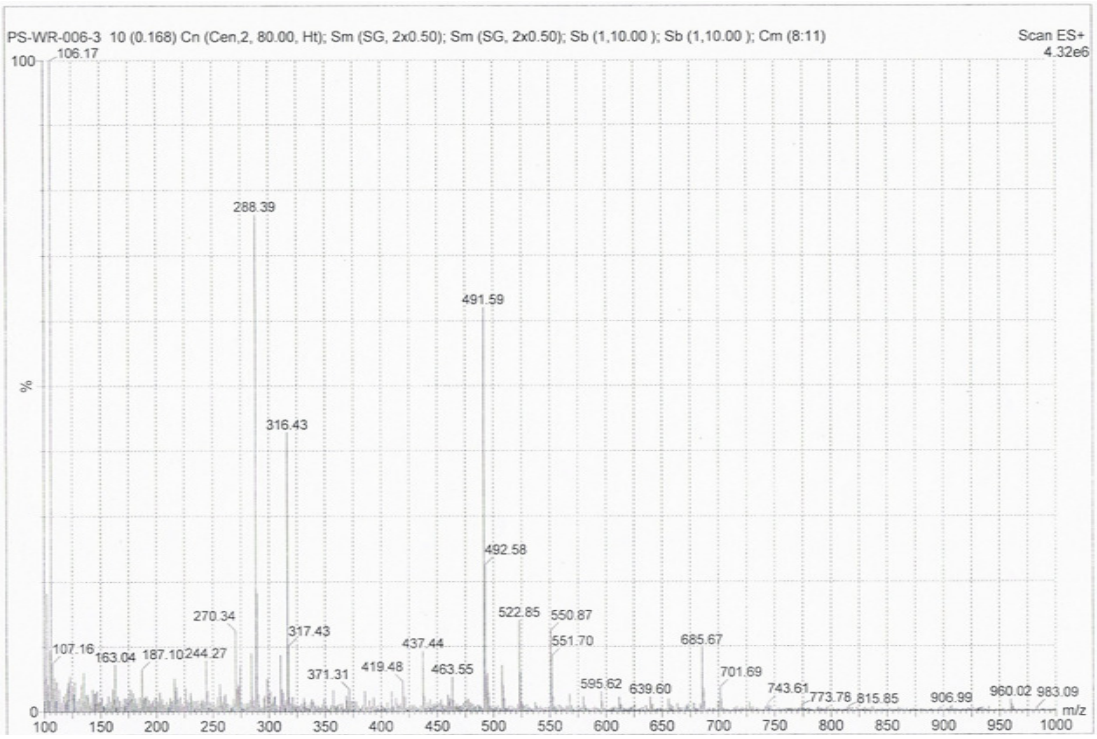

Figure A-3 The positive mass spectrum of compound **1**.

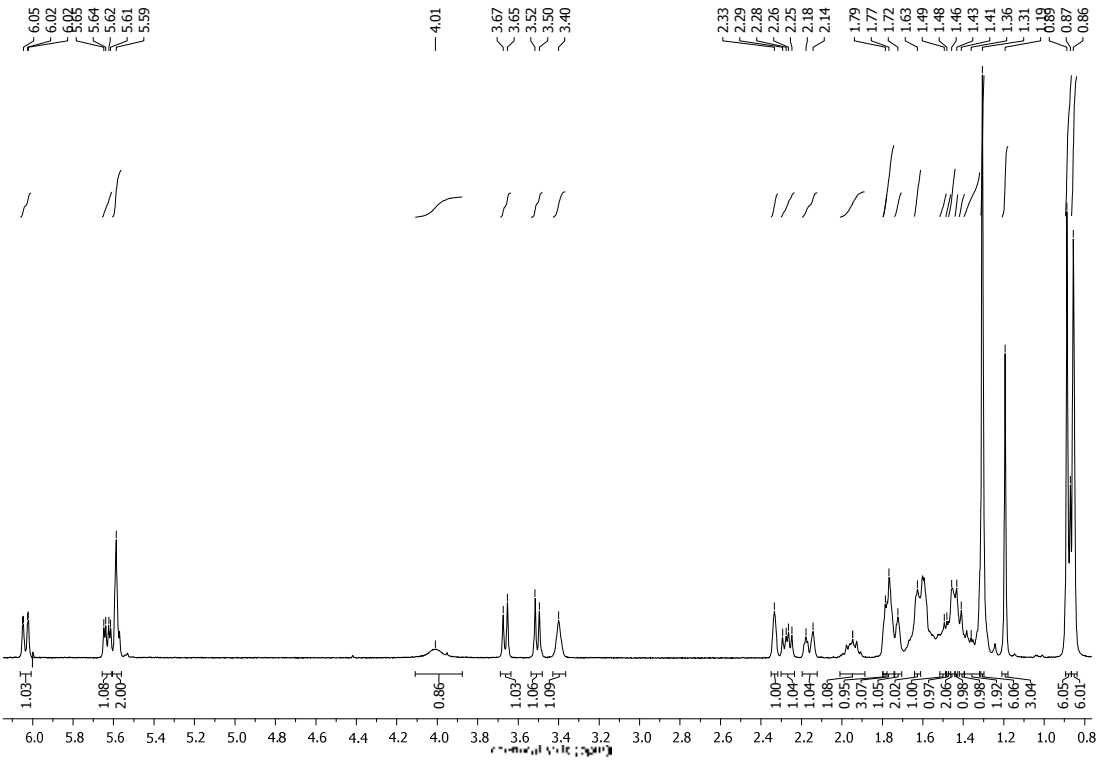

Figure A-4 The ^{1}H-NMR spectrum ($CDCl_3$) of compound **2**.

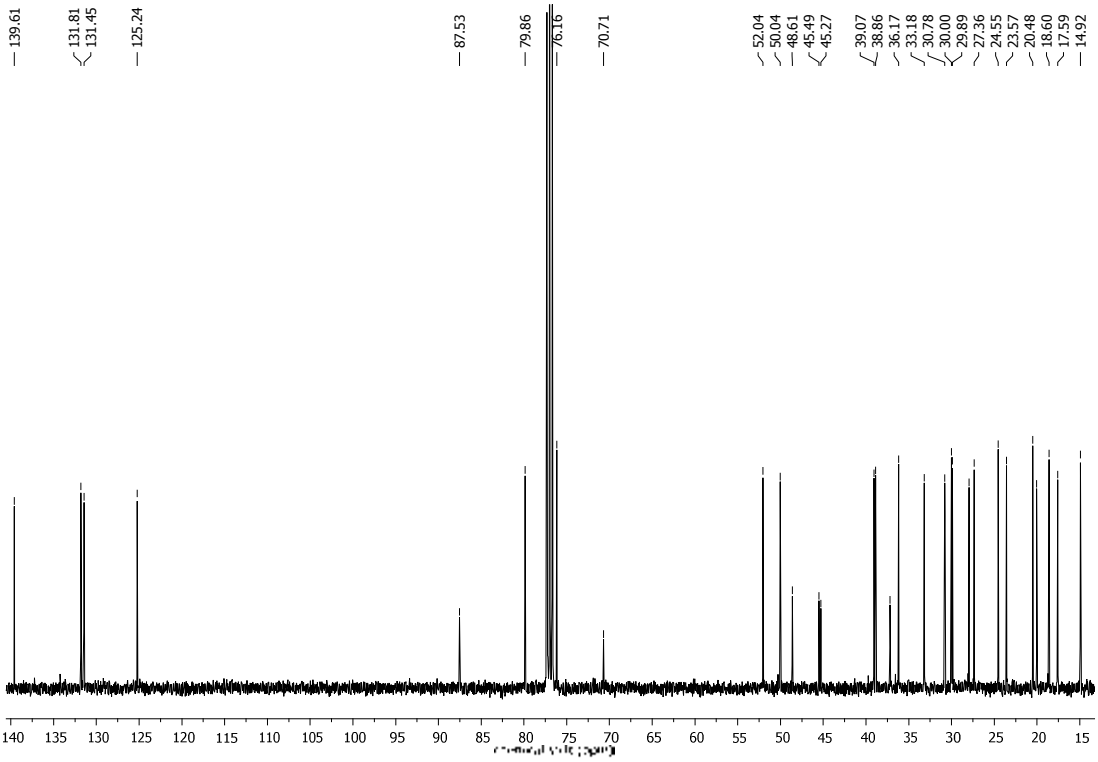

Figure A-5 The ^{13}C-NMR spectrum ($CDCl_3$) of compound **2**.

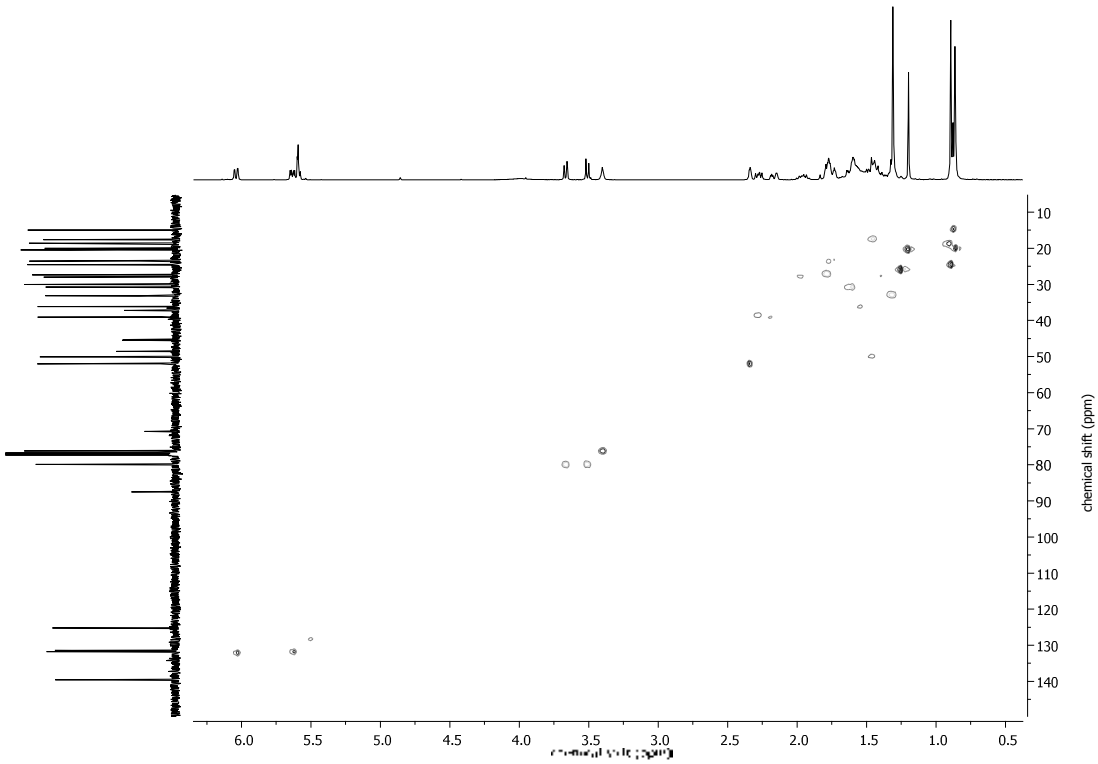

Figure A-6 The HSQC spectrum ($CDCl_3$) of compound **2**.

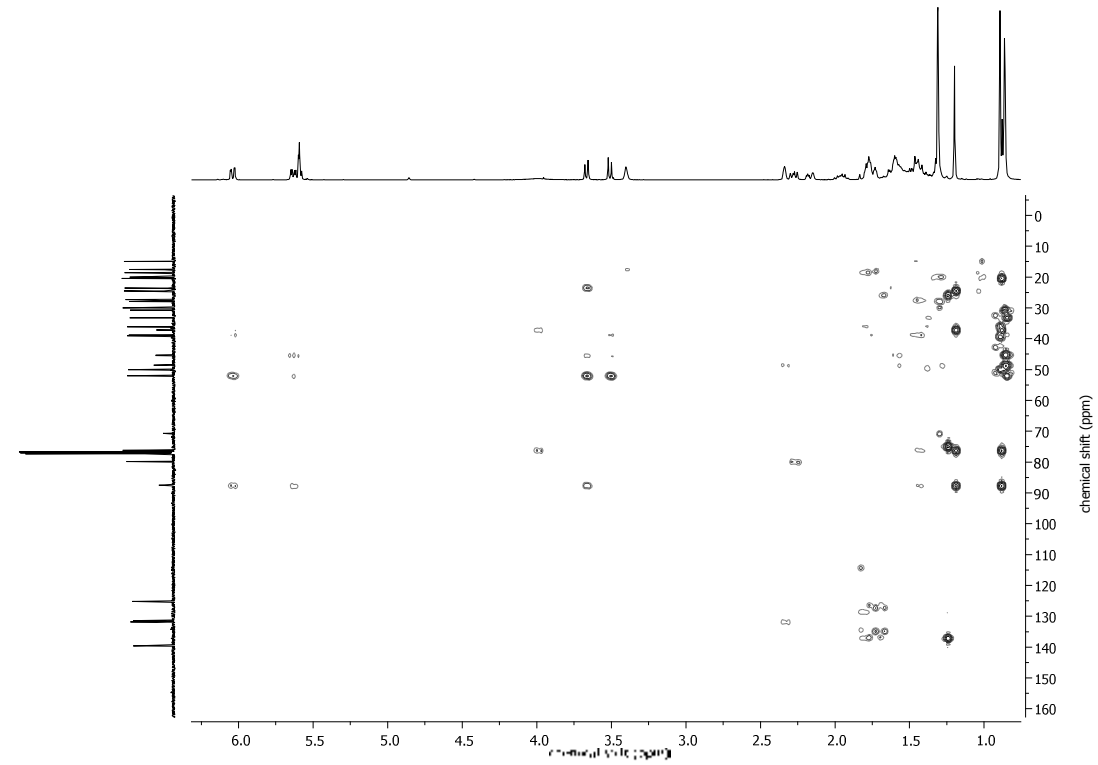

Figure A-7 The HMBC spectrum ($CDCl_3$) of compound **2**.

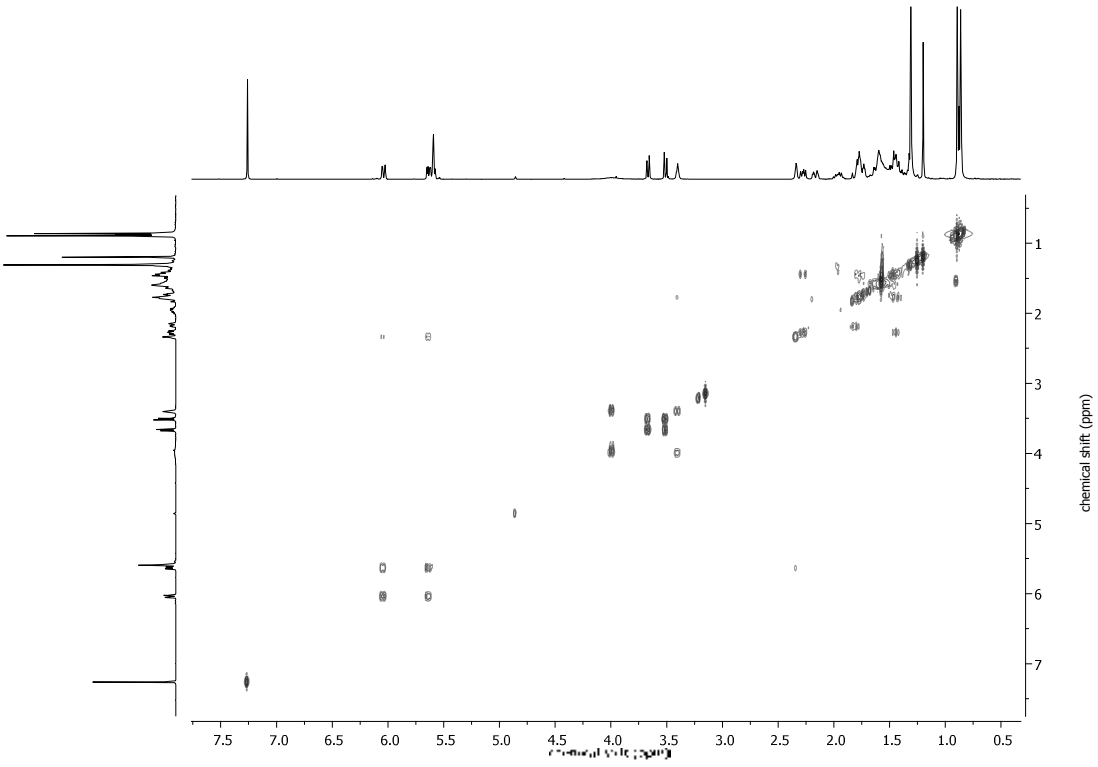

Figure A-8 The COSY spectrum ($CDCl_3$) of compound **2**.

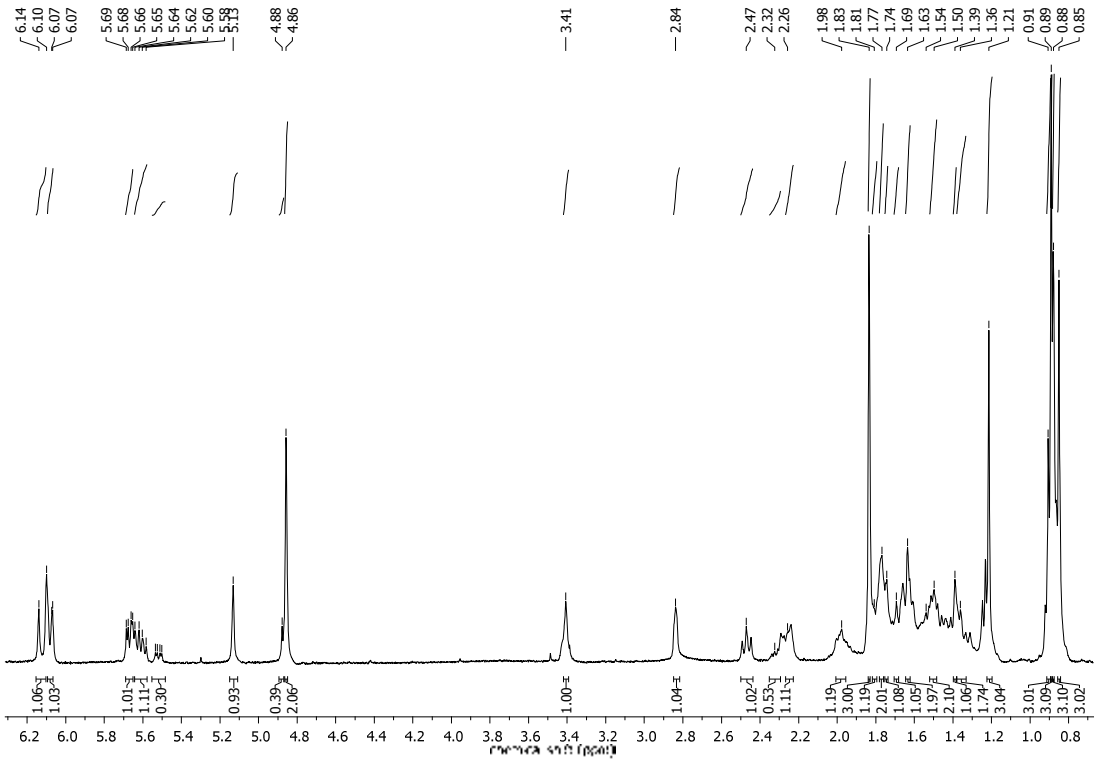

Figure A-9 The ^{1}H-NMR spectrum ($CDCl_3$) of mixture **3**.

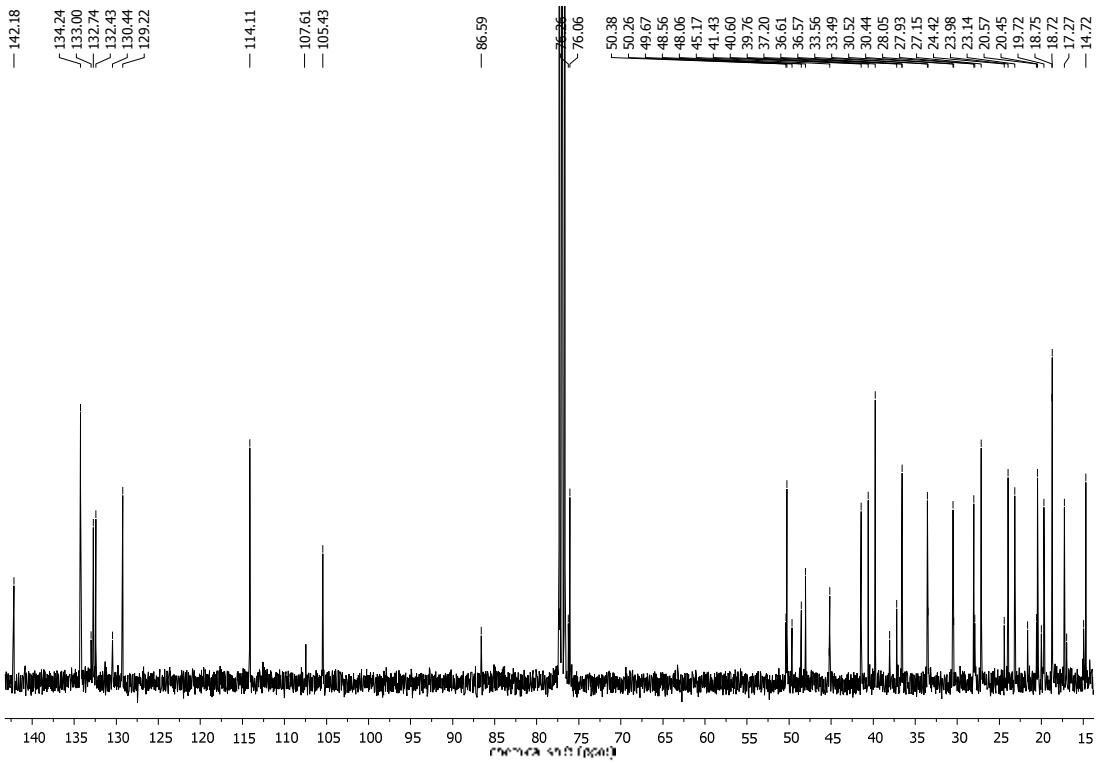

Figure A-10 The ^{13}C-NMR spectrum ($CDCl_3$) of mixture **3**.

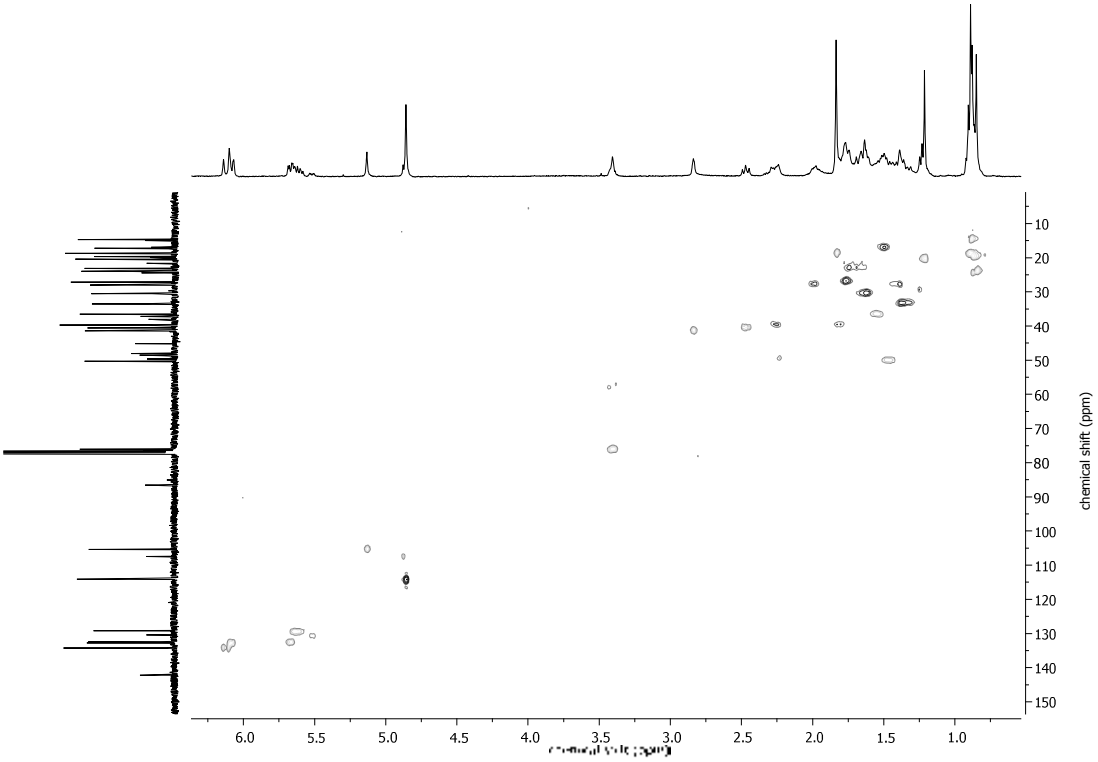

Figure A-11 The HSQC spectrum ($CDCl_3$) of mixture **3**.

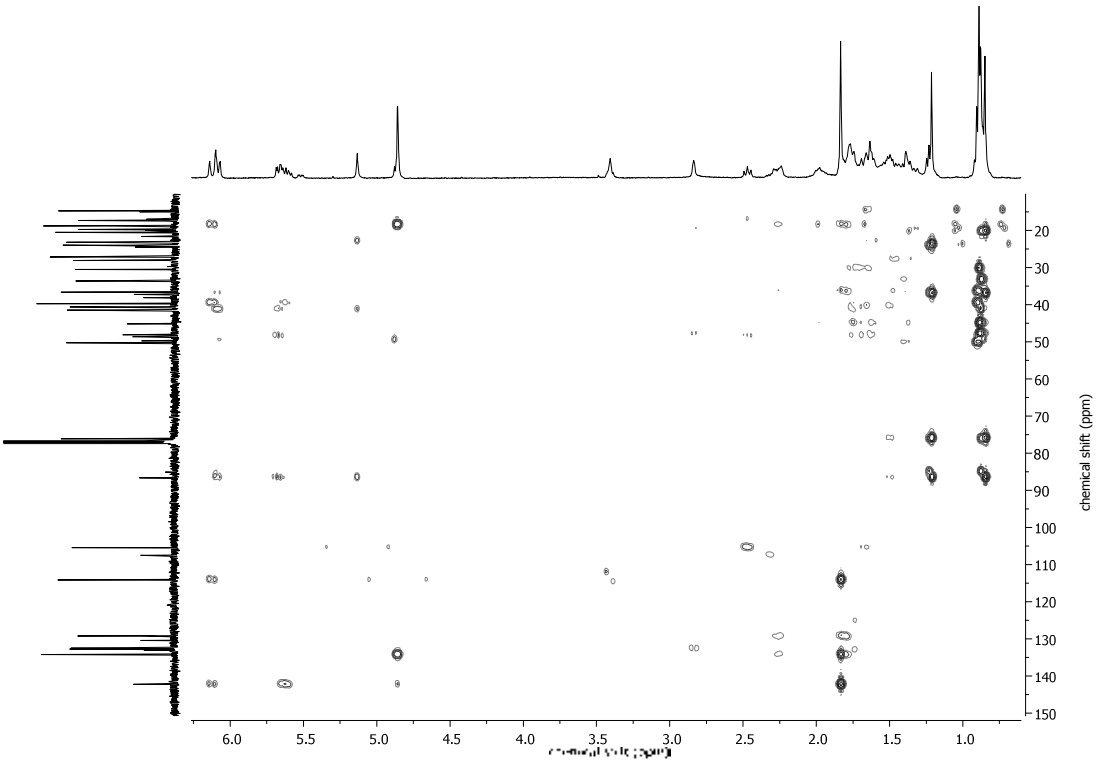

Figure A-12 The HMBC spectrum ($CDCl_3$) of mixture **3**.

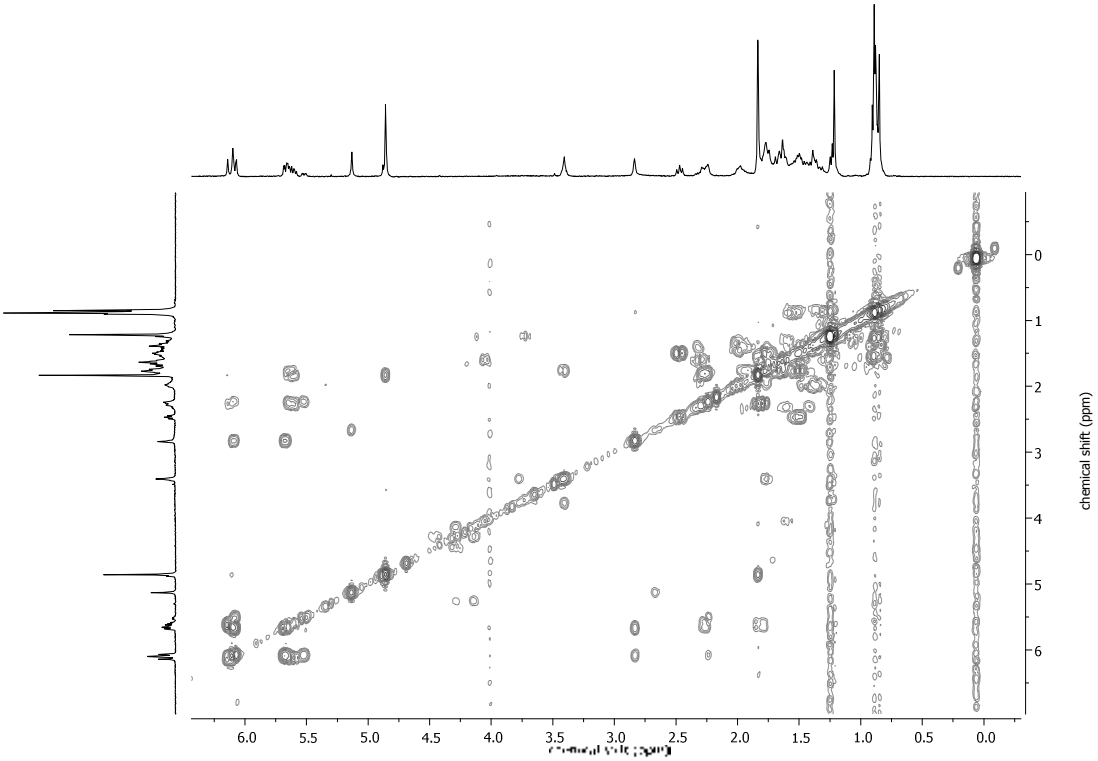

Figure A-13 The COSY spectrum ($CDCl_3$) of mixture **3**.

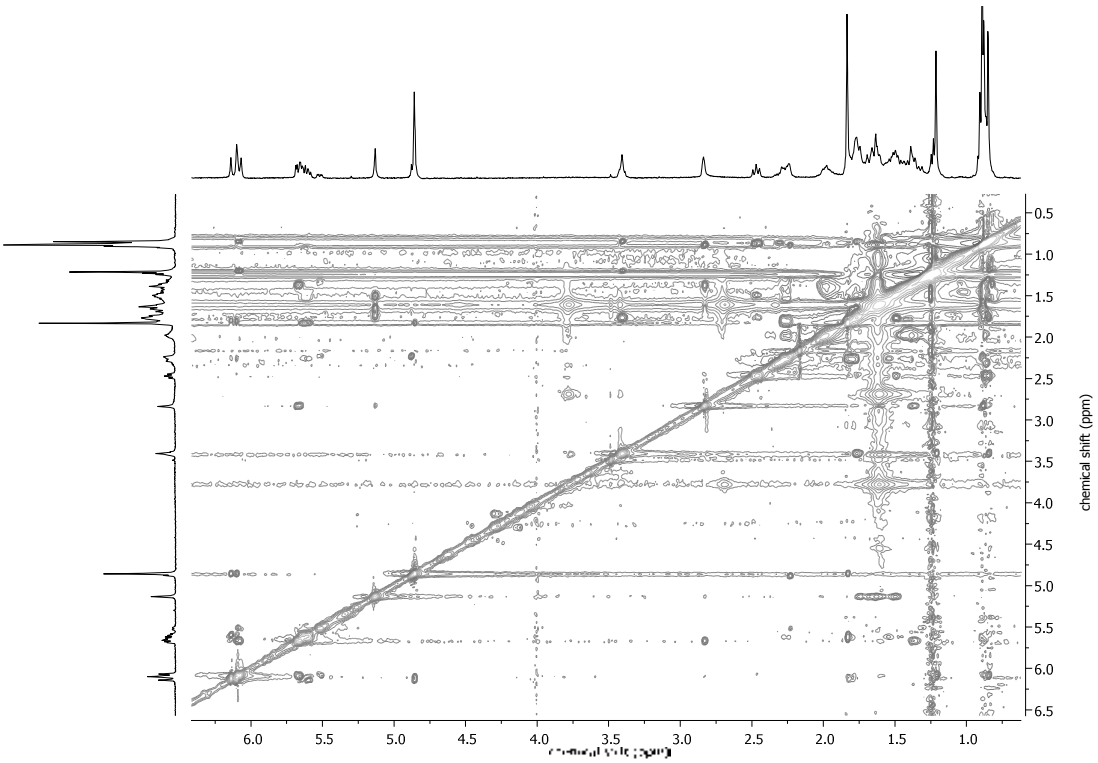

Figure A-14 The NOSEY spectrum ($CDCl_3$) of mixture **3**.

Acquisition Parameter

Source Type	ESI	Ion Polarity	Positive	Set Nebulizer	0.3 Bar
Focus	Not active	Set Capillary	4500 V	Set Dry Heater	180 °C
Scan Begin	50 m/z	Set End Plate Offset	-500 V	Set Dry Gas	4.0 l/min
Scan End	1000 m/z	Set Collision Cell RF	150.0 Vpp	Set Divert Valve	Waste

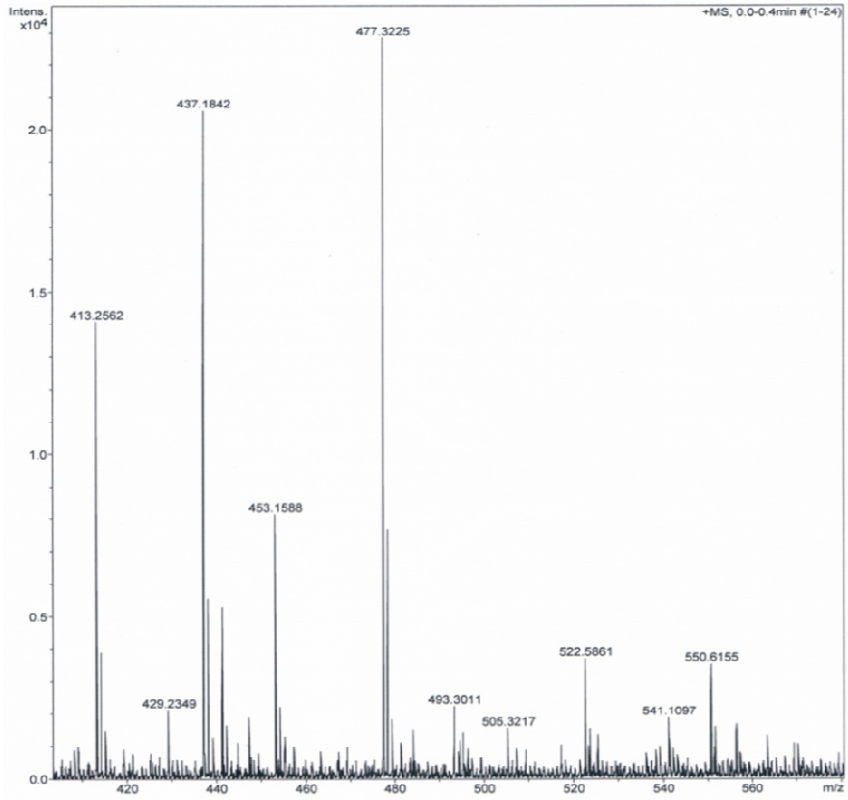

Figure A-15 The positive mass spectrum of mixture **3**.

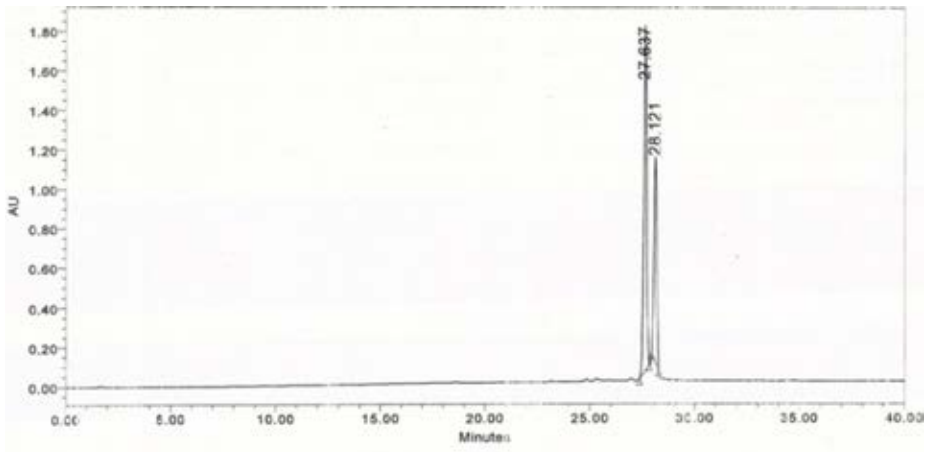

	RT	Area	% Area	Height
1	27.637	1645954	62.53	1755142
2	28.121	986289	37.47	1042680

Figure A-16 The HPLC chromatogram of mixture **3** (a mobile phase of a gradient MeOH:H_2O (50:50 to 100:0 in 20 min and 100:0 in 20 min at λ 230 nm).

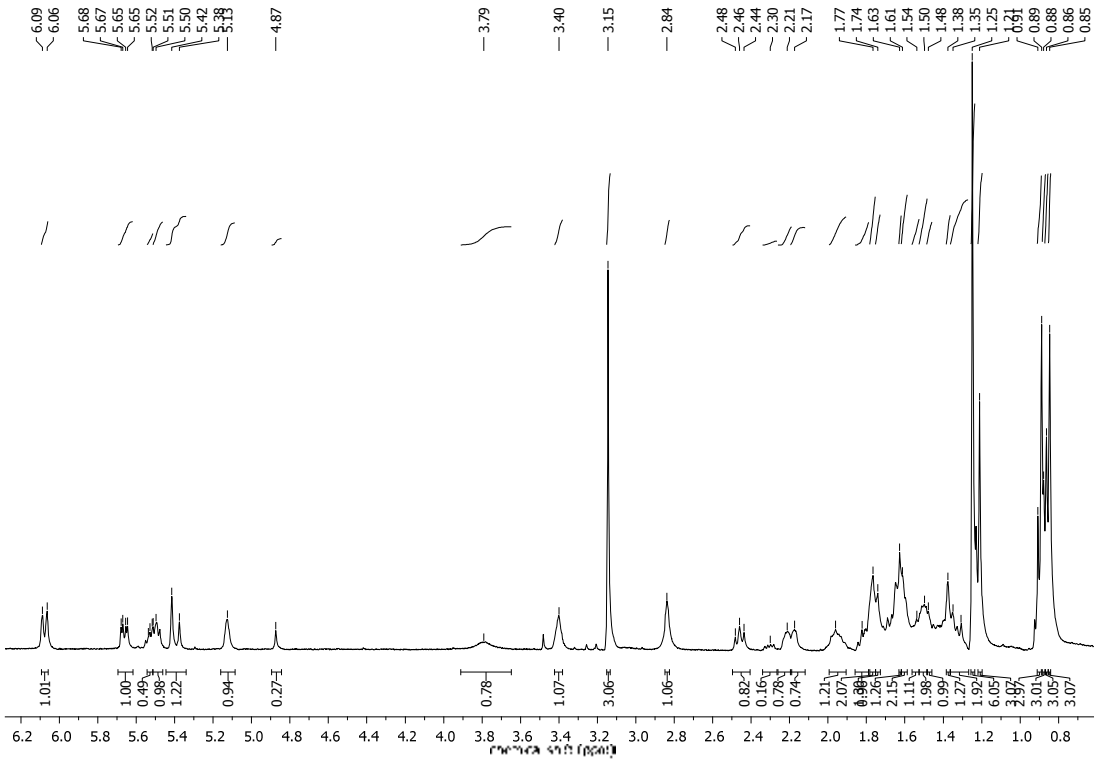

Figure A-17 The ^{1}H-NMR spectrum ($CDCl_3$) of mixture **4**.

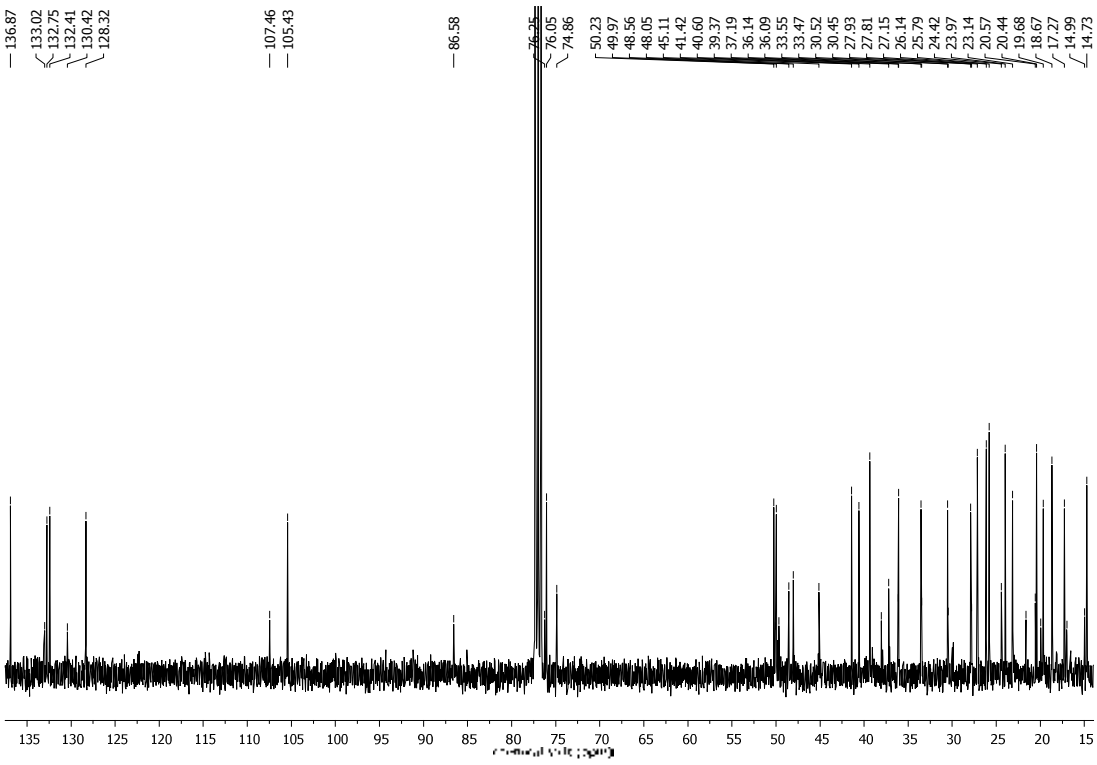

Figure A-18 The ^{13}C-NMR spectrum ($CDCl_3$) of mixture **4**.

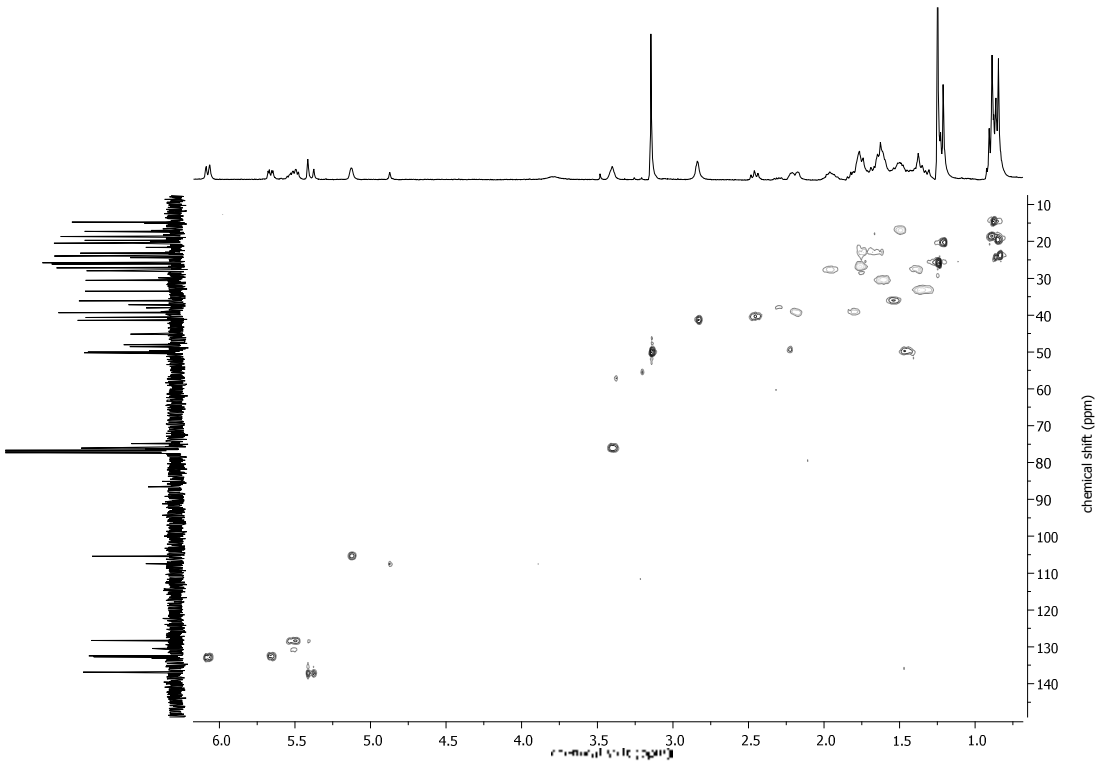

Figure A-19 The HSQC spectrum ($CDCl_3$) of mixture **4**.

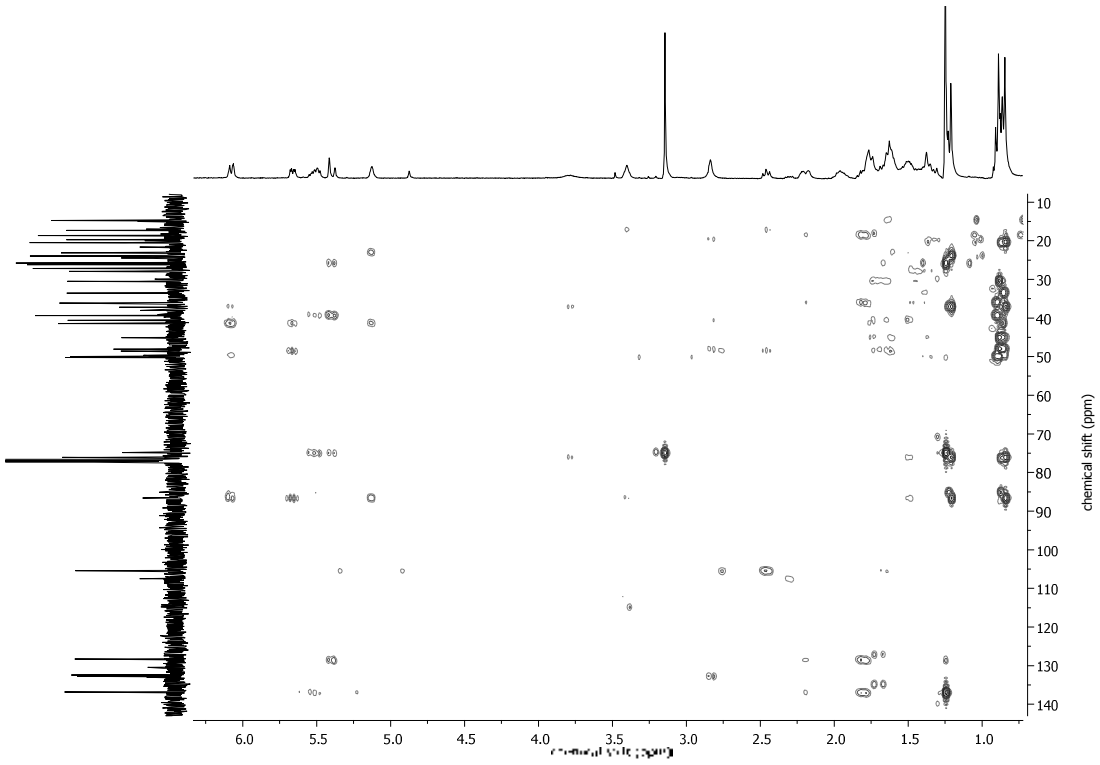

Figure A-20 The HMBC spectrum ($CDCl_3$) of mixture **4**.

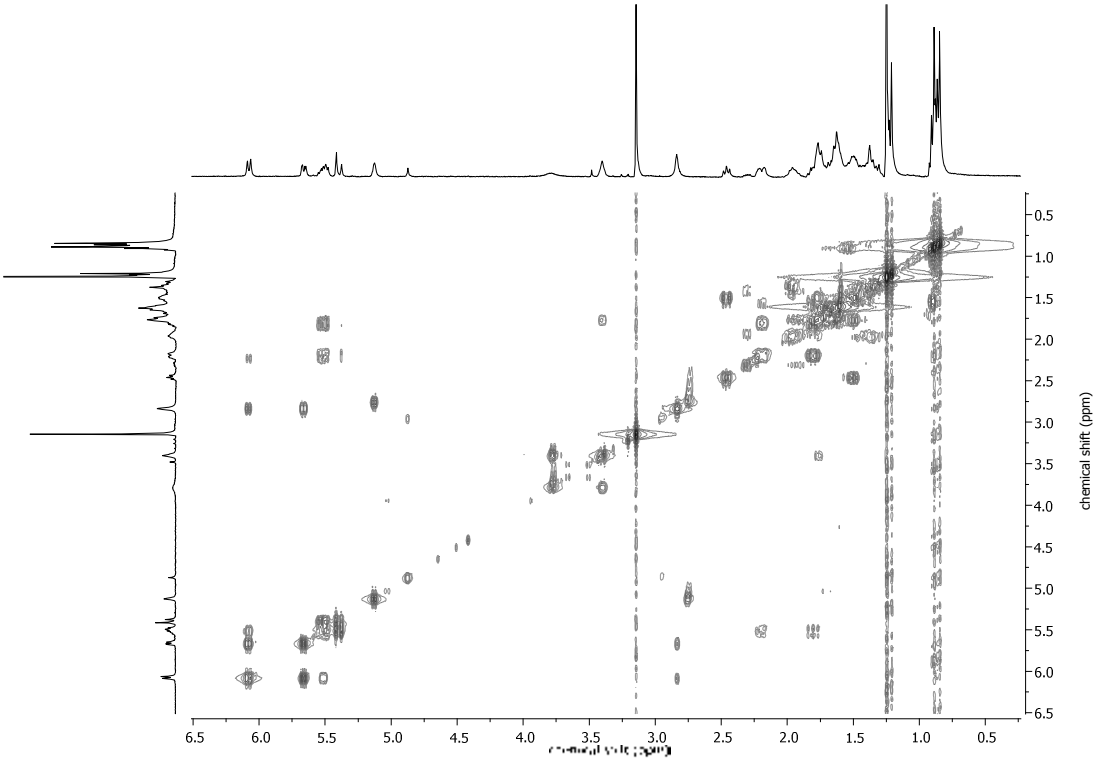

Figure A-21 The COSY spectrum ($CDCl_3$) of mixture **4**.

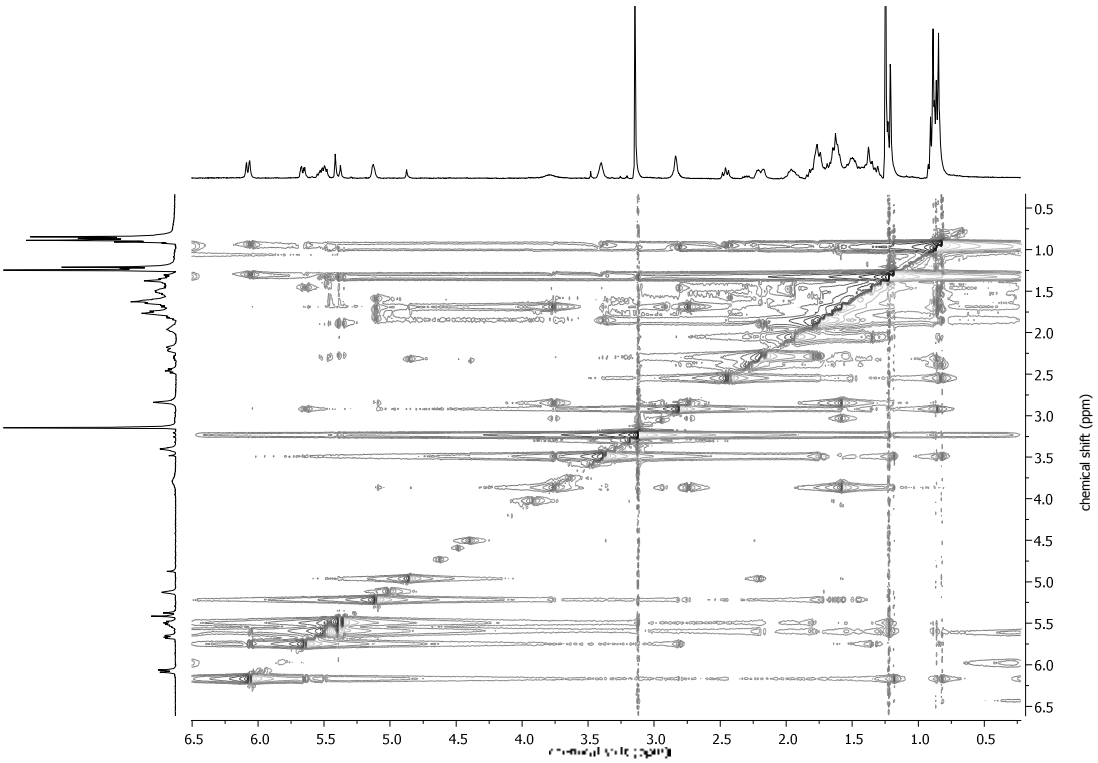

Figure A-22 The NOSEY spectrum ($CDCl_3$) of mixture **4**.

Acquisition Parameter

Source Type	ESI	Ion Polarity	Positive	Set Nebulizer	0.3 Bar
Focus	Not active	Set Capillary	4500 V	Set Dry Heater	180 °C
Scan Begin	50 m/z	Set End Plate Offset	-500 V	Set Dry Gas	4.0 l/min
Scan End	1000 m/z	Set Collision Cell RF	150.0 Vpp	Set Divert Valve	Waste

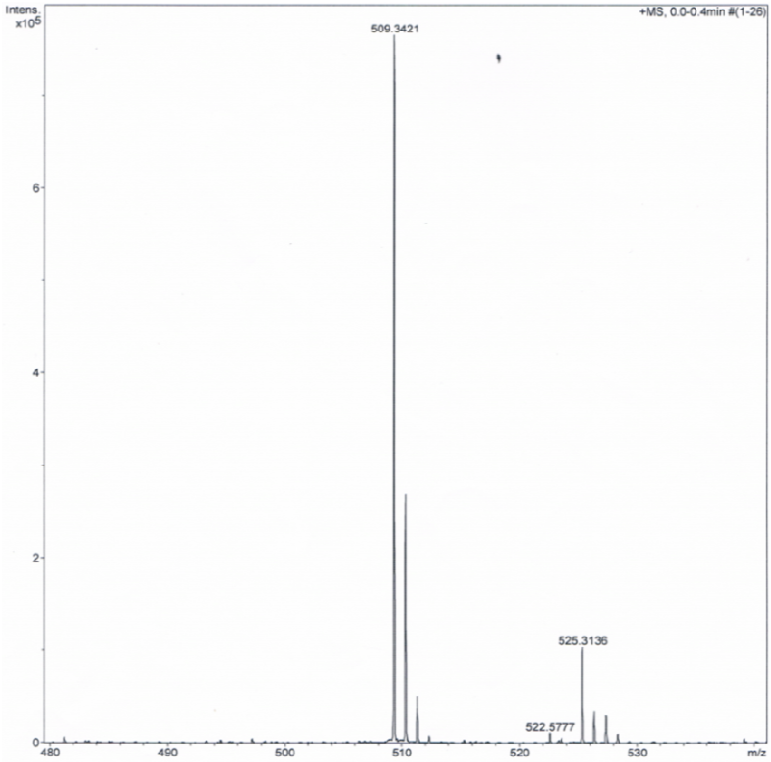

Figure A-23 The positive mass spectrum of mixture **4**.

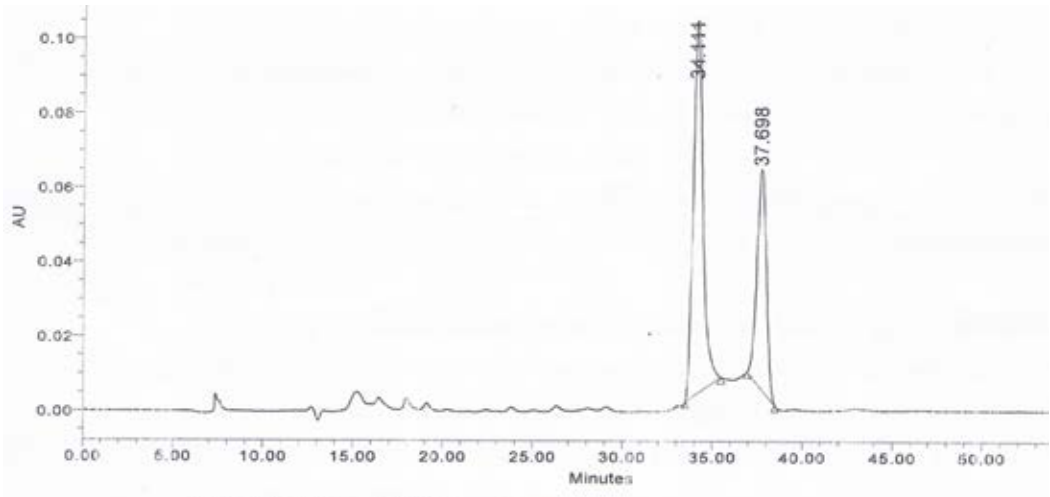

	RT	Area	% Area	Height
1	34.111	3777130	63.50	100744
2	37.698	2171016	36.50	59213

Figure A-24 The HPLC chromatogram of mixture **4** (a mobile phase of 100% MeOH at λ 230 nm).

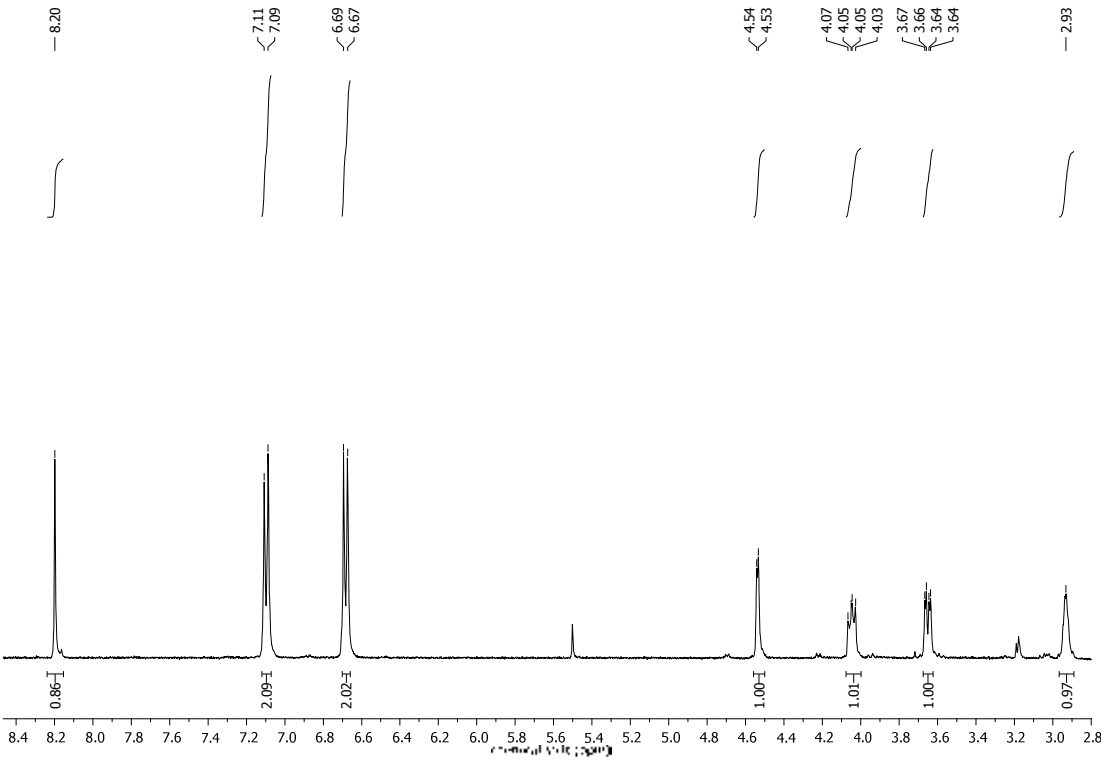

Figure A-25 The ^{1}H-NMR spectrum (acetone-d_6) of compound **5**.

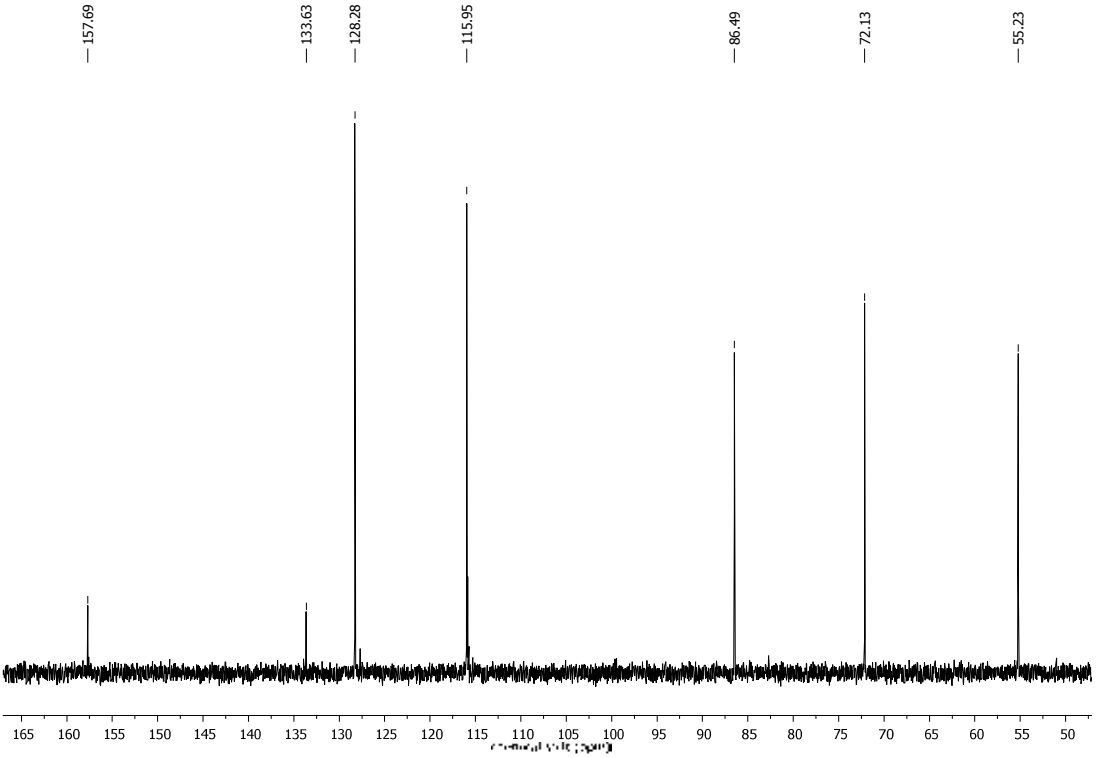

Figure A-26 The ^{13}C-NMR spectrum (acetone-d_6) of compound **5**.

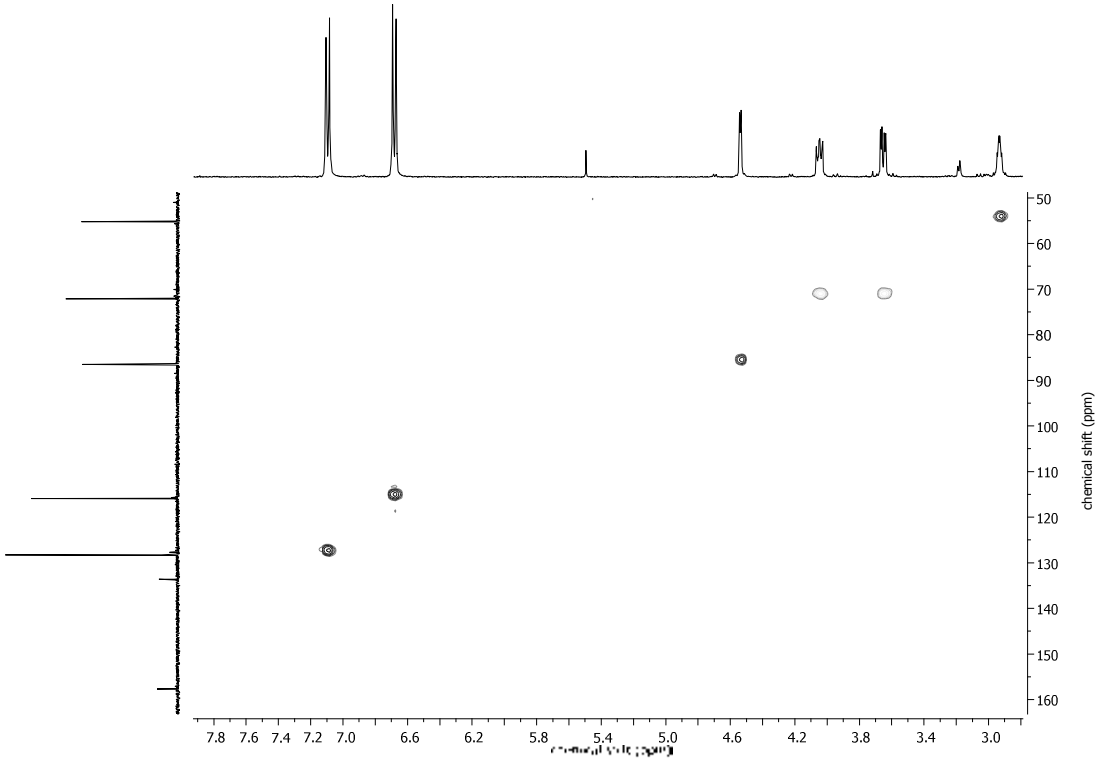

Figure A-27 The HSQC spectrum (acetone-d_6) of compound **5**.

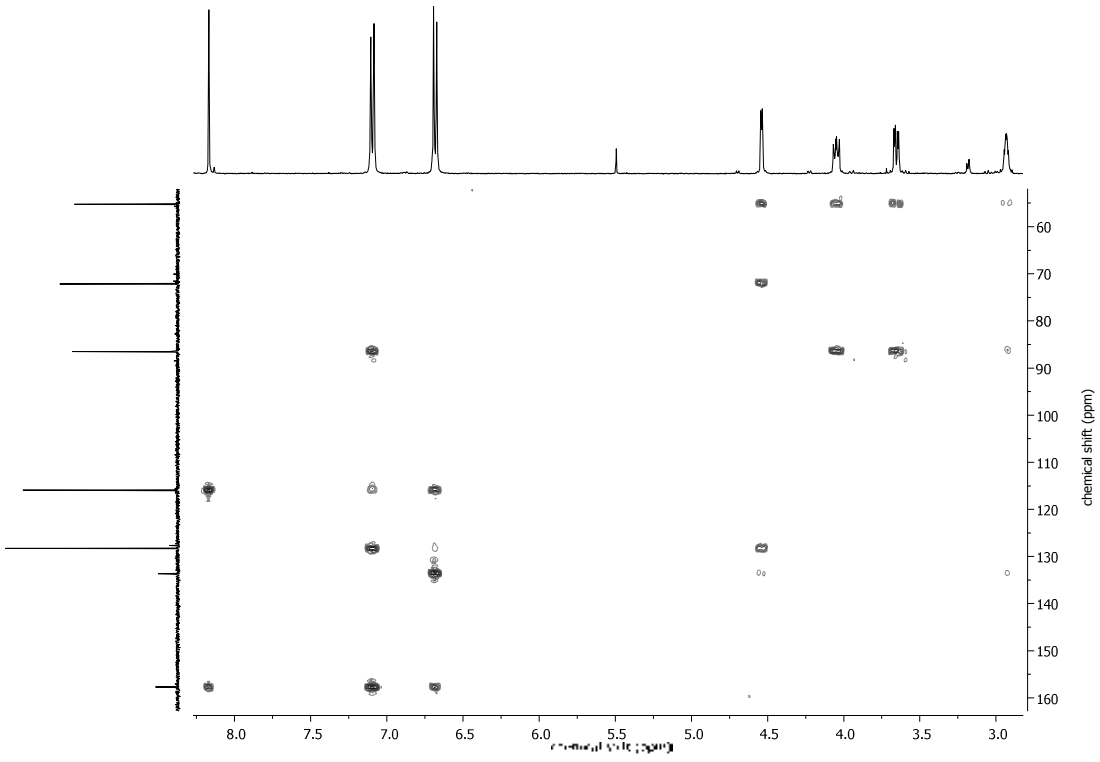

Figure A-28 The HMBC spectrum (acetone-d_6) of compound **5**.

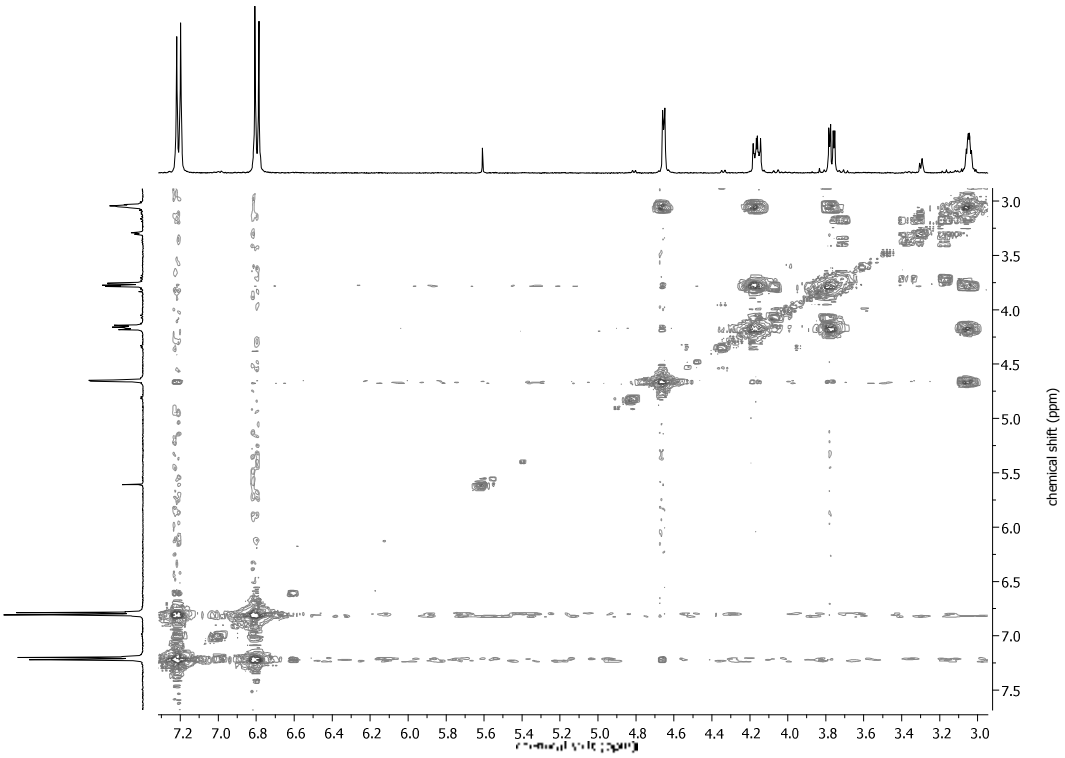

Figure A-29 The COSY spectrum (acetone-d_6) of compound **5**.

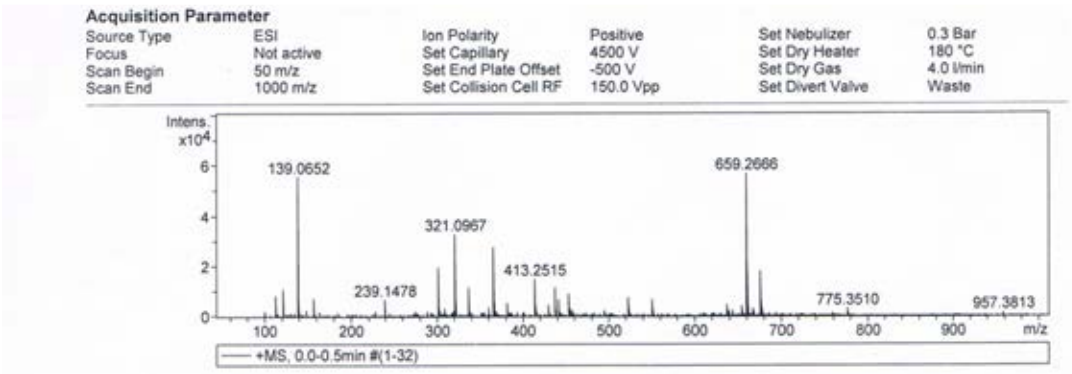

Figure A-30 The positive mass spectrum of compound **5**.

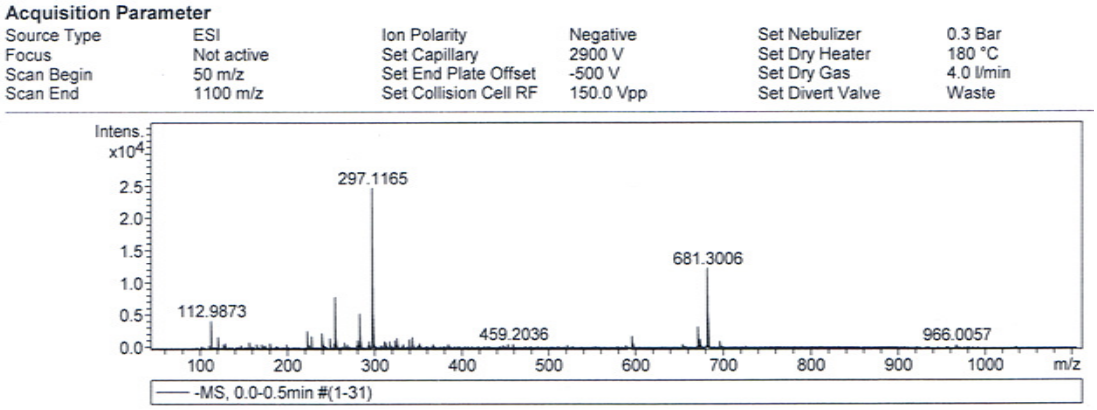

Figure A-31 The negative mass spectrum of compound **5**.

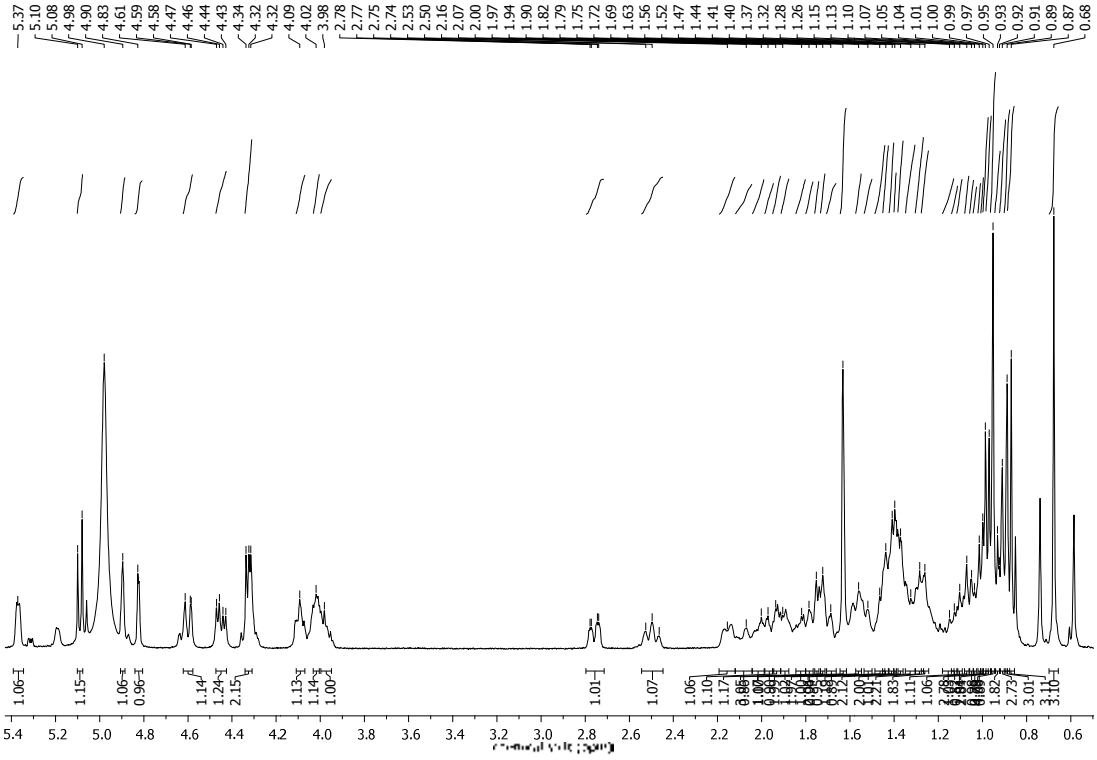

Figure A-32 The ^{1}H-NMR spectrum (pyridine-d_5) of mixture **6**.

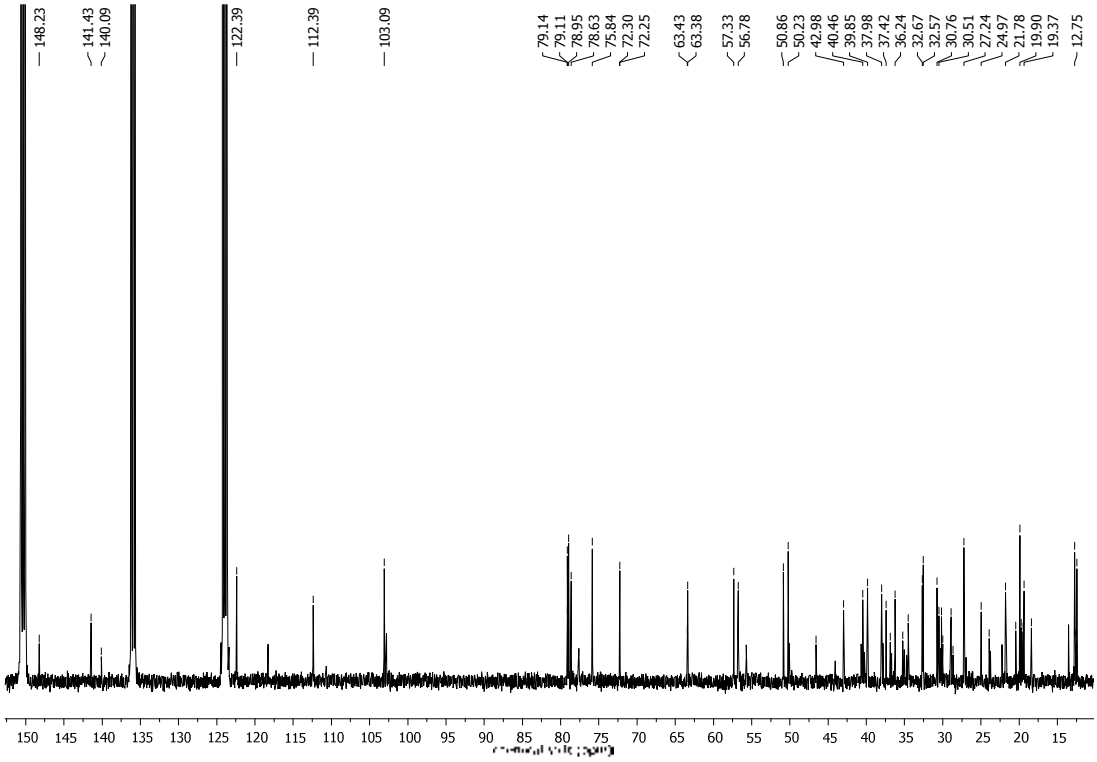

Figure A-33 The ^{13}C-NMR spectrum (pyridine-d_5) of mixture **6**.

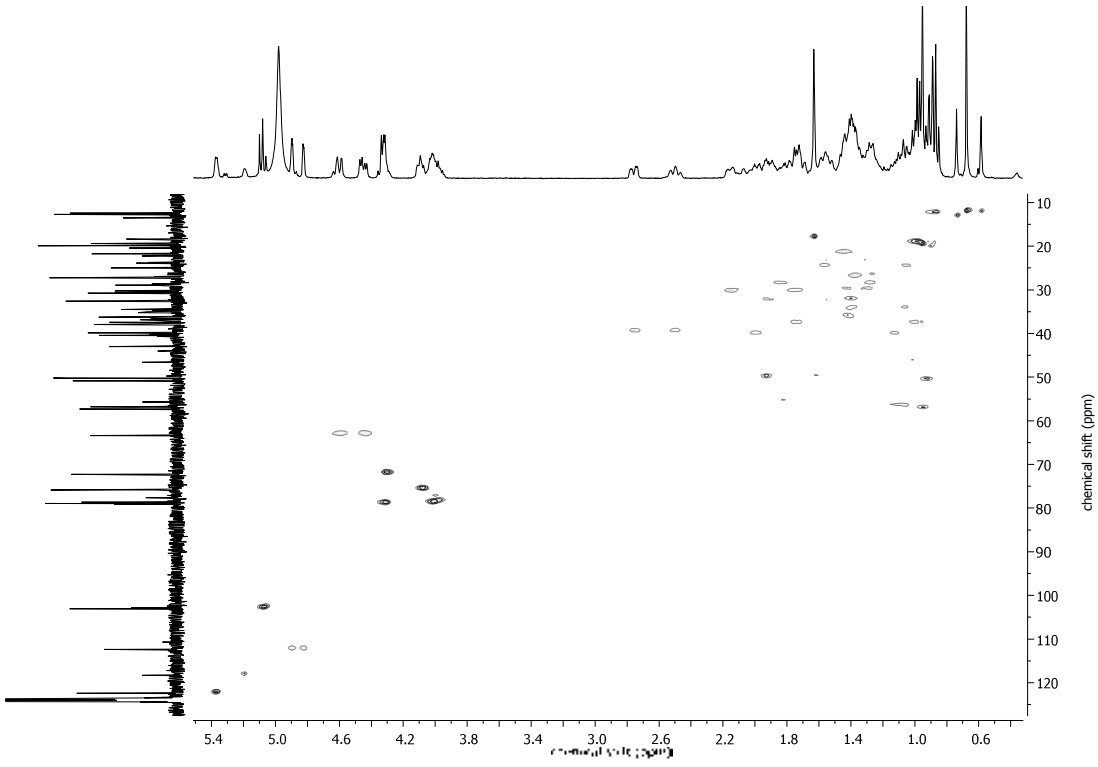

Figure A-34 The HSQC spectrum (pyridine-d_5) of mixture **6**.

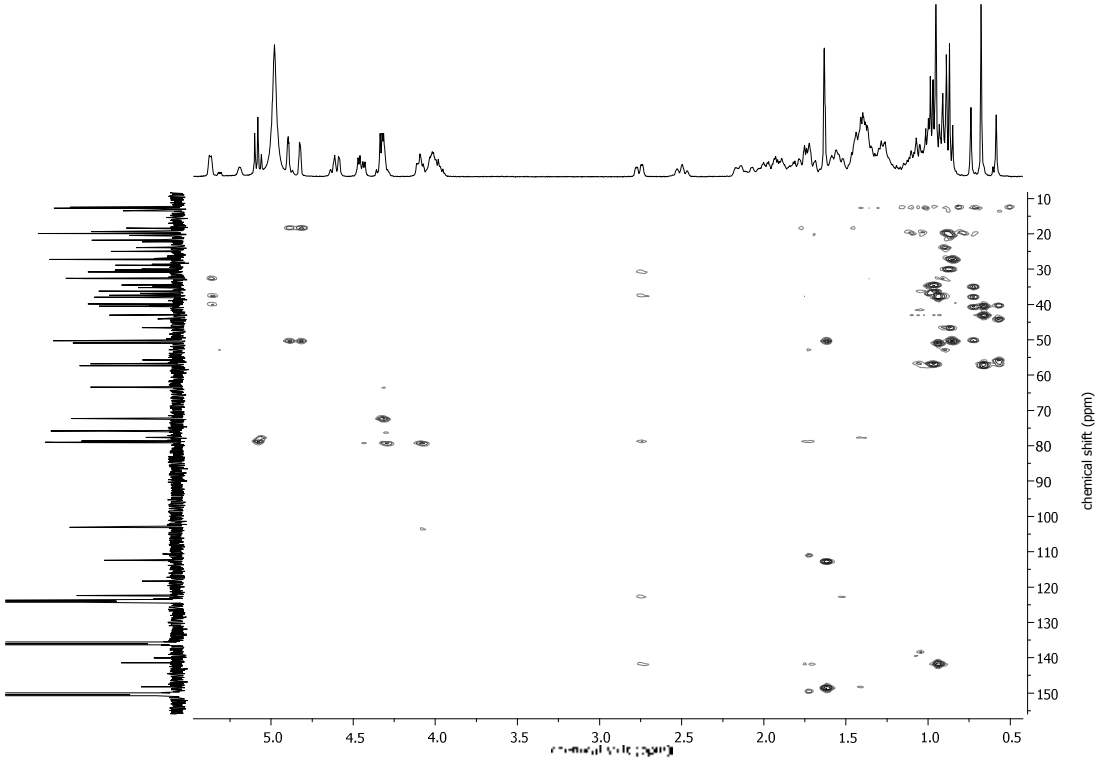

Figure A-35 The HMBC spectrum (pyridine-d_5) of mixture **6**.

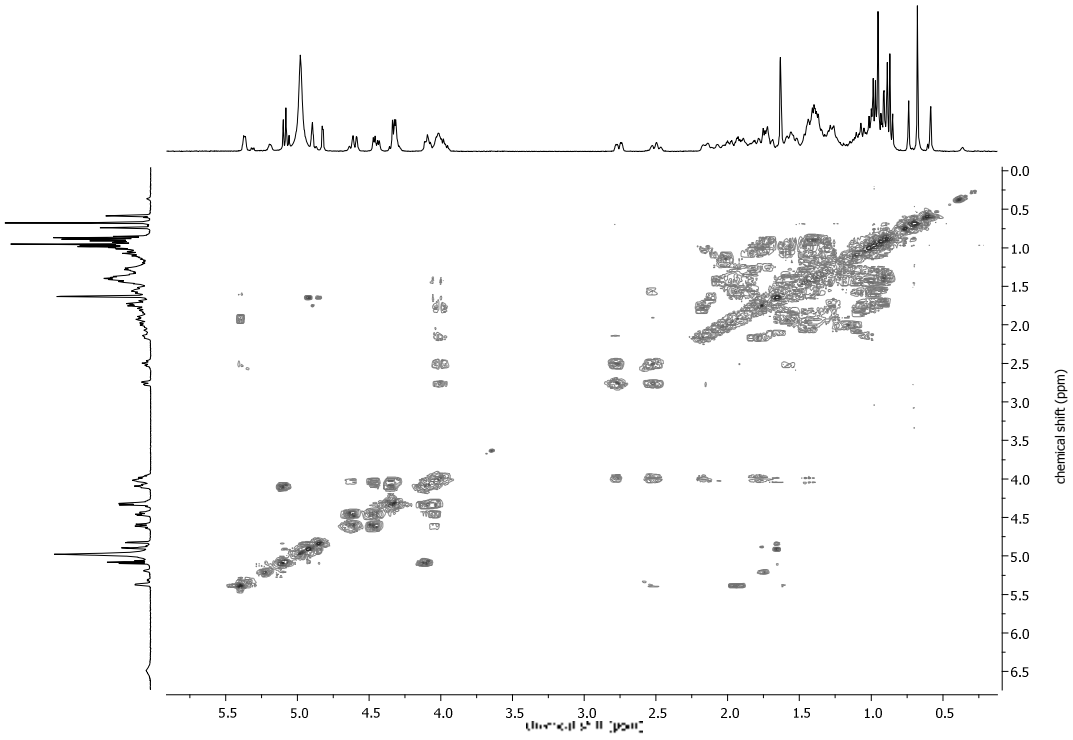

Figure A-36 The COSY spectrum (pyridine-d_5) of mixture **6**.

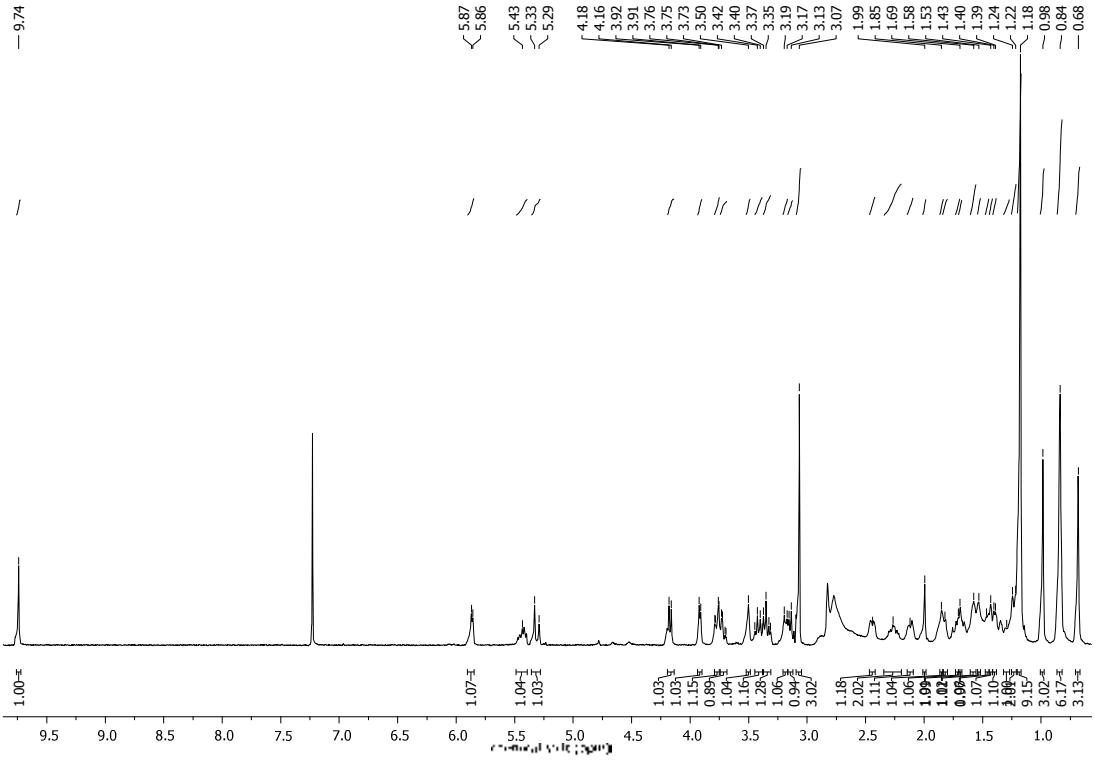

Figure A-37 The ^{1}H-NMR spectrum ($CDCl_3$) of compound **7**.

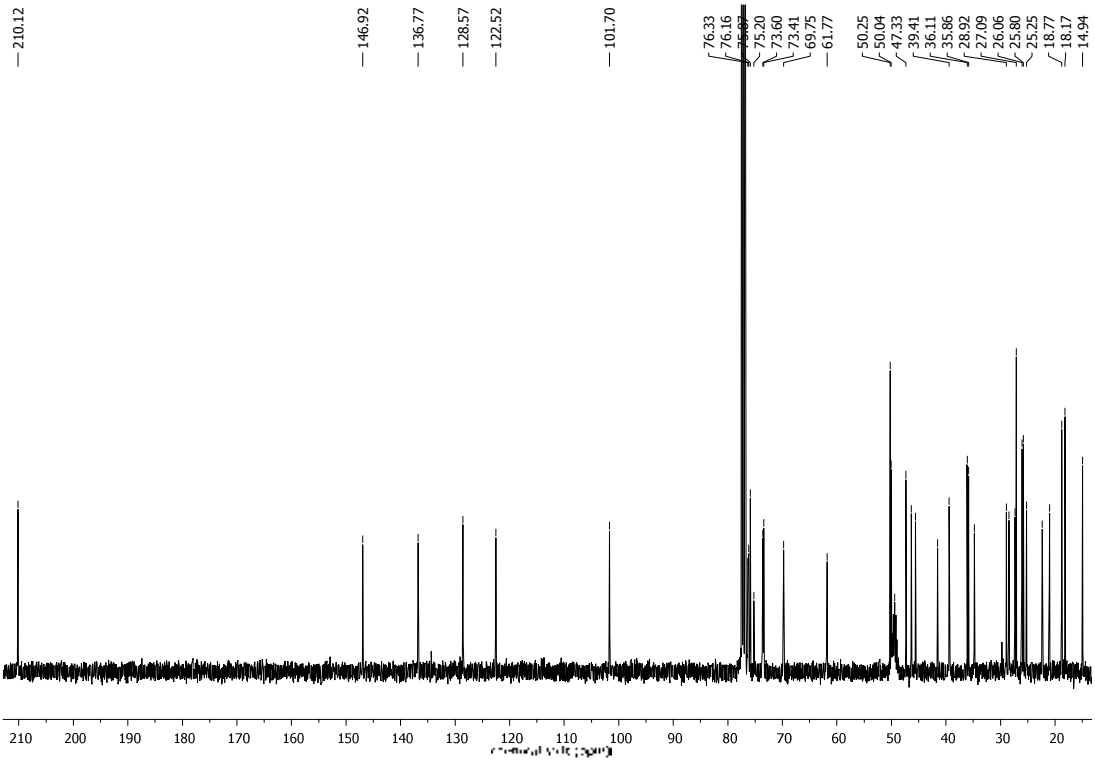

Figure A-38 The ^{13}C-NMR spectrum ($CDCl_3$) of compound **7**.

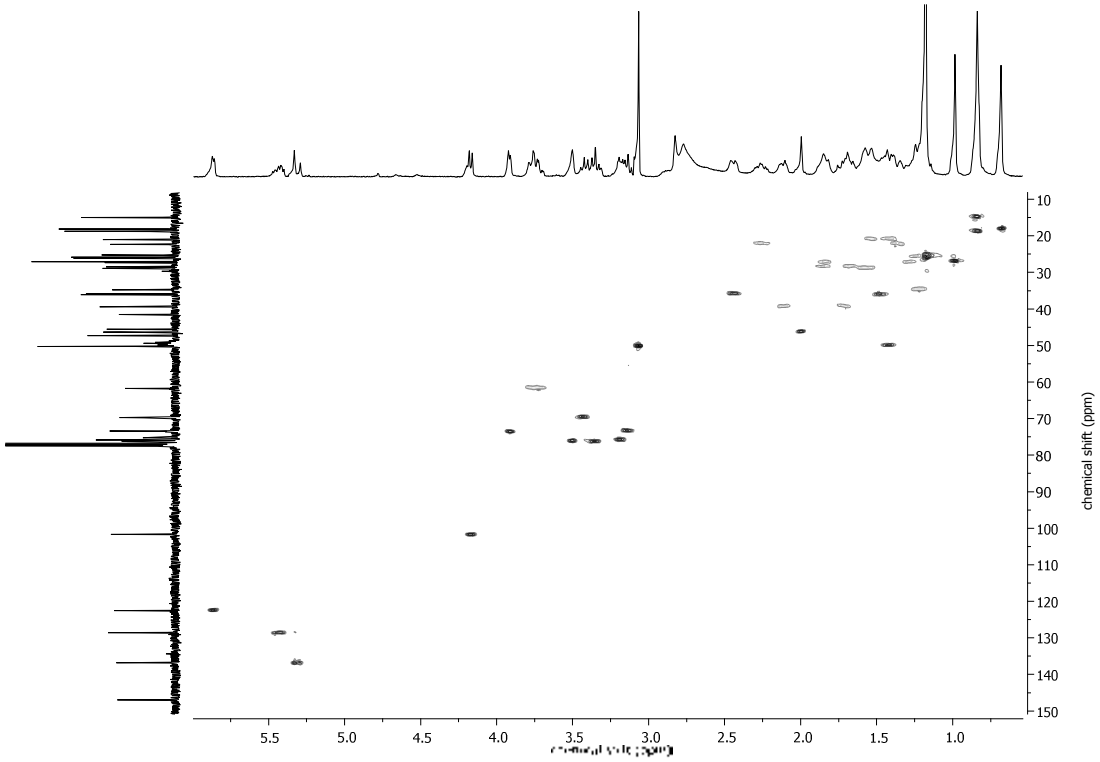

Figure A-39 The HSQC spectrum ($CDCl_3$) of compound **7**.

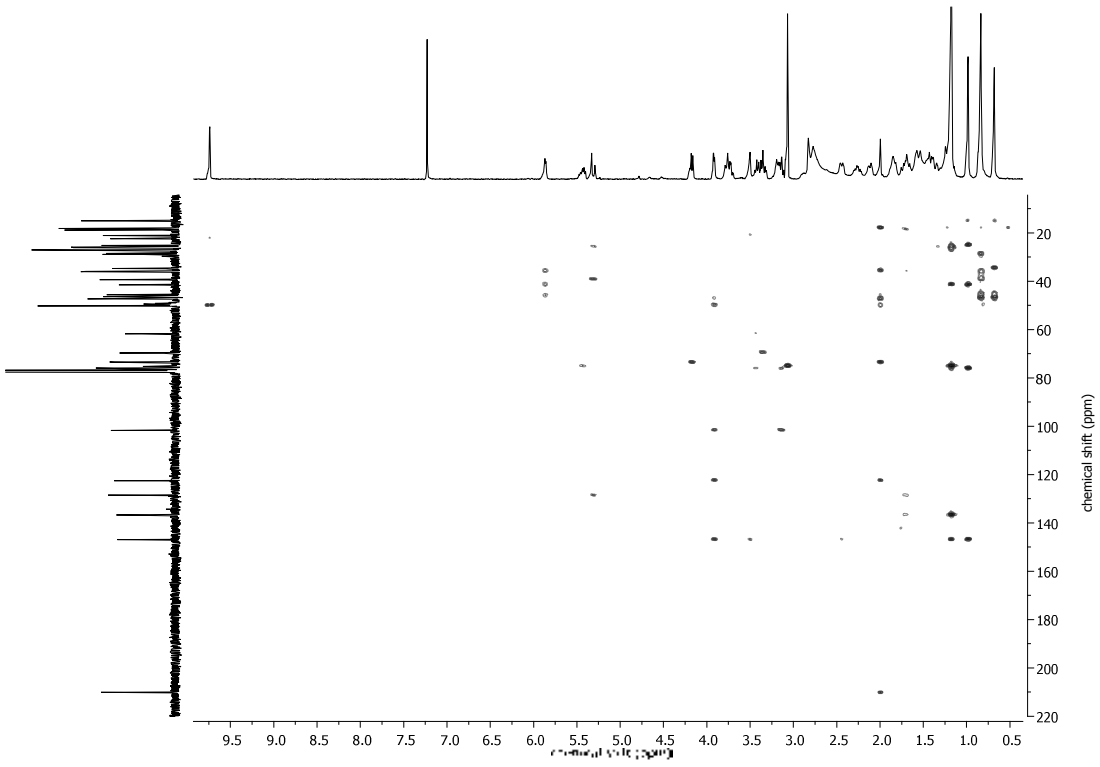

Figure A-40 The HMBC spectrum ($CDCl_3$) of compound **7**.

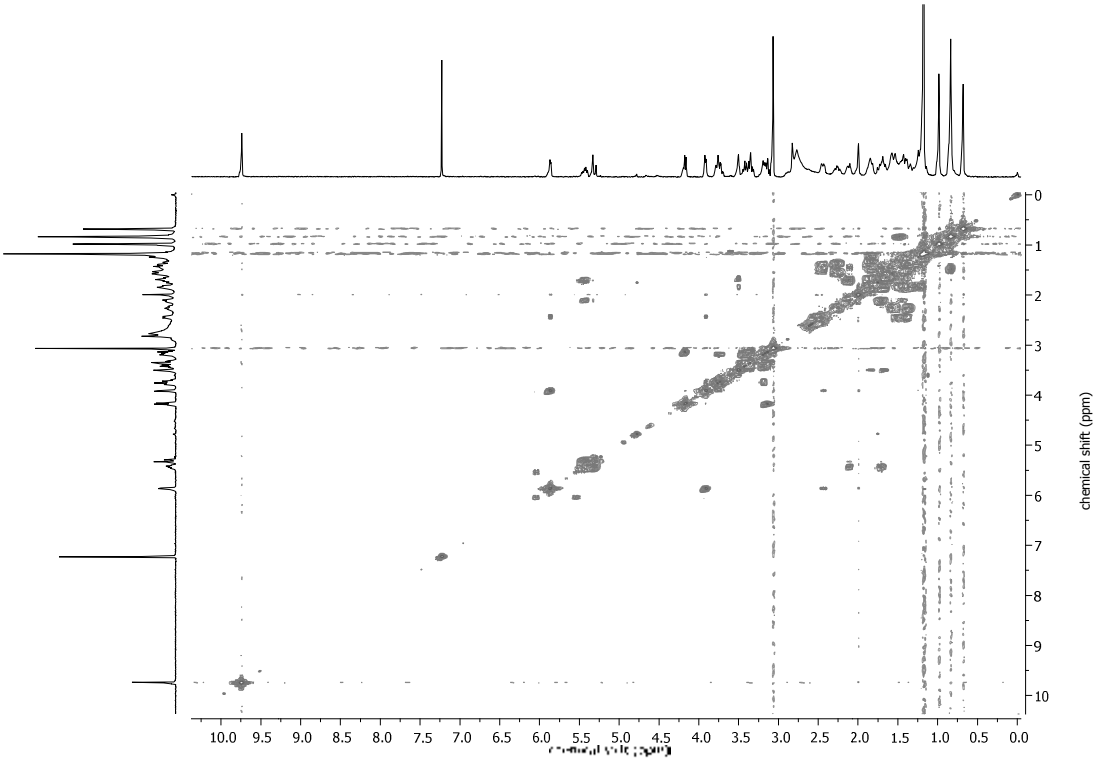

Figure A-41 The COSY spectrum ($CDCl_3$) of compound **7**.

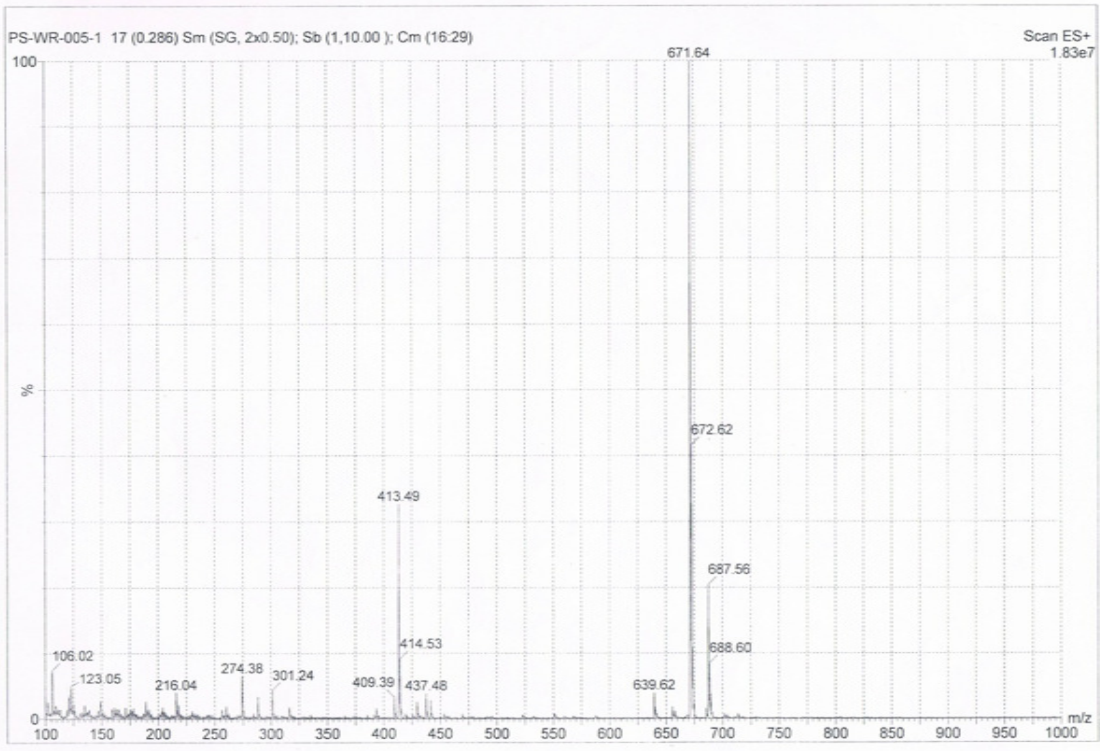

Figure A-42 The positive mass spectrum of compound **7**.

VITA

Miss Wichuta Kuanhut was born on September 14, 1986 in Lopburi Province, Thailand. She graduated with Bachelor's Degree of Engineering, major in Petrochemicals and Polymeric Materials from Faculty of Engineering and Industrial Technology, Silpakorn University, in 2009. She then continued her graduate degree at the Department of Chemistry, Chulalongkorn University. During the time she was studying in the Master of Science program at the Department of Chemistry.

Her present address is 68 Moo 12, Tambon Bangkhu, Amphoe Thawung, Lopburi Province, Thailand, 15150, Tel: 083-9109279.